

**Aus dem Lehrstuhl für Physiologie  
Schwerpunkt Neurophysiologie  
der Universität Würzburg  
Vorstand: Prof. Dr. med. Manfred Heckmann**

**Effects of Transgenic Expression of Botulinum Toxins in Drosophila**

**Inaugural - Dissertation  
zur Erlangung der Doktorwürde der  
Medizinischen Fakultät  
der  
Julius-Maximilians-Universität Würzburg**

**vorgelegt von  
Philipp Backhaus  
aus Paderborn**

**Würzburg, Juni 2016**





**Referent bzw. Referentin:** Prof. Dr. med. Tobias Langenhan, D.Phil.

**Korreferent bzw. Korreferentin:** Prof. Dr. Christian Stigloher

**Dekan:** Prof. Dr. med. Matthias Frosch

**Tag der mündlichen Prüfung: 20.01.2017**

**Der Promovend ist Arzt**



# **Dedication**

To my wife Christina,

our sons Theodor, Karl, Mattis and Kurt



# Table of contents

<b>1</b>	<b>Introduction.....</b>	<b>1</b>
1.1	Clostridial neurotoxins and the SNARE apparatus.....	1
1.2	The <i>GAL4/UAS</i> -system in <i>Drosophila melanogaster</i> .....	4
1.3	Effector genes in <i>Drosophila melanogaster</i> .....	5
1.4	CNTs fail to disrupt neuroexocytosis in specific cell types.....	6
1.5	The visual system of <i>Drosophila melanogaster</i> .....	7
1.6	Project summary.....	8
<b>2</b>	<b>Methods.....</b>	<b>10</b>
2.1	Materials.....	10
2.2	Molecular biology.....	18
2.3	S2 cell culture.....	20
2.4	Western blots.....	20
2.5	Imaging .....	22
2.6	Lethality assays .....	23
2.7	Behavior .....	23
2.8	Statistics.....	35
<b>3</b>	<b>Results .....</b>	<b>36</b>
3.1	Generation of transgenic botulinum toxin DNA.....	36
3.2	Verification of BoNT mediated proteolysis <i>in vitro</i> using western blots.....	46
3.3	Generation of transgenic flies .....	52
3.4	CNT effect on survival and development.....	54
3.5	Effects of CNT expression on larval behavior .....	58
3.6	CNT effect in the visual system .....	61
<b>4</b>	<b>Discussion.....</b>	<b>76</b>
4.1	Generation of transgenic <i>UAS-BoNT</i> -flies .....	76
4.2	Varying effectivity of <i>UAS-BoNT</i> constructs in larval survival and behavior.....	77
4.3	Effect of BoNT-expression in the visual system of <i>Drosophila</i> .....	80
<b>5</b>	<b>Conclusion .....</b>	<b>85</b>
<b>6</b>	<b>References .....</b>	<b>86</b>

## Table of figures

Figure 1.1 Clostridial neurotoxins and the SNARE complex	2
Figure 1.2 <i>GAL4/UAS</i> -system	5
Figure 1.3 Overview on anatomy of the fly visual system	8
Figure 2.1 Sketch of the "Buchner-ball" setup	27
Figure 2.2 Photographs of the "Buchner-ball" setup	28
Figure 2.3 Heating trace	31
Figure 3.1 Alignment Synaptobrevin	37
Figure 3.2 Alignment SNAP-25	39
Figure 3.3 Alignment Syntaxin-1A	40
Figure 3.4 Scheme of the BoNT gene locus and the expressed protein	42
Figure 3.5 Scheme of the modified BoNT-F construct	43
Figure 3.6 Scheme of expression plasmids for western blots	44
Figure 3.7 Stainings of BoNTs in S2 cells	45
Figure 3.8 Localization of Syx-1A in S2 cells	47
Figure 3.9 Overview on western blots of BoNT mediated proteolysis of SNARE proteins	49
Figure 3.10 Original western blot	51
Figure 3.11 Original western blot	51
Figure 3.12 Original western blot	52
Figure 3.13 Assessment of lethality after expression in neurons	55
Figure 3.14 Assessment of lethality after expression in muscles	56
Figure 3.15 Decrease of larval activity after induction of CNT expression in neurons	59
Figure 3.16 Eye morphology after CNT expression	62
Figure 3.17 Effect of pan-neuronal <i>Shibire<sup>ts</sup></i> expression	63
Figure 3.18 Influence of different stimulus variables on OMR	65
Figure 3.19 OMR of <i>ombH<sup>31</sup></i> vs <i>WTB</i>	67
Figure 3.20 <i>GMR-GAL4 &gt; UAS-TNT</i> effect on OMR in the adult fly	68
Figure 3.21 <i>GMR-GAL4 &gt; UAS-Shibire<sup>ts</sup></i> effect on OMR	69
Figure 3.22 <i>GMR-GAL4 &gt; UAS-BoNT-B</i> effect on OMR in the adult fly	71
Figure 3.23 OMR after expression of different effectors with <i>Rh1-GAL4</i>	72
Figure 3.24 <i>Rh1-GAL4 (on 2<sup>nd</sup>) &gt; UAS-Shibire<sup>ts</sup></i>	74



## Table of tables

Table 2.1 Enzymes	10
Table 2.2 Bacterial strains	13
Table 2.3 External plasmids	13
Table 2.4 Internal plasmids	14
Table 2.5 Personal plasmids	16
Table 2.6 Primer	18
Table 2.7 Crosses for lethality experiments	23
Table 2.8 Genotypes corresponding to Figure 3.15 on p. 59	24
Table 2.9 Genotypes corresponding to Figure 3.20 on p. 68 and Figure 3.22 on p. 71	24
Table 2.10 Genotypes corresponding to Figure 3.21 on p. 69	24
Table 2.11 Genotypes corresponding to Figure 3.23 on p. 72	24
Table 2.12 Genotypes corresponding to Figure 3.24 on p. 74	25
Table 3.1 GC-content and codon adaption of different CNT cDNA variants	41
Table 3.2 SNARE protein and fragment molecular weight	48
Table 3.3 Success of Injection	53
Table 3.4 Lethal effect of <i>UAS-Cre</i> dependent <i>UAS-BoNT-F</i> expression	57
Table 3.5 Overview on BoNT <i>in vitro</i> cleavage, transgenesis and induced lethality	58

# 1 Introduction

## 1.1 Clostridial neurotoxins and the SNARE apparatus

In the course of evolution a great variety of species have developed toxins in order to increase their chance of survival. Taken into account the crucial role of neuronal cells in mediating animal behavior, neuronal structures are common targets of toxins. Since many of these neurotoxins interfere highly specifically with well defined molecular processes, they can be employed to analyze neuronal physiology. This way, neurotoxins have contributed to a variety of fundamental discoveries in neuroscience (Adams and Olivera, 1994).

Bacteria of the species *Clostridia* host 8 structurally closely related neurotoxins: Tetanus toxin (TNT) and the seven different botulinum toxin types (BoNT-A, -B, -C, -D, -E, -F and -G). The extracellular active forms of these clostridial neurotoxins (CNTs) are composed of two components, a light and a heavy chain (Figure 1.1, A). Specific binding of the heavy chain component to either motoneurons (in the case of botulinum toxins) or inhibitory neurons (in the case of tetanus toxin) leads to dissemination of the dichain toxin and translocation of the light chain into the intracellular presynaptic compartment. The light chain then acts as a specific protease cleaving presynaptic proteins with high specificity, leading to disruption of neurotransmitter release (Schiavo et al., 2000 for review).

CNTs have been used in various model organisms as pharmacological tools or expressible transgenes to study the physiology of neurotransmitter release or to functionally block specific neuronal subsets in order to assess their involvement in network function (Sakaba et al., 2005; Neuser et al., 2008)

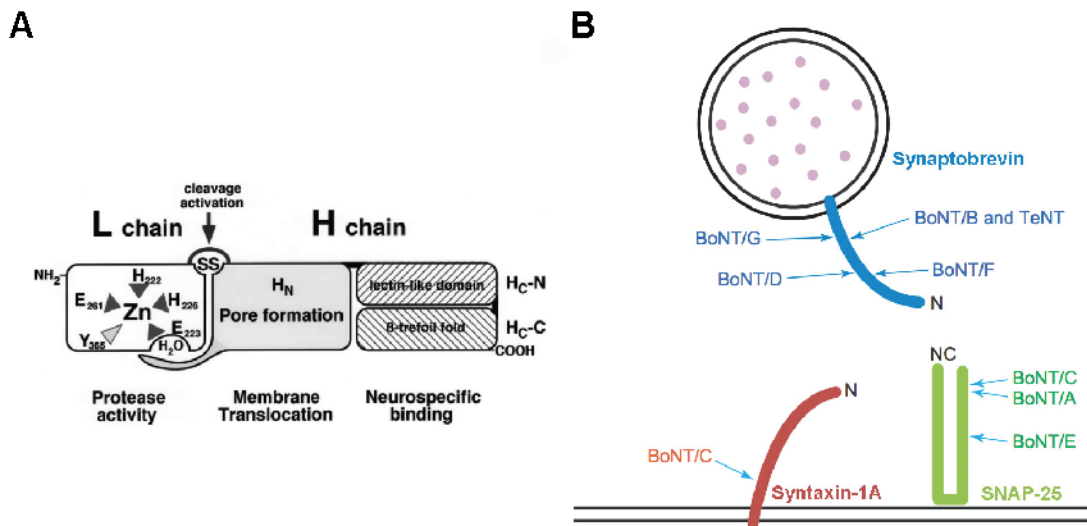


**Figure 1.1 Clostridial neurotoxins and the SNARE complex**

**A:** Common structure of all CNTs, from Schiavo et al., 2000. The extracellular active forms of these clostridial neurotoxins (CNTs) are composed of two components, a light and a heavy chain **B:** SNARE complex and cleavage sites of CNTs, modified from Breidenbach and Brunger, 2005. Synaptobrevin is vesicle-bound whereas Syntaxin-1A and SNAP-25 are associated with the presynaptic plasma membrane. “N” and “C” specify the respective N- and C-terminal.

Ca<sup>2+</sup>-triggered exocytosis of neurotransmitter containing vesicles takes place at the active zone, an electron-dense structure at the presynaptic plasma membrane. It is preceded by a complex cascade including accumulation of neurotransmitter into vesicles and directing the vesicles to the point of release in proximity to voltage gated Ca<sup>2+</sup>-channels. After exocytosis, vesicles are recycled by endocytosis in order to maintain ongoing neurotransmitter release. The molecular processes underlying this presynaptic “cycling” of vesicles involve complex and dynamically changing protein-protein interactions and as many details remain unclear to date, are under ongoing investigation (Südhof, 2012).

One of the presynaptic key players involved in these processes that has been identified and studied to a great extent is the SNARE (soluble N-Ethylmaleinimide-sensitive-factor attachment receptor) apparatus. It is composed of three components: the v-SNARE Synaptobrevin (n-Syb), which resides on the vesicular membrane and the t-SNAREs Syntaxin (Syx) and SNAP-25, which are associated with the presynaptic plasma membrane. Upon elevation of the presynaptic Ca<sup>2+</sup> concentration, these proteins form a dense complex that pulls the vesicle

membrane to the plasma membrane initiating fusion of the two lipid bilayers (Chen and Scheller, 2001; Bruns and Jahn, 2002). Accordingly, exocytosis of the vesicle content occurs. In addition to their widely studied role in neuroexocytosis, SNARE protein isoforms are also involved in non-neuronal vesicular secretion and membrane trafficking (DiAntonio et al., 1993; McMahon et al., 1993; Schulze et al., 1995).

All CNT light chains exert their toxic effect by cleaving parts of the SNARE apparatus, but differ in terms of their target recognition and cleavage sites. Whereas TNT, BoNT-B, -D, -F and -G cleave neuronal Synaptobrevin, BoNT-A and BoNT-E act on SNAP-25 and BoNT-C exerts a dual specificity for SNAP-25 and Syntaxin-1a (Figure 1.1, B). These distinct molecular target sites cause specific effects on synaptic properties during the decay of synaptic function. For instance, a study that made use of toxin injection into the calyx of Held discovered that BoNT-A mediated SNAP-25 cleavage primarily reduces the  $Ca^{2+}$  sensitivity of neurotransmitter containing vesicles (Sakaba et al., 2005). The same study showed that TNT mediated Synaptobrevin cleavage seems to modify the coupling of release competent vesicles to  $Ca^{2+}$ -channels, whereas BoNT-C mediated Syntaxin cleavage neither seems to effect the sensitivity to  $Ca^{2+}$  nor the coupling to  $Ca^{2+}$ -channels of remaining release competent vesicles. Other studies on *Crayfish* motoneurons could show that although BoNT-B and TNT cleave neuronal Synaptobrevin at the identical peptide bond, their effectivity in blocking neurotransmitter release varies greatly depending on the activity state of the synapse (Hua and Charlton, 1999; Prashad and Charlton, 2014): TNT mediated SNARE cleavage depends on ongoing neurotransmitter release, whereas BoNT-B cleaves its substrate independent of synaptic activity. The base for these different properties are differently located CNT binding sites on neuronal Synaptobrevin. At inactive synapses, the SNARE complex is tightly zippered exposing only the binding site for BoNT-B, but not for TNT (Hua et al., 1998). As these studies exemplify, comparison of the distinct effects of different CNTs can provide valuable insight into the molecular processes governing neurotransmitter release.

## 1.2 The *GAL4/UAS*-system in *Drosophila melanogaster*

Tissue- and cell-specific expression of effector proteins, used to precisely alter and report cell functions, as well as to visualize cell types can be conveniently conducted in *Drosophila melanogaster* using the *GAL4/UAS*-system (Brand and Perrimon, 1993). In this yeast-derived binary expression system, a gene encoding the yeast transcriptional activator GAL4 and its binding site *UAS* (*upstream activated sequence*) are inserted either randomly (Brand and Perrimon, 1993) or via site specific integration (Pfeiffer et al., 2010) into the *Drosophila* genome. The “driver line” carrying the *GAL4*-transcription factor downstream to a tissue specific enhancer, encodes “where” a protein is expressed. The “reporter line” carrying the *UAS*-promoter upstream of an effector gene, encodes “what” is expressed in the *GAL4* positive cells. After crossing these two lines, the GAL4 is tissue-specifically expressed and thus promotes transgene expression after binding at *UAS* only in *GAL4* positive cell types (Figure 1.2, A). After establishment of this system in 1993, multiple large stock collections (i.e. Jenett et al., 2012) have been generated that contain specific *GAL4*-lines for nearly every cell-type in *Drosophila*. Many *GAL4*-lines promote transgene expression throughout different developmental stages in various tissue- and cell-types. Thus it is difficult to examine effects of transgenes restricted to a specific developmental stage and cell type. This problem can be circumvented by usage of the heat sensitive *tub-GAL80<sup>ts</sup>* construct (McGuire et al., 2003; Figure 1.2, B) that blocks GAL4 activity at restrictive temperatures (18 °C) and allows effector gene expression only at the permissive temperature (31 °C).

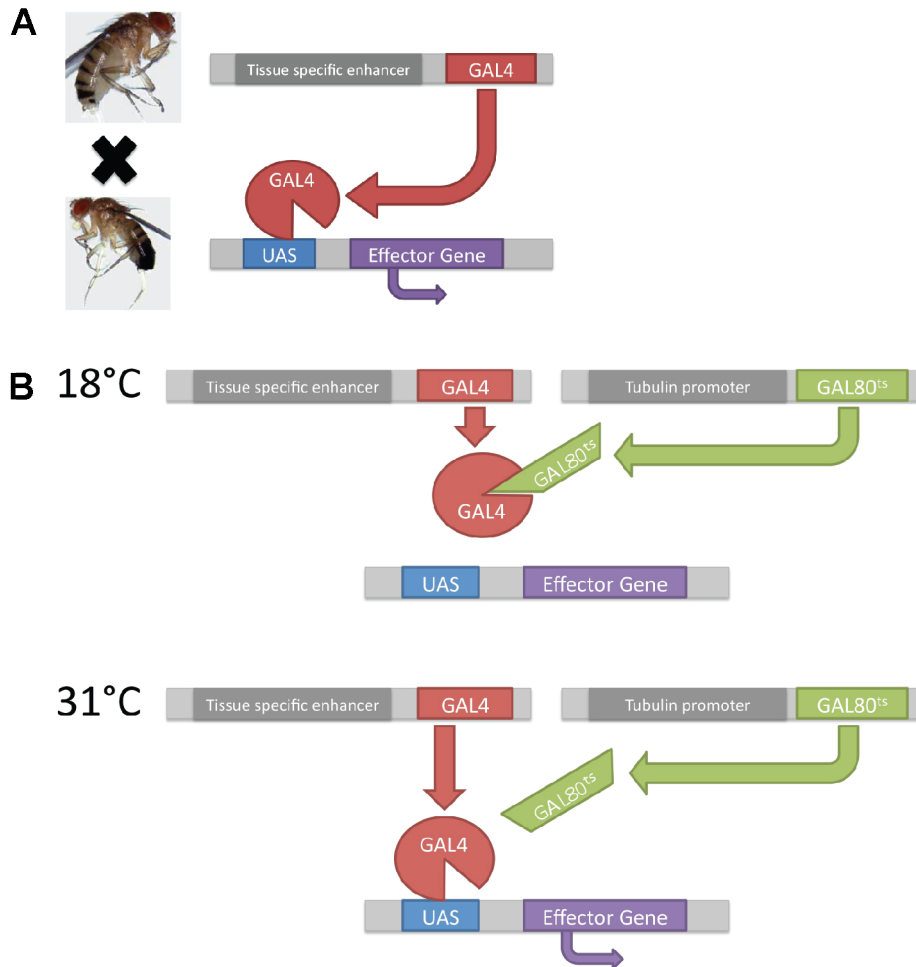


### Figure 1.2 *GAL4/UAS*-system

**A:** Scheme of the *GAL4/UAS*-system. Crossing of a *GAL4*-line to an *UAS*-line leads to tissue-specific *GAL4*-binding to *UAS* and consequently to tissue-specific gene expression. **B:** Temperature dependent conformational changes confine the ability of *GAL80<sup>ts</sup>* to inhibit *GAL4* binding to low “restrictive” temperatures.

### 1.3 Effector genes in *Drosophila melanogaster*

By use of the *GAL4/UAS*-system a variety of different effector genes can be expressed in *Drosophila* that at a broad spectrum of specificity either interfere with general neuronal / cell function or specific neuronal processes. For instance the gene *reaper* induces cell lethality by activating apoptosis in neuronal and non-neuronal cells (White et al., 1996) whereas the mutated Diphtheria toxin A-chain DTI executes its lethal effects by unspecifically blocking protein synthesis (Han et al., 2000).

One prominent example for a neuron-specific effector is the heat-sensitive *dynammin*-mutant *shibire<sup>ts</sup>*. At low “permissive” temperatures (18 °C) the transgene-product acts as the wild type Dynamin, promoting endocytosis. After elevation to the “restrictive” temperature (31 °C), the protein undergoes a conformational change leading to a block of endocytosis and a resulting subsequent block of exocytosis (Kitamoto, 2001), which is rapidly reversible after switching back to the permissive temperature.

The *clostridial* neurotoxin TNT (Sweeney et al., 1995) acts by proteolysing neuronal Synaptobrevin and thus directly targets a molecule crucial for neuroexocytosis. It is so far the only CNT available as an effector gene in *Drosophila* and *UAS-TNT* has been successfully used in *Drosophila* in a multitude of studies to silence groups of neurons in order to identify their role in network function (i.e. Neuser et al., 2008; Umezaki et al., 2011)

#### **1.4 CNTs fail to disrupt neuroexocytosis in specific cell types**

Despite the many examples of potent application of *UAS-TNT*, it appears ineffective in blocking neurotransmitter release in specific *Drosophila* cell types such as mushroom body neurons (Thum et al., 2006) and lamina monopolar neurons (Zhu et al., 2009). Ineffectiveness has also been reported in photoreceptor cells, as *UAS-TNT* expression did not lead to a loss of photoreceptor synaptic activity and vision dependent behavior (Rister and Heisenberg, 2006). As the authors mentioned, this ineffectiveness could be based on the following two hypotheses: n-Syb might be protected from cleavage by Calmodulin, a protein that binds to n-Syb overlapping with the cleavage site for TNT and BoNT-B (Figure 3.1, De Haro et al., 2003). Alternatively, neurotransmitter release could work independent of n-Syb in *Drosophila* photoreceptors. A similar specific lack of CNTs to disrupt neurotransmitter release has been reported in mice: A recent study found that neither BoNT-C, -D nor -E interfere with mouse inner hair cell neuroexocytosis after toxin injection via the patch pipette. The authors concluded that inner hair cell “exocytosis is unconventional and may operate independently of neuronal SNAREs” (Nouvian et al., 2011). Interestingly, *Drosophila* photoreceptor cells and

mouse inner hair cells share some common features, as both do not exhibit action potentials but transmit vesicles as a direct function of stimulus input. In addition, both are involved in transmitting high frequency stimuli and flies possess a manifold higher optical temporal resolution than for example humans. Thus, testing whether CNTs other than TNT are effective in interfering with *Drosophila* photoreceptor function could help to identify the molecular basis for the insensitivity to TNT and to reveal the proteinbox of the vesicle release machinery in different cell types. Accordingly, botulinum toxins might provide effective alternatives for silencing neuronal cells where *UAS-TNT* is ineffective.

### **1.5 The visual system of *Drosophila melanogaster***

Just as it is common in all insects the *Drosophila* retina is composed of multiple repetitive elements called ommatidia. In *Drosophila melanogaster* every ommatidium contains one of each of the 8 different photoreceptor cell types R1-R8 that propagate and transmit their signals into the optic lobes (Figure 1.3, A). Phototransduction (the transduction of an electromagnetic wave into an intracellular electric signal) takes place inside the rhabdomere of photoreceptors. The process is mediated by a complex molecular cascade that is initiated by a conformational change of the protein Rhodopsin upon absorption of a photon that finally leads to depolarization of the cell after the opening of Ca<sup>2+</sup>-channels. Although phototransduction of insects and vertebrates share a lot of similarities, some fundamental differences exist. (1) Whereas vertebrate photoreceptor cells hyperpolarize upon illumination, insect photoreceptors depolarize as response to photons. (2) Insects as flies can putatively discriminate between single “images” a lot faster than vertebrates. Whereas humans cannot discriminate between single images on a regular television-program running with < 50 hz, some insects can generate distinct electrical responses in their photoreceptors to changing visual stimuli up to 300 Hz (see Borst, 2009 for review).



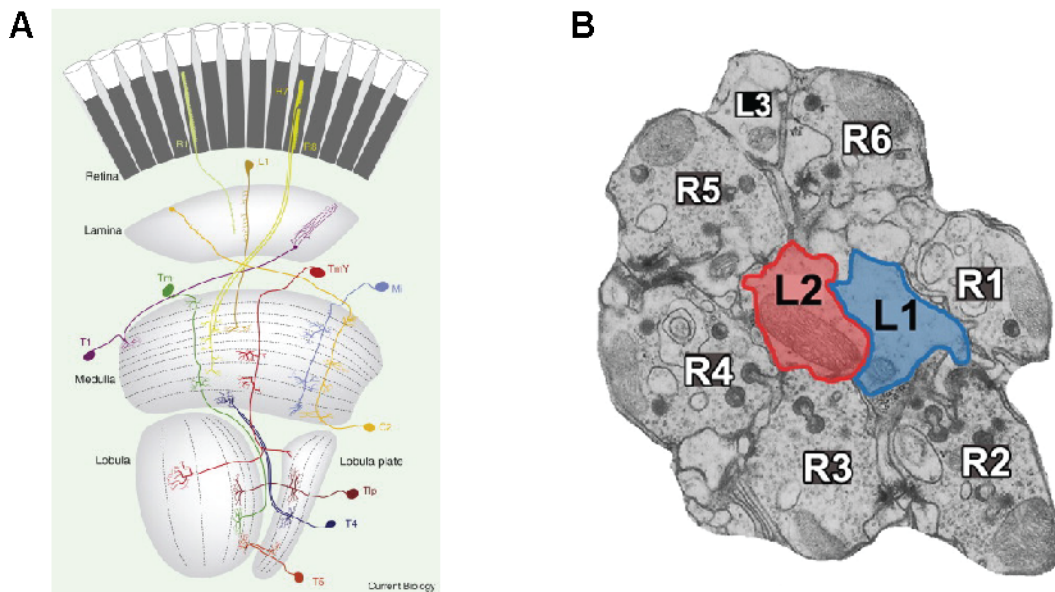


### Figure 1.3 Overview on anatomy of the fly visual system

**A:** Scheme of propagation of different photoreceptors and neurons through the *Drosophila* retina and optic lobes, taken from Borst, 2009. **B:** Electron microscopy cross-section through a lamina “cartridge” showing photoreceptors R1-R6 surrounding Lamina monopolar neurons L1 and L2, taken from Rister et al., 2007.

Of the 8 photoreceptor subtypes, only R1-R6 are involved in motion vision and transfer their signal via histaminergic synapses onto the Lamina monopolar cells L1-L3 (Figure 1.3, B). The photoreceptor cells and the Lamina monopolar cells are part of a neuronal circuitry that drives a fundamental behavioural reflex in flies: the optomotor response (OMR). As the world moves, flies try to follow the movement syndirectionally, thus trying to stabilize their gaze. This behaviour can be assessed by measuring head or body movement during flight or walking and has been examined in this study using a behavioural setup known as the “Buchner-ball-apparatus” (Buchner, 1976), where a tethered fly is walking on a Styrofoam ball that is floating on an air stream.

## 1.6 Project summary

We generated transgenic *UAS-BoNT* flies that allow for expression of different botulinum toxin light chains. This way, CNTs can be conveniently combined with various other genetic manipulations including gene knock-outs, RNAi mediated cell-specific expression knock-downs (Dietzl et al., 2007) or specific mutations of

proteins that interact with the SNARE apparatus to further gather insight into the complex molecular interactions of presynaptic proteins. We performed biochemical assays to assess the susceptibility of *Drosophila* SNARE to BoNT-mediated proteolysis. Further, we analyzed the facility of BoNTs to induce lethality after expression in neuronal and non-neuronal cells and quantified the impact of induced toxin expression on larval motor behavior. To evaluate the influence of these toxins in the visual system of adult *Drosophila melanogaster*, we built up a behavioral setup allowing the measurement of flies' optomotor response. After evaluation of the setup, we assessed the ability of the newly generated toxins to interfere with visually induced motion behavior after expression in the "TNT-insensitive" photoreceptors.

## 2 Methods

### 2.1 Materials

All chemicals were, if not specified otherwise, purchased from Roth (Karlsruhe), Sigma (Diesenhofen) or Merck (Darmstadt). All oligonucleotides were synthesized by Eurofins MWG (Ebersberg). All molecular biology kits used for DNA extraction and purification were obtained from Qiagen (Hilden) or Macherey-Nagel (Dueren). All PCRs were performed with the Thermocycler T3, T3000 (Biometra, Göttingen).

#### 2.1.1 Enzymes

Enzyme	Supplier
Various restriction enzymes	NEB (Frankfurt)
Accustar Polymerase	Eurogentec (Belgium)
MasterMix	NEB (Frankfurt)
T4-Ligase	Roche (Mannheim)
LR-Clonase Enzyme-mix	Invitrogen (USA)
Proteinase K	Invitrogen (USA)
Cre-recombinase	NEB (Frankfurt)

**Table 2.1 Enzymes**

#### 2.1.2 Buffers and media

<i>Drosophila</i> food medium	1 l H <sub>2</sub> O 4.5 g agar 20 g sugar beet syrup 72.2 g malt 16.6 g yeast 9 g soybean meal 72.2 g cornmeal 1.45 g methylparaben 5.7 g propionic acid
LB medium	20 g of LB Broth Base ad 1 l dH <sub>2</sub> O autoclave
LB plates	20 g of LB Broth Base

	<p>15 g of Agar-Agar  ad 1 l d H<sub>2</sub>O  adjust pH to 7.5  autoclave  cool to 50 °C  add antibiotics  pour into Petri dishes  store at 4 °C</p>
Loading buffer (6x)	<p>2.5 ml of bromphenol blue (1 %)  3 ml of glycerol  ad 10 ml d H<sub>2</sub>O</p>
TAE (50x)	<p>2 M Tris-Base  50 mM EDTA, pH 8.0  57.1 ml of glacial acetic acid (100 %)  ad 1 l d H<sub>2</sub>O</p>
Agarose gels	<p>1 x TAE + 0.5-1 % Agarose</p>
Laemmli buffer (2x)	<p>4 % SDS  10 % 2-mercaptoethanol  20 % glycerol  0,004 % bromophenol blue  0.125 M Tris HCl  adjust to pH 6.8</p>
Denaturing RIPA-buffer	<p>150 mM NaCl  10 mM TrisBase (pH 7.4)  1 % (w/w) Nonidet P-40  0.1 % SDS  1 % (w/v) Na-Deoxycholate  0.1 % Triton X-100  Protease Inhibition Cocktail  (P8340-1ML, Sigma)  1 mM EDTA (372 mg/l)  184 mg/l Na-Orthovanadate  1 mM NaF</p>
1,5M TrisHCl, pH 8,8	<p>18.15 g TrisBase/100 ml H<sub>2</sub>O  adjust to pH 8.8 with 6N HCl  store at 4 °C</p>
0,5M TrisHCl, pH 6,8	<p>6 g Tris base/100ml H<sub>2</sub>O  adjust to pH 6.8 with 6N HCl  store at 4 °C</p>

Electrode (Running) Buffer, pH 8,3	3.03 g TrisBase 14.4 g glycine 1 g SDS ad 1 l d H <sub>2</sub> O store at 4 °C
Blottin-/Towbin-Buffer	3,03 g TrisBase 14.4 g glycine 200 ml MetOH ad 1 l d H <sub>2</sub> O
TBS-T	2.42 g TrisBase 8 g NaCl Adjust to pH 7.6 with 30 % HCL (for 10x) ad 1 l d H <sub>2</sub> O 1 ml Tween 20
Resolving Gel (15%)	2.4 ml d H <sub>2</sub> O 5 ml 30 % Acrylamid/Bis (Rotiphorese Gel 30) 2.5 ml 1.5 M TrisHCL pH 8.8 100 µl 10 % SDS 50 µl 10 % Ammonium persulfate 5 µl Temed (Tetramethylethylenediamine)
Stacking Gel (5 %)	5.7 ml d H <sub>2</sub> O 1.7 ml 30 % Acrylamid/Bis (Rotiphorese Gel 30) 2.5 ml 0.5 M TrisHCL pH 6.8 100 µl 10 % SDS 50 µl 10 % Ammonium persulfate 10 µl Temed (Tetramethylethylenediamine)
Stripping Buffer	20 ml SDS 10 % 12.5 ml TrisHCL 6.8 0.8 ml 2-Mercaptoethanol

### 2.1.3 Stock solution

Ampicillin	50 mg/ml in H <sub>2</sub> O
Chloramphenicol	12.5 mg/ml in H <sub>2</sub> O
Kanamycin	10 mg/ml in H <sub>2</sub> O

## 2.1.4 Size marker

Hyper Ladder  
ColorPlus 7709s

Bioline, Luckenwalde  
Invitrogen

## 2.1.5 Bacterial strains

Strain	Manufacturer	Genotype
<i>XL1-blue</i>	Stratagene	<i>RecA1 endA1 gyrA96 thi-1 hsdR17 supE44 relA1 lac [F'proAB laqqZDM15 TN10 (Tet<sup>r</sup>)]</i>
<i>DB 3.1</i>	Invitrogen	<i>F-gyrA462 endA1 Δ(sr!-recA) mcrB mrr hsdS20(rB-, mB-) supE44 ara-14 galK2 lacY1 proA2 rpsL20(SmR) xyl-5 λ-leu mtl 1</i>

**Table 2.2 Bacterial strains**

## 2.1.6 Plasmids

Plasmid	Purchased at / provided by	Description
<i>GH28821 (pPB23)</i>	DGRC (Bloomington)	cDNA of <i>Dm</i> SNAP-25
<i>pPB2</i>	GeneArt® (California)	Synthetic cDNA of BoNT-A light chain modified by GeneOptimizer® software
<i>pPB3</i>	GeneArt® (California)	Synthetic cDNA of BoNT-B light chain modified by GeneOptimizer® software
<i>pPB4</i>	GeneArt® (California)	Synthetic cDNA of BoNT-C light chain modified by GeneOptimizer® software
<i>pPB5</i>	GeneArt® (California)	Synthetic cDNA of BoNT-F light chain modified by GeneOptimizer® software
<i>pPB6</i>	GeneArt® (California)	Synthetic cDNA of BoNT-G light chain modified by GeneOptimizer® software
<i>pPB42</i>	GeneArt® (California)	Synthetic cDNA of BoNT-D light chain modified by GeneOptimizer® software
<i>pJFRC7-20XUAS-IVS-mCD8-GFP</i>	(Pfeiffer et al., 2010)	Vector containing 20 x <i>UAS</i>
<i>pSB2 (pPB34)</i>	T. Binz (Hannover)	<i>Rattus norvegicus</i> <i>VAMP2</i>
<i>PSP37 (pPB36)</i>	T. Binz (Hannover)	<i>Rn</i> <i>SNAP-25</i>
<i>pHPC1A (pPB37)</i>	T. Binz (Hannover)	<i>Rn</i> <i>Syntaxin1A</i>

**Table 2.3 External plasmids**

Plasmid	Constructed by	Description
<i>pTL140</i>	T. Langenhan	<i>Dm-n-syb</i> cDNA inserted in <i>pENTR1ADual</i>
<i>pTL146</i>	T. Langenhan	<i>Dm-syx</i> cDNA inserted in <i>pENTR1ADual</i>
<i>pTL148</i>	T. Langenhan	<i>pUAST::Venus-4xGGSlinker-syx</i>
<i>pTL152</i>	T. Langenhan	<i>pUAST::n-syb-A5linker-RFP</i>
<i>pNH27</i>	N. Hartmann	<i>amCFP</i> in <i>pENTR-3C</i>
<i>pNH28</i>	N. Hartmann	<i>amCFP::5G::Brp17AA-Stop-3C</i>
<i>pNH42</i>	N. Hartmann	<i>UAS-mCD8::EGFP::Stop</i>
<i>pENTR1ADual</i>	Invitrogen	Gateway® entry vector
<i>pAWF</i>	Murphy LAB	Gateway® destination vector: <i>Actin5C</i> -promotor, Gateway cassette, 3 x <i>Flag</i>
<i>pTVW</i>	Murphy LAB	Gateway® destination plasmid: <i>UAS</i> -promotor, Gateway cassette, Venus
<i>pTWF</i>	Murphy LAB	Gateway® destination plasmid: <i>UAS</i> -promotor, Gateway cassette, 3 x <i>Flag</i>
<i>pBPGAL4.2::p65Uw</i>	origin not available	Contains <i>GAL4</i>
	origin not available	Contains <i>GAL4</i> under <i>Actin</i> -promotor control
<i>pTWH-attB</i>	(Bischof et al., 2007)	Contains <i>phiC31 attB</i>

**Table 2.4 Internal plasmids**

Plasmid	Content	Method of Construction
<i>pPB1</i>	Intermediate product	PCR from <i>pAWF</i> with <i>tL_346F</i> and <i>tL_347R</i> -> 02. Digest of 02 and <i>pJFRC7-20XUAS-IVS-mCD8-GFP</i> with <i>AscI</i> and <i>HindIII</i> and ligation of the products-> 03. PCR from <i>pTWF</i> with <i>tL_348F</i> and <i>tL_349R</i> ->04. Digest of 04 with <i>AvrII</i> and <i>XhoI</i> and Digest of 03 with <i>XhoI</i> and <i>XbaI</i> -> Ligation
<i>pPB7</i>	<i>BoNT-A</i> in <i>pENTR1ADual</i>	<i>pPB2</i> was digested with <i>XhoI</i> and <i>EcoRV</i> and ligated into <i>pENTR1ADual</i> after digestion with <i>XhoI</i> and <i>DraI</i> .
<i>pPB8</i>	<i>BoNT-B</i> in <i>pENTR1ADual</i>	<i>pPB3</i> was digested with <i>XhoI</i> and <i>EcoRV</i> and ligated into <i>pENTR1ADual</i> after digestion with <i>XhoI</i> and <i>DraI</i> .
<i>pPB9</i>	<i>BoNT-C</i> in	<i>pPB4</i> was digested with <i>Sall</i> and <i>EcoRV</i> and

	<i>pENTR1ADual</i>	ligated into <i>pENTR1ADual</i> after digestion with <i>XhoI</i> and <i>DraI</i> .
<i>pPB10</i>	<i>BoNT-F</i> in <i>pENTR1ADual</i>	<i>pPB5</i> was digested with <i>XhoI</i> and <i>EcoRV</i> and ligated into <i>pENTR1ADual</i> after digestion with <i>XhoI</i> and <i>DraI</i> .
<i>pPB11</i>	<i>BoNT-G</i> in <i>pENTR1ADual</i>	<i>pPB6</i> was digested with <i>XhoI</i> and <i>EcoRV</i> and ligated into <i>pENTR1ADual</i> after digestion with <i>XhoI</i> and <i>DraI</i> .
<i>pPB12</i>	Dest. Vector with <i>PhiC31</i> recombination side and C-terminal 3x <i>flag-tag</i>	Both, <i>pTWH-attB</i> and <i>pPB1</i> were digested with <i>NotI-HF</i> and <i>AgeI-HF</i> and ligated after phosphoralisation of the <i>pTWH-attB</i> -digest.
<i>pPB13</i>	<i>BoNT-A</i> in <i>pPB12</i>	LR <i>pPB12</i> and <i>pPB7</i>
<i>pPB14</i>	<i>BoNT-B</i> in <i>pPB12</i>	LR <i>pPB12</i> and <i>pPB8</i>
<i>pPB15</i>	<i>BoNT-C</i> in <i>pPB12</i>	LR <i>pPB12</i> and <i>pPB9</i>
<i>pPB16</i>	<i>BoNT-F</i> in <i>pPB12</i>	LR <i>pPB12</i> and <i>pPB10</i>
<i>pPB17</i>	<i>BoNT-G</i> in <i>pPB12</i>	LR <i>pPB12</i> and <i>pPB11</i>
<i>pPB18</i>	Dest. Vector: Contains LR side with 20X Codon-optimized UAS, C-Terminal 3 x <i>Flag-tag</i> , rev. comp. <i>Actin-GAL4</i> .	PCR of <i>pBPGAL4.2::p65Uw</i> with <i>pb_19F</i> and <i>pb_20R</i> ->Digest with <i>PvuII</i> and <i>Ascl</i> . Digest of <i>pPB1</i> with <i>Ascl</i> and <i>EcoRV</i> ->Ligation
<i>pPB19</i>	<i>Dm-SNAP-25</i> in <i>pENTR1ADual</i>	PCR from <i>GH28821</i> with <i>pb_21F</i> and <i>pb_22R</i> . Ligation with <i>pENTR1ADual</i> after digest with <i>XhoI</i> and <i>DraI</i> .
<i>pPB20</i>	UAS-LR-side with N-terminal V5- and C-terminal <i>HA-tag</i>	PCR from <i>pTWH_attB</i> with <i>pb_23F</i> and <i>pb_24R</i> . Digest from PCR product and <i>pTWH_attB</i> with <i>NotI</i> and <i>BglII</i> ->Ligation
<i>pPB21</i>	<i>CFP</i> in <i>pPB18</i>	LR from <i>pNH27</i> and <i>pPB18</i>
<i>pPB22</i>	<i>Dm-n-Syb</i> in <i>PPB20</i>	LR of <i>pPB20</i> and <i>PTL140</i>
<i>pPB24</i>	<i>BoNT-A</i> in <i>pPB18</i>	LR <i>pPB7</i> X <i>pPB18</i>
<i>pPB25</i>	<i>BoNT-B</i> in <i>pPB18</i>	LR <i>pPB8</i> X <i>pPB18</i>
<i>pPB26</i>	<i>BoNT-C</i> in <i>pPB18</i>	LR <i>pPB9</i> X <i>pPB18</i>
<i>pPB27</i>	<i>BoNT-F</i> in <i>pPB18</i>	LR <i>pPB10</i> X <i>pPB18</i>
<i>pPB28</i>	<i>BoNT-G</i> in <i>pPB18</i>	LR <i>pPB11</i> X <i>pPB18</i>
<i>pPB29</i>	<i>Dm syntaxin-1A</i> in <i>pPB20</i>	LR <i>pTL146</i> X <i>pPB20</i>
<i>pPB30</i>	<i>Dm SNAP-25</i> in <i>pPB20</i>	<i>pPB19</i> X <i>pPB20</i>
<i>pPB31</i>	<i>Rattus norvegicus VAMP2</i> in <i>pENTR1ADual</i>	PCR of <i>pSB2</i> with <i>pb_27F</i> and <i>pb_28R</i> was digested with <i>EcoRV-HF</i> and <i>XhoI</i> and ligated with <i>pENTR1ADual</i> after digest with <i>DraI</i> and <i>XhoI</i>



pPB32	<i>Rattus norvegicus</i> Syntaxin-1A in pENTR1ADual	PCR of pHPC1A with pb_29F and pb_30R was digested with EcoRV-HF and XhoI and ligated with pENTR1ADual after digest with DraI and XhoI
pPB33	<i>Rattus norvegicus</i> SNAP-25 in pENTR1ADual	PCR of pSP37 with pb_25F and pb_26R was digested with EcoRV-HF and XhoI and ligated with pENTR1ADual after digest with DraI and XhoI
pPB37	<i>Rattus norvegicus</i> VAMP-2 in pPB20	LR pPB31 with pPB20
pPB38	<i>Rattus norvegicus</i> syntaxin-1A in pPB20	LR pPB32 with pPB20
pPB39	<i>Rattus norvegicus</i> SNAP-25 in pPB20	LR pPB33 with pPB20
pPB40	BoNT-B in pTWF	LR pTWF with pPB8
pPB41	BoNT-F in pTWF	LR pTWF with pPB10
pPB43	BoNT-F in pENTR1ADual (Intermediate product)	PCR of pPB10 with pb_31F and pb_32R was digested with BssHII and XhoI and ligated with pENTR1ADual after digest with BssHII and XhoI
pPB44	WT Dm syx-1a_Stop	PCR of pPB29 with pb_35F and pb_36R was digested with XhoI and EcoRV and ligated with pENTR1ADual after digest with XhoI and DraI
pPB48	Rat-SNAP-25_stop in pENTR1ADual	PCR of pPB33 with pb_25F and pb_42R was digested with EcoRV and XhoI and ligated with pENTR1ADual after digest with DraI and XhoI
pPB49	BoNT-D in pENTR1ADual	Digest of pPB42 with XhoI and EcoRV was ligated with pENTR1ADual after digest with XhoI and DraI
pPB50	LoxP_Venus_Stop_Lox P_BoNT-F	PCR of pTVWR with pb_33F and pb_34R was digested with BssHII and Sall and ligated to digest of pPB43 with BssHII and Sall
pPB51	LoxP_Venus_Stop_Lox P_BoNT-F in pTWF	LR pPB50 with pTWF
pPB52	LoxP_Venus_Stop_Lox P_BoNT-F in pPB18	LR pPB50 with pPB18
pPB53	Rat-SNAP-25_stop in pTWH-attB	LR pTWH-attB with pPB48
pPB54	BoNT-D in pTWF	LR pPB49 with pTWF
pPB55	BoNT-D in pPB18	LR pPB49 with pPB18
pPB56	LoxP_BoNT-F	pPB52 after <i>in vitro</i> Cre-Recombination

**Table 2.5 Personal plasmids**

## 2.1.7 Primer

Name	Sequence
<i>pb_1F</i>	acgcgctcgacatcaacatgccatttgtaataaacaattta
<i>pb_2R</i>	agatatccggccttattgtatcctttatcta
<i>pb_3F</i>	acgcgctcgacatcaacatgccagttacaataaataattta
<i>pb_4R</i>	agatatcctttaacacttttacacatttgatc
<i>pb_5F</i>	acgcgctcgacatcaacatgccaataacaattaacaactta
<i>pb_6R</i>	agatatcctttattatataatgatctaccatct
<i>pb_7F</i>	acgcgctcgacatcaacatgccagttgtaataaatagttta
<i>pb_8R</i>	agatatcctttctaggaataacgctcttaca
<i>pb_9F</i>	acgcgctcgacatcaacatgccagttaataaaaaactta
<i>pb_10R</i>	agatatccattttgtacattacaggctgcac
<i>pb_11R</i>	atagtttagcggccgcgcttaacacttttacacatttgatc
<i>pb_12R</i>	atagtttagcggccgcgcttattatataatgatctaccatct
<i>pb_13R</i>	atagtttagcggccgcgctttctaggaataacgctcttaca
<i>pb_14R</i>	atagtttagcggccgcgctttgtacattacaggctgcac
<i>pb_15F</i>	tagaatatagaattgcatgc
<i>pb_16F</i>	tatacacagccagtctgcag
<i>pb_19F</i>	acagctgaagcttgaagcaagcctcaatc
<i>pb_20R</i>	atggcgcgcctctagaactagtggatctaaac
<i>pb_21F</i>	tacacttttaaaatcaacatgccagcggatccatctgaaga
<i>pb_22R</i>	ccgctcgagcccttaatagttgatgtgccctt
<i>pb_23F</i>	acagatctatcaacatgggcaagccatcccaaccccctgctgggctggattccaccagatcgaca agttgtacaaa
<i>pb_24R</i>	atagtttagcggccgcatagtgactggatagtgtg
<i>pb_25F</i>	agatatcatcaacatggccgaggacgcagacat
<i>pb_26R</i>	ccgctcgagccaccacttcccagcatcttg
<i>pb_27F</i>	agatatcatcaacatgtcggctaccgctgccac
<i>pb_28R</i>	ccgctcgagccagagctgaagtaaacgatga
<i>pb_29F</i>	agatatcatcaacatgaaggaccgaaccagga
<i>pb_30R</i>	ccgctcgagcctcaaagatgccccgatgg
<i>pb_31F</i>	gaagcgcgcataacttcgtatagcatacattatacgaagtatccgctcgatcaacagcttc
<i>pb_32R</i>	tcttctcagggccttgcggggat
<i>pb_33F</i>	aaggctcgacatcaacatgataacttcgtatagcatacattatacgaagtatatatggtagcaagggcg agga
<i>pb_34R</i>	cttgcgcgcccctactgtacagctcgtccatgc

Name	Sequence
<i>pb_35F</i>	aagaagatatcatcaacatgactaaagacag
<i>pb_36R</i>	tcttctcgaggcctacatgaaataactgctaacat
<i>pb_42R</i>	ccgctcgagccctaaccacttcccagcatcttg
<i>pb_43F</i>	ccagataacagtatgctgattt

**Table 2.6 Primer**

## 2.2 Molecular biology

### 2.2.1 Synthesis of cDNA

cDNA for the light chains of botulinumtoxin A, B, C, D, F and G were synthesized by GeneArt®, Life Technologies®. GeneOptimizer® was used to adapt cDNA for expression in *Drosophila melanogaster*.

### 2.2.2 Sequencing

Sequencing was performed by Eurofins MWG. Primers and Plasmids for sequencing were provided according to company's instructions.

### 2.2.3 Cloning

Cloning from synthetic BoNT-A light chain into a vector for expression in *Drosophila* S2 cells is specified in example below. The illustrated methods were used for all other plasmids (Table 2.5). The Invitrogen Gateway® system was used for transferring inserts into different target plasmids.

#### ***Entry plasmid***

To create the *BoNT-A* Entry plasmid *pPB7*, two restriction digests were performed: 1 µg *pPB1* with *XhoI* and *EcoRV* and 2 µg *pENTR1ADual* with *XhoI* and *DraI*. Digests were always incubated for at least 3 hours at 37 °C. Fragments were separated in 1 % Agarose-Gel containing 7 µl Sybr® Safe at 100 V. The proper DNA bonds (1.4 kbp for *pPB1* and 2.2 kbp for *pENTR1ADual*) were cut out with a scalpel. DNA fragments were extracted using QIAGEN QIAEX® II Gel Extraction Kit (500) according to manufacturer's instructions. Ligation was performed at 16 °C over night. Ligation product was transformed into XL-Blue, plated on an agar plate

containing Kanamycin and incubated at 37 °C over night. Single colonies were picked and transferred into liquid medium and again incubated at 37 °C over night under constant agitation. DNA was prepared using MACHEREY-NAGEL NucleoSpin® Plasmid preparation kit according to manufacturer's instructions. Insert was sequenced for verification purposes, as was always done for inserts or elements that were modified or amplified via PCR (for some amplified segments that were not direct objects of investigation of this study, only functional testing was performed).

### ***Destination plasmid***

*pPB18* was constructed in 3 steps. Only the last step is specified here. PCR of *pBGAL4.2-P65UW* was performed as in section 2.2.4. Primers were *pB19F* and 20R. In this specific case, PFU polymerase was used. Fragments were separated, purified above. The whole purification yield was digested with *PvuII* and *AcsI* and again digested. Ligation was performed as above. Ligation product was transferred into *DB 3.1* bacteria and plated on agar containing Chloramphenicol and Ampicillin. Harvest and purification was done as above.

### ***LR-Reaction***

To insert the BoNT-A light chain cDNA of *pPB7* into *pPB18*, an Invitrogen Gateway® LR-reaction was performed. Reaction preparation was composed of 5 µl in total and contained 150 ng/µl of *pPB18*. Equal molecular amount of *pPB7* and 1 µl LR Clonase was added. Incubation was done at 25 °C for 1 hour. Then 1 µl of Proteinase K was added to the solution and incubated at 37 °C for 10 minutes. Product was transformed, plated and purified as above.

### **2.2.4 PCR**

Biometra® T3 Thermocycler was used for PCR. Preparation of 50 µl containing 1 µl of each primer, 2 µl template, 1 µl dNTP and 0.5 µl Accustar Polymerase was used, standard protocol was:

2 min 94 °C

25 x 30 sec 94 °C

30 sec 55 °C

1 min / 1 kbp PCR fragment size 68 °C

10 min 72 °C

For a list of primers, see Table 2.6 on page 18.

## **2.3 S2 cell culture**

### **2.3.1 Handling**

*Drosophila* S2 cells (Invitrogen, #R690-07) were held at 27 °C and regularly split every 3-4 days. Cells were raised in Schneider's *Drosophila* medium (R69007, ThermoFisher Scientific) + 10 % fetal calf serum (Biochrom) in 50 ml culture flasks (Cellstar).

### **2.3.2 Transfection**

Cells were disseminated on 24-well multidishes (Nunclon). For imaging, cells were raised on coverslips placed in the wells. S2 cells were transfected in accordance with the appropriate transfection protocol of Invitrogen using Lipofectamine 2000 (Invitrogen, #11668027). Used DNA concentrations were modified in order to transfect with equal plasmid quantities. If transfected plasmids did not contain *GAL4*, *Actin-5C-GAL4* plasmid was added in equal quantity. After transfection, cells were incubated for additional 48 hours at 27 °C for imaging or 31 °C for western blots.

## **2.4 Western blots**

### **2.4.1 Preparation of protein**

After incubation at 31 °C for 48 hours, cells were washed with ice-cold PBS and then continuously kept on ice. Cells were harvested with ice-cold PBS and centrifuged for 5 min at 380 g (2000 rpm) at 4 °C (BIOFUGE 15). After removal of the supernatant, the palled was lysed in 30 µl of denaturing RIPA-buffer

containing 1:1000 anti-proteases cocktail (P8340-1ML, Sigma-Aldrich) and centrifuged with 6081 g (8000 rpm) for 10 min at 4 °C. 3 µl - 10 µl of the supernatant containing the proteins were used for western blots.

### **2.4.2 Blotting and immunostaining**

Protein was transferred into Laemmli-buffer, denaturated at 65 °C for 10 minutes and loaded into wells of a two-sectioned polyacrylamide gel. At first, the proteins were collected in the section containing 5 % acrylamide (“stacking gel”) at 80 V for about 1 hour. After the front had reached the 2<sup>nd</sup> section of the polyacrylamide gel that contained 15 % acrylamide (“resolving gel”), voltage was switched to 120 V for another 80 minutes. The marker was Colorplus 7709s (Invitrogen). Western blotting was performed with 0.35 A for 30 min onto a polyvinylidene fluoride membrane (Immobilon-P, Merck Millipore). All electrophoresis steps were performed at 4 °C. Membranes were blocked with TBST + 4 % milk powder for 1 hour. Incubation with the first antibody was performed overnight at 4 °C in TBST + 4 % milk powder with mouse anti-V5 (for SNAP-25, 1:5000, monoclonal, Invitrogen #R960-25) or mouse anti-HA (1:2500 for n-syb + BoNT-D or 1:5000 for remaining blots, monoclonal, Covance HA.11 Clone 16B12). Blots were subsequently washed with TBST 5 times at room temperature and incubated with secondary goat anti-mouse HRP conjugated antibodies (1:2500, polyclonal, Dianova #115-035-166) for 2 hours at room temperature. After development of the first immunoreaction, blots were stripped for 25 min at 60°C with stripping solution, washed with TBST and incubated with primary mouse anti-beta-tubulin antibody for BoNT-D (1:1000, monoclonal, DSHB #E7) or rabbit anti-alpha-tubulin antibody (1:1000, polyclonal, Santa Cruz Biotechnology (E-19)-R #sc-12462-R) for remaining blots and afterwards incubated with secondary goat anti-mouse HRP conjugated antibodies (1:5000, see above) and goat anti-rabbit HRP conjugated antibodies (1:5000, polyclonal, Dianova #111-035-144), respectively.

### **2.4.3 Photography and digital processing**

Peroxidase signals were recorded on regular radiographic film (Kodak Biomax Light Film, BLM-1) and developed (Curix 60, AGFA; GV-60, Vision X). Films were

scanned natively and additionally with blot membranes in background. Adobe Photoshop (CS5) was used to digitally extract marker from blot membranes and add to native films.

## **2.5 Imaging**

For native imaging of S2 cells (Figure 3.8 on p. 47), coverslips containing the transfected cells were washed with PBS (10 minutes) and fixed with 4 % PFA for 10 minutes at room temperature and subsequently washed with PBS for 4 times (1 quick wash + 4 x 10 minutes). Then coverslips were taken out of the wells (24-well multidishes (Nunclon)), flipped and embedded in Vectashield (Vector) on an object slide and sealed with colourless nail polish.

For imaging of stained S2 cells (Figure 3.7 on p. 45), transfected cells were washed with PBS and fixed with 6.4 % PFA for 15 minutes at room temperature and incubated with PBS containing 0.5 % SDS for 20 minutes and subsequently washed 3 times with PBS (1 quick wash + 2 x 10 minutes). Incubation with primary mouse anti-Flag antibody (1:1000, monoclonal, Chemicon, #MAB3118)/ rabbit anti-GFP antibody (1:1000, polyclonal, Invitrogen) was performed in 0.1 % PBT solution (PBS containing 0.1% Triton TX100) containing 0.5 ng/ml BSA over night. After 5 washing steps with PBT (2 x quick wash, 3 x 20 min), incubation with secondary antibody Cy3-anti-mouse (1:1000, polyclonal, Jackson ImmunoResearch) / Alexa-488-anti-rabbit (1:1000, polyclonal, Invitrogen) was performed over night. After 5 washing steps with PBT (2 x quick wash, 3 x 20 min), coverslips were taken out of the wells, flipped and embedded in Vectashield on an object slide and sealed with nail polish.

Confocal images were obtained with a linescanning confocal LSM 5 system (Zeiss) equipped with a 1.25 numerical aperture 63 x oil-immersion objective (Figure 3.7 A-F, Figure 3.8 on p. 47) or a 20 x objective (Figure 3.7 G-I).

## 2.6 Lethality assays

$w^+;;UAS-BoNT-A2/TM3,Sb$	$x w^+/Y;OK6-GAL4;$
$w^+;OK6-GAL4/CyO-GFP;$	$x w^{1118}/Y;UAS-BoNT-B1;$
$w^+;;UAS-BoNT-C1/TM3,Sb$	$x w^+/Y;OK6-GAL4;$
$w^+;;UAS-BoNT-G1/TM3,Sb$	$x w^+/Y;OK6-GAL4;$
$w^+;OK6-GAL4;$	$x w^+/Y;UAS-TNT-E/CyO;$
$w^+, elav-GAL4;;$	$x w^-/Y;;UAS-BoNT-A2/TM3,Sb$
$w^+, elav-GAL4;;$	$x w^{1118}/Y;UAS-BoNT-B1/CyO;$
$w^+, elav-GAL4;;$	$x w^-/Y;;UAS-BoNT-C1/TM3,Sb$
$w^+, elav-GAL4;;$	$x w^-/Y;;UAS-BoNT-G1/TM3,Sb$
$w^+, elav-GAL4;;$	$x w^+/Y;UAS-TNT-E/CyO;$
$w^+;G7-GAL4/CyO-GFP;$	$x w^{1118}/Y;;$
$w^+;G7-GAL4/CyO-GFP;$	$x w^{1118}/Y;UAS-BoNT-B1;$
$w^+;G7-GAL4/CyO-GFP;$	$x w^-/Y;;UAS-BoNT-C$
$w^+;G7-GAL4/CyO-GFP;$	$x w^+/Y;UAS-TNT-E;$

**Table 2.7 Crosses for lethality experiments**

For lethality assays, either the *GAL4*-line or the *UAS-CNT*-line was crossed to a balancer chromosome with a dominant marker (*CyO* or *TM3-Sb* for adult flies, *CyO-GFP* for larvae). These balanced *GAL4*- or *UAS*-lines were then crossed to the respective homozygous *UAS*- or *GAL4*-lines. This way only balancer-negative (balancer-) flies carry both, the *GAL4*-line and the *UAS*-transgenes required for toxin expression. Expression of an effective toxin led to progeny only consisting of balancer-positive flies whereas ineffective toxin expression led to a Mendelian ratio of balancer-positive and balancer-negative flies. The progeny was collected at 4 - 8 (*elav-GAL4* and *OK6-GAL4*) consecutive days after the first adult flies hatched. For *G7-GAL4*, 3<sup>rd</sup> instar larvae were counted twice in two consecutive crossings for each genotype.

## 2.7 Behavior

### 2.7.1 Fly lines

#### *Culture condition*

Flies were raised at a 12h/12h day/night cycle at either 18 °, 21 ° or 25 ° (as specified for different experiments) and 60% humidity on a standard cornmeal and molasses medium (Ashburner, 1989).



### Genotypes for larval motor behavior

$w^*/w^{1118};OK6-GAL4/+; // w^*/Y;OK6-GAL4/+;$
$w^*, elav-GAL4/w^{1118}; // w^*, elav-GAL4/Y;;$
$w^{1118}/w^*;+/UAS-BoNT-B1;+/tub-GAL80^{ts} // w^{1118}/Y;+/UAS-BoNT-B1;+/tub-GAL80^{ts}$
$w^{1118}/w^*;+/tub-GAL80^{ts};+/UAS-BoNT-C1 // w^{1118}/Y;+/tub-GAL80^{ts};+/UAS-BoNT-C1$
$w^{1118}/w^*;+/UAS-TNT-E;+/tub-GAL80^{ts} // w^{1118}/Y;+/UAS-TNT-E;+/tub-GAL80^{ts}$
$w^*;OK6-GAL4/UAS-BoNT-B1;+/tub-GAL80^{ts} // w^*/Y;OK6-GAL4/UAS-BoNT-B1;+/tub-GAL80^{ts}$
$w^*/w^*;OK6-GAL4/tub-GAL80^{ts};+/UAS-BoNT-C1 // w^*/Y;OK6-GAL4/tub-GAL80^{ts};+/UAS-BoNT-C1$
$w^*;OK6-GAL4/UAS-TNT-E;+/tub-GAL80^{ts} // w^*/Y;OK6-GAL4/UAS-TNT-E;+/tub-GAL80^{ts}$
$w^*, elav-GAL4/w^*;+/UAS-BoNT-B1;+/tub-GAL80^{ts} // w^*, elav-GAL4/Y;+/UAS-BoNT-B1;+/tub-GAL80^{ts}$
$w^*, elav-GAL4/w^*;+/tub-GAL80^{ts};+/UAS-BoNT-C1 // w^*, elav-GAL4/Y;+/tub-GAL80^{ts};+/UAS-BoNT-C1$
$w^*, elav-GAL4/w^*;+/UAS-TNT-E;+/tub-GAL80^{ts} // w^*, elav-GAL4/Y;+/UAS-TNT-E;+/tub-GAL80^{ts}$

**Table 2.8 Genotypes corresponding to Figure 3.15 on p. 59**

### Genotypes for OMR behavior

$w^*/w^{1118};GMR-GAL4/+;$
$w^{1118}/w^*;+/UAS-TNT-E;+/tub-GAL80^{ts}$
$WTB/w^*;+/UAS-BoNT-B1;+/tub-GAL80^{ts}$
$w^*;GMR-GAL4/UAS-TNT-E;+/tub-GAL80^{ts}$
$w^*;GMR-GAL4/UAS-BoNT-B1;+/tub-GAL80^{ts}$

**Table 2.9 Genotypes corresponding to Figure 3.20 on p. 68 and Figure 3.22 on p. 71**

$w^*/w^{1118};GMR-GAL4/+;$
$w^{1118}/w^*;UAS-Shi^{ts1}; +/UAS-Shi^{ts1}$
$w^*/w^*, UAS-Shi^{ts1};GMR-GAL4/+; +/UAS-Shi^{ts1}$

**Table 2.10 Genotypes corresponding to Figure 3.21 on p. 69**

$w^+/w^{1118};Rh1-GAL4/+$
$w^{1118};+/UAS-BoNT-C$
$w^+/w^{1118};Rh1-GAL4/UAS-BoNT-C$
$w^*/w^{1118};+/UAS-BoNT-B;UAS-TAG64/+$
$w^+/w^{1118};+/UAS-BoNT-B;Rh1-GAL4/+$
$w^{1118}/w^*;UAS-shi^{ts1}; +/UAS-shi^{ts1}$
$w^+/w^*,UAS-shi^{ts1}; Rh1-GAL4/UAS-shi^{ts1}$
$w^*/w^{1118};+/UAS-TNT-E;UAS-TAG64/+$
$w^+/w^{1118};+/UAS-TNT-E;rh1-GAL4/+$

**Table 2.11 Genotypes corresponding to Figure 3.23 on p. 72**

$w^*/WTB;Rh1-GAL4/+;$
$w^{1118}/w^*,UAS-Shi^{ts1};,+/UAS-Shi^{ts1}$
$w^*/w^*,UAS-Shi^{ts1};Rh1-GAL4/+;,+/UAS-Shi^{ts1}$

**Table 2.12 Genotypes corresponding to Figure 3.24 on p. 74**

## 2.7.2 Larval peristaltic

After distinct length of incubation at 31 °C (1 h, 5 h, 10 h, 15 h, 20 h, 25 h or 40 h), third instar larvae were transferred to a Petri dish (Sarstedt, 92 mm) filled with 1 % agarose (Biozym, #84004). Front and back peristaltic movements (Suster and Bate, 2002) were equally counted by eye for 90 seconds for each larva as long as peristaltic movements propagated through the whole body. Larvae were observed through a binocular microscope with two flexible light sources from above. If larvae reached the rim of the Petri dish, time was stopped and larvae were returned to the middle of the dish. Then, after a couple of seconds to allow the larvae to recover from the manipulation, the measurement was continued. Experiments were performed at 25 - 27 °C ambient temperature. All genotypes were tested at the same day in an alternating manner.

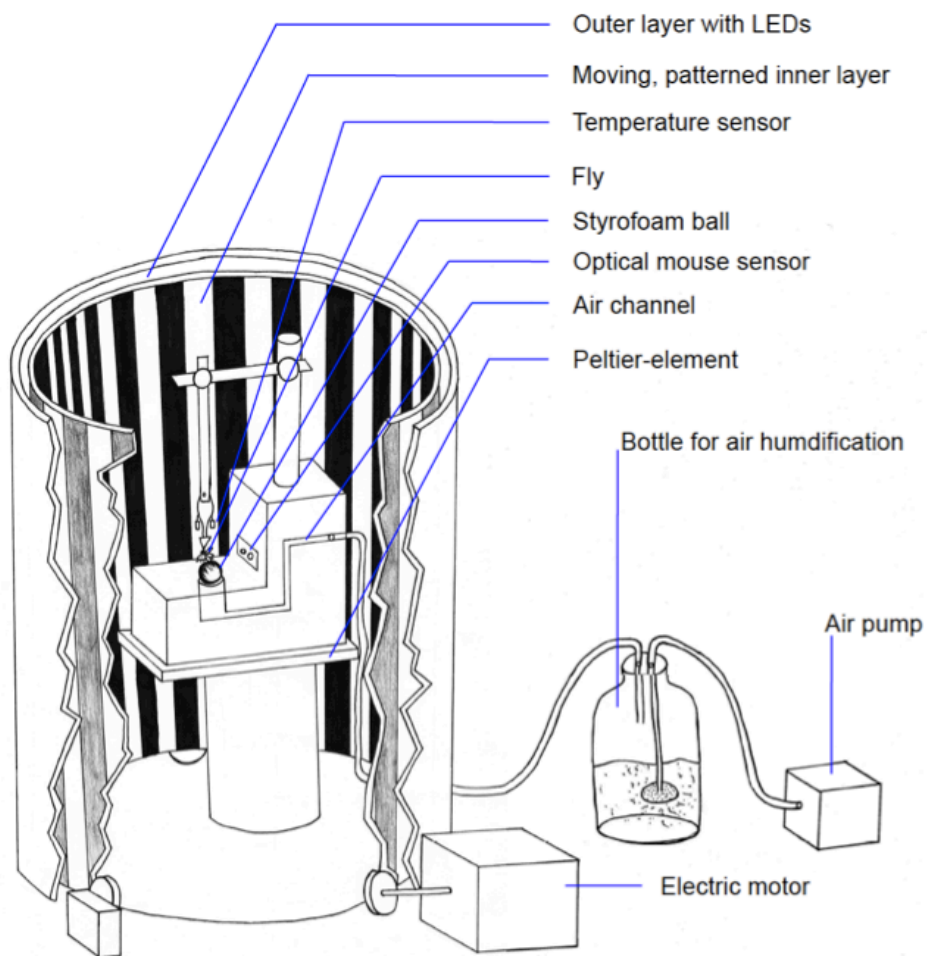
## 2.7.3 Optomotor behavior

### 2.7.3.1 Setup

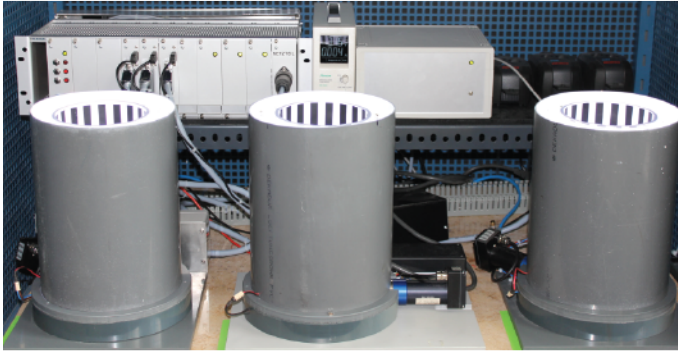
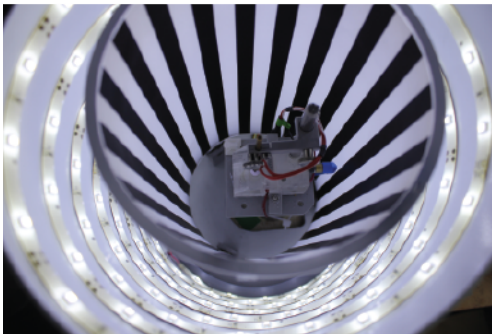
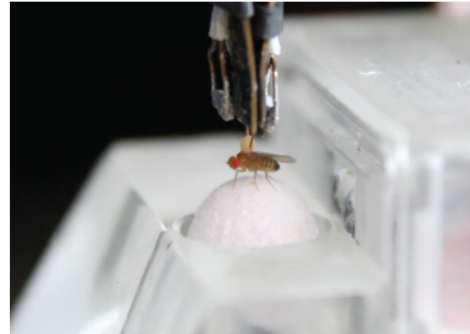
#### *Composition of the setup*

The setup (Figure 2.1 and Figure 2.2) consists of a custom made acrylic glass block with drilling holes that connect to an air channel. A Styrofoam ball is placed into the top hole of the air channel. The air pressure is provided by an air pump, regulated by a valve and humidified in bottles containing distilled water. The temperature of these bottles is kept constantly at 12 °C. The ball's movement is monitored by an optical mouse sensor that is mounted directly next to the ball. The processing hardware is fixed right under the acrylic glass block. Two tiny temperature sensors are connected 2-3 mm above the flies' body at the tips of the fly holder without directly contacting it. Another temperature sensor is glued to the backside of the acrylic glass block, a couple of millimeters above a Peltier

element mounted directly between the acrylic glass block and the optical mouse sensor processing hardware. The Peltier element is connected to the acrylic glass block with heat transfer paste. It is feedback regulated by the temperature sensors above the fly allowing to keep the fly temperature constant. To apply visual input to the fly, the acrylic glass block is located such that the Styrofoam ball is right in the middle of a surrounding patterned drum. This drum runs on three guides. Two are freely rotating on bearings and the other one surrounds the driving shaft of the electric engine that powers the drum's rotation. Rubber rings surround all guides to increase friction between the drum and the guides. The drums are 25 cm high with an inner diameter of 12.3 cm covering the fly's vertical view field of approximately  $126^\circ$  and the complete horizontal field. For calibration purposes a tiny magnet in the lower part of the inner drum allows contactless switching of a sensor located directly next to the drum. The patterned drum is surrounded by another drum with an inner diameter of 20 cm. The inner surface of the outer drum is coated in reflective white. A LED stripe with 50 equally distributed LEDs is glued to the inner surface of the drum. The setup is placed in a cage which is shaded with black board and a black curtain.



**Figure 2.1 Sketch of the "Buchner-ball" setup**

**A****B****C**

**Figure 2.2 Photographs of the “Buchner-ball” setup**

### ***Peripheral hardware - computer interface***

Data of the optical mouse sensor are directly fed into the computer via an USB-cable. Communication with the electric engine is provided by a serial port. All other input-output operations are performed across the Labjack: LED illumination (analogous output), all 3 temperature sensors (analogous input), digital signal for power supply associated with the Peltier element. The magnet sensor signal is directly processed by the electric engine.

### ***Software***

The software was written in JAVA with implanted native C-methods. The software provides a GUI (graphical user interface). It allows controlling of all relevant measurement variables: Drum direction and speed as well as absolute and relative drum positioning, illumination strength and temperature of the fly. Stimulus conditions sequences can be arranged into “journals” that allow for fully automatic measurement sequences. Calibration of the electric engine for turning frequencies and proper relative and absolute positioning is also accessible through the GUI.

Data are stored into a data file. Usually every 40 ms turning of the ball in two dimensions, time and eventual “events” are documented in the data file. Events are either steps in the measurement protocol (journal), temperature warnings and markers that can be added online during the measurement at special events, as disconnection of a fly of its holder. The flies’ movements, documented by the rotation of the ball, are displayed during the measurement and can also be loaded and displayed afterwards. The software also supports fully automatic data processing as well as manual analysis.

### ***Contribution***

Plexiglas blocks, Styrofoam balls and fly holder were manufactured and kindly provided by the workshop of the “Biozentrum der Universität Würzburg” (Am Hubland, 97074 Würzburg, Germany). All other fine mechanical work was performed at the workshop of the Institute of Physiology (Röntgenring 9, 97070 Würzburg, Germany) by Franz-Josef Sauer, Armin Liebenstein and Max Wiesen. All electrotechnical work as well as design and production of custom made boards were performed by Christian Geiger, Institute of Physiology (Röntgenring 9, 97070 Würzburg, Germany). The software was written by Philipp Backhaus. The development of the setup was managed and supervised by Kirscha Neuser und Philipp Backhaus.

### ***Technical components***

The electric engine that drives the rotating drum is a Faulhaber “Motion Control System” (3564K024B CS, MCBL 3003/06 S) with an attached planetary gear manufactured by Mattke (PG 28/2). The optical mouse sensor was taken from a Digtius 3-button laser mouse (Avago ADNS-7550). An EHEIM 200 air pump (aquarium supply) is used to generate the air stream. A Labjack U12 is used as digital and analog input-output source. Platinum-chip temperature sensors (JUMO, # 90.6125) are used to monitor the air stream temperature.

### **2.7.3.2 Stimulus and environment**

#### ***Temperature***

The temperature of the airstream is regulated by a Peltier element placed right under the acrylic glass block in proximity to the air channel. During measurements the temperature of the two temperature sensors above the flies head (2-3 mm above the flies' body) is analyzed every 5 seconds. The sensor inside the plexiglas-block directly switches off heating at temperatures  $> 65\text{ }^{\circ}\text{C}$  to prevent heat damage to the electronic components. The computer software compares the arithmetic mean of the value of the two sensors with the target temperature and calculates a target heating-value that is a fraction of 1. An output digital signal is transferred to the circuit breaker of the power supply for the Peltier element that closes or opens the circuit proportional to the heating-value. The heating-value is calculated by a complex self-written feedback controller that adjusts regulation on a short- and long time scale: It assures that the previously set temperature boundaries ( $\pm 0.7\text{ }^{\circ}\text{C}$ ) are met and that the arithmetic mean of the actual temperature corresponds to the previously set target temperature on a longer time scale. If the boundaries are crossed the software writes a warning message into the data file. Proper temperature adjustment of the fly by the setup was not only demonstrated by behavioral experiments but also by placing another temperature sensor directly over the ball where the fly is usually placed.

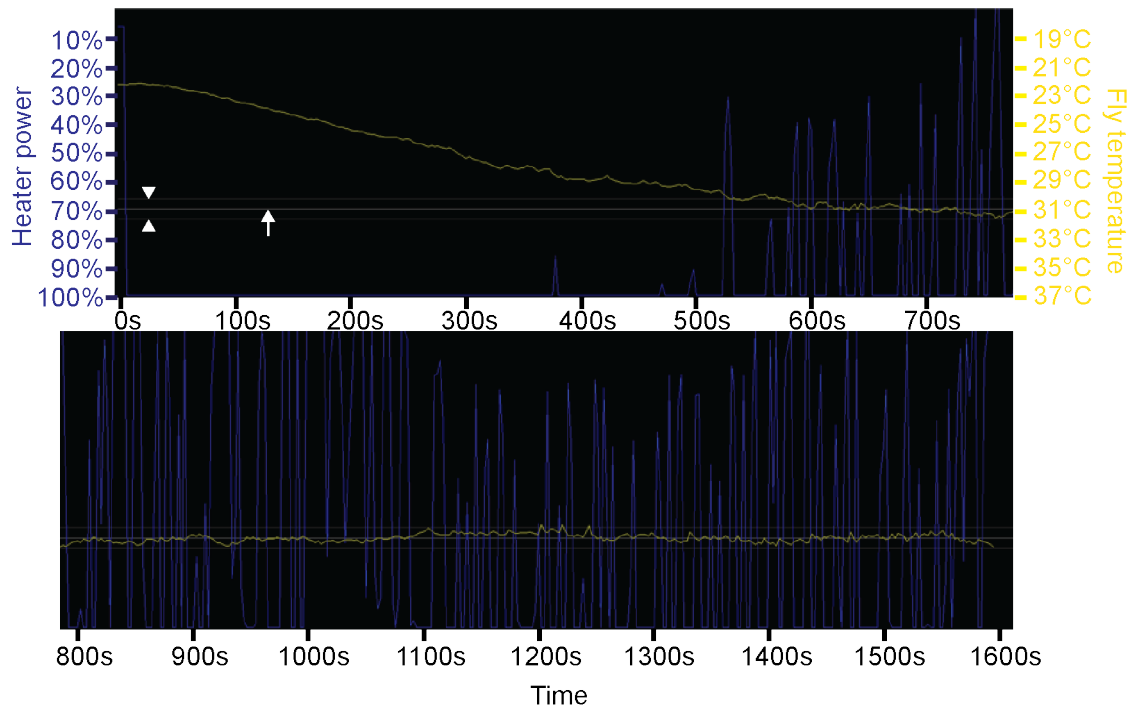


**Figure 2.3 Heating trace**

Modified screenshot from recording software displaying typical traces of temperature (yellow) and relative heater power (blue) over time. White line (arrow) displays target temperature, gray lines (arrow heads) are temperature boundaries ( $\pm 0.7^\circ\text{C}$ ).

### ***Drum rotation***

For the calibration, the drum rotates with a given speed until 100 complete rotations are performed as measured by the magnet sensor. Based on the time needed for 100 turns, a factor that translates speed signals for the electric engine into rounds per minute is calculated.

### ***Drum patterns***

Patterns were printed out by a Xerox 700 DC printer on tracing-paper from Papyrus (90 g / m<sup>2</sup>) and were glued to the inner surface of the transparent drum. For highest contrast, a rubber-like black intransparent and non-reflecting surface sheet was cut by plot-cutter and glued to the tracing paper. Patterns were generated in Adobe Indesign and correspond to 0 %, 2 %, 5 %, 20 % and 100 % on the greyscale. To further diffuse the light of the LEDs another blank tracing paper was glued to the outer surface of the drum. For the human eye the inner, patterned layer appears to be illuminated homogenously. Patterns contain 18 black and 18



white stripes. The variable ‘pattern frequency’ expresses how many pairs of 1 black and 1 white stripe pass one point in the view field of the fly in one second.

### ***Surrounding light and temperature***

The whole setup is located in a cage with attached black card and a black curtain. For the human eye, the room is completely dark. No special control of environmental temperature is performed. During measurements, the inner of the cage could heat up to 28 °C. Measurements with target temperature under 28 °C were performed with open curtains at daylight.

### ***Humidity***

Flies’ perseverance and activity critically depend on humidity of the air stream. The air passes a bottle filled 10 cm with distilled water to saturate the air stream with humidity. To allow constant humidity saturation of the stream independent of surrounding temperature, the temperature of the container bearing the water bottles is regulated. For experiments it was held at 12 °C.

### ***Air stream***

The air stream is tuned for each experiment until the ball floats quietly without fast autonomic turnings and without dipping to the bottom.

### **2.7.3.3 Fly preparation**

Flies were between 3 and 7 days old at the time of measurement. Only female flies were taken for analysis, because of their overall bigger body size and to reduce variance in experiments. The raising temperature depended on the experiment and usually was 18 °C for *tub-GAL80<sup>ts</sup>* constructs and 20 °C for *UAS-Shi<sup>ts</sup>* constructs. 24 hours (+/- 1 h) before the experiment, flies were CO<sub>2</sub> anaesthetized and isolated into small vials that only contained moist filter paper, but no food. The vials were incubated at 31 °C, “not incubated” controls were kept at 18 °C, *UAS-Shi<sup>ts</sup>* constructs and respective controls at 25 °C. Before the experiment the vials were placed on ice until flies did not show spontaneous movement anymore (usually 3-10 minutes). Flies were transferred onto an ice-cold Petri dish cover and manipulated with a brush to expose the dorsal thorax. A triangle formed hook

made of 0.1 mm strong copper filament was grasped with the fly holder and a small glue dot of about the size of the width of the fly thorax was attached to the exposed corner of the triangle. UV-hardening dental glue was used. The hook was attached to a mechanic micromanipulator and lowered until the glue contacted with the thorax. The glue was hardened with a UV-pistol (LED.B Curing Light, Woodpecker Medical Instrument) for 15 seconds from behind the fly. All flies were checked under a binocular microscope if all legs were intact and freely moving. Wings should also be freely moveable. Most flies showed spontaneous fly attempts. The holder is attached to the setup and the fly is carefully lowered onto the centre of the Styrofoam ball, so that the fly is walking on it without being squeezed and with its body axis parallel to the length axis of the Plexiglas block. The ball should keep its initial height as it was before the fly made contact with it.

#### **2.7.3.4 Measurement**

Measurements were carried out at 31 °C (if not specified otherwise). After positioning the fly into the setup, it was heated until the target temperature of 31 °C was reached in a stable manner (usually 5-10 minutes). During heating, the drum did not move and illumination was turned on. Directly after reaching the target temperature, the drum started rotating. 10 different measurement units of 90 seconds were applied (-0.1 Hz, 0.1 Hz, -1 Hz, 1 Hz, -10 Hz, 10 Hz, -30 Hz, 30 Hz, -45 Hz, 45 Hz pattern frequency). All 10 units were executed 9 times, while the order of the units was randomized. A whole measurement usually took 2 hours and 20 - 35 minutes (90 seconds x 10 x 9 + time for initial heating + time for drum rotation changes). All groups that are displayed in one graph were measured as part of one measurement-set that usually spanned 1-2 weeks. All groups were measured alternating.

#### **2.7.3.5 Data processing and analysis**

Every 40 ms, X (left/right) and Y (for-and backward) movements were recorded and stored into a data file as in the following example:

Time (ms)	X-value	Y-Value	Comment
...	...	...	...
3381240	45	33	TEMPERATURE_31_READY
3381280	20	21	START_TURNING_3RPM
...	...	...	...

Ball movements around the horizontal axis parallel to the flies' anterior-posterior body axis were not measured. X- and Y-values were saved in arbitrary units as edited by the optical mouse sensor. Positive values indicated counter-clockwise ball turning which corresponded to an intent of the fly to turn clockwise and vice versa. Fly measurements with obvious errors were primarily excluded (i.e. derailing of the stimulation drum, unintentional release of the fly, dropping of the Styrofoam ball). Secondly, an activity threshold (overall activity < 2 (arbitrary units)) was applied for each individual fly and intra-threshold flies were excluded from analysis. The fraction of flies excluded this way ranged between 10 – 20 %. Data processing was carried out by our custom written software. Of the typically measured 9 sets of measurement units, only the latter 6 were taken into account for analysis, to allow the flies to acclimatize to the recording situation for 3 sets. The randomized 90 s stimulus windows of the remaining 6 measurement unit sets were sorted by their direction and pattern frequency. All stimulus windows for each frequency and direction were put in line and connected, as if they were measured consecutively (i. e. all six 90 s 10 Hz measurements were put in line as if 10 Hz were measured once for 540 s). Then the actual measurement interval (usually 40 ms) was adapted to the analysis interval (120 ms, simple addition of 3 consecutive X and Y-values). The threshold (usually absolute value  $\geq 4$ ) was applied for X and Y values individually. When supra-threshold X values corresponded to syn-directional fly turning (positive values for clockwise pattern turning or negative values for counter-clockwise pattern turning), 1 was added to the counter and when supra-threshold X-values corresponded to contra-directional fly turning, -1 was added to the counter. The following counter was divided by the number of time points with either X or Y over threshold. This leads to a number between -1 and 1 whereas 1 indicates perfect syn-directional turning,

0 random turning and -1 perfect contra-directional turning. Thus only the relative time the fly followed the drum rotation was measured, but not the absolute amount of ball rotation, although the latter has a certain influence, because of the threshold for X-movements of 4. The upper method of analysis only considers data points where the fly showed supra-threshold activity. This leads to an increasing error of analysis of flies with very low activity, which was circumvented by sorting out flies with very low activity as described above.

## 2.8 Statistics

For pairwise comparison in larval motor behavior experiments and OMR-experiments the Mann-Whitney-U-Test was used (Prism 5). For comparisons with zero the Wilcoxon Signed Rank Test was used (Prism 5). The multiple comparisons represent an explorative statistical analysis. Thus no corrections as the Bonferroni correction were performed. For calculation of the incubation length required for a 50 % suppression of larval motor behavior, a logistic curve fit was applied. The respective values represent the time points where the curve reaches half of its maximum. For data analysis of lethality tests the fraction of balancer positive flies has been calculated for each genotype. A fraction of 1 indicates a lethality of 100 % as no flies carrying both the *GAL4* driver and the toxin could be counted. A fraction of 0.5 indicates no influence on lethality. Two-tailed p-values were calculated using a binominal test based on a success probability of 0.5 (<http://graphpad.com/quickcalcs/binomial1>). Percentage ID of sequence alignments were calculated with Jalview (Waterhouse et al., 2009). \* reflects  $p < 0.05$ , \*\*  $p < 0.01$  and \*\*\*  $p < 0.001$ .

## 3 Results

### 3.1 Generation of transgenic botulinum toxin DNA

The following steps were performed in order to generate transgenic flies expressing the different botulinum toxin light chains under *UAS*-control. In order to determine the putative probability of *Drosophila* neuronal SNARE proteins to be effectively cleaved by BoNTs, their conservation was analysed at first. Then appropriate transgenic vectors were generated via injection into *Drosophila* embryos by an external company (BestGene Inc.). Simultaneously, vectors were generated that allowed for verification of the construct and its cleavage effectiveness using immunohistochemistry as well as western blots.

#### 3.1.1 Analysis of primary structure conservation

*Drosophila* neuronal SNARE primary structure is moderately conserved in respect to its vertebrate isoforms (*Drosophila melanogaster* (*Dm*) n-Syb vs. *Rattus norvegicus* (*Rn*) VAMP2: Percentage ID = 61 %; *Dm* Syntaxin-1A vs. *Rn* Syntaxin-1A: Percentage ID = 69 %; *Dm* SNAP-25 vs. *Rn* SNAP-25: Percentage ID = 60 %). The success of creating BoNTs as effective tools in *Drosophila* critically depends on the BoNTs' ability to cleave *Drosophila* neuronal SNARE isoforms. Different studies concerning the influence of SNARE protein mutations on their cleavability by CNTs are present in the literature that will be analyzed in the following sections. In general, two regions of SNARE proteins are critical for cleavage: The region around the cleavage site and typically one of the 2-4 SNARE domains where the CNT binds to its targets (Schiavo et al., 2000). While the importance for successful cleavage of most neighbouring amino acids varies among the different SNARE proteins and BoNTs, conservation of the P1' amino acid (the first C-terminal amino acid in respect to the cleavage site) appears to be absolutely critical for proper cleavage (Schmidt and Bostian, 1997; Vaidyanathan et al., 1999; Sikorra et al., 2008). The following passages summarize an estimation of the susceptibility to the different BoNTs based on primary structure

conservation of *Drosophila* SNARE. These results were the basis of BoNT-selection for integration into the *Drosophila* genome.

### 3.1.1.1 Synaptobrevin

Synaptobrevin is cleaved by TNT, BoNT-B, BoNT-D, BoNT-F and BoNT-G (Figure 3.1) Two synaptobrevin isoforms have been identified in *Drosophila* (Chin et al., 1993; DiAntonio et al., 1993; Hua et al., 1998). Synaptobrevin (Syb) is expressed ubiquitously while neuronal Synaptobrevin (n-Syb) is exclusively expressed in neurons and localizes to synapses. An ideal neurotoxin should exclusively cleave n-Syb and should not interfere with Syb. The influence of Synaptobrevin mutations on CNT-cleavage has been analysed in great detail in a systematic mutation study (Sikorra et al., 2008). The following interpretations on the cleavage efficiency of different CNTs on n-Syb and Syb are based on this study if not quoted otherwise.

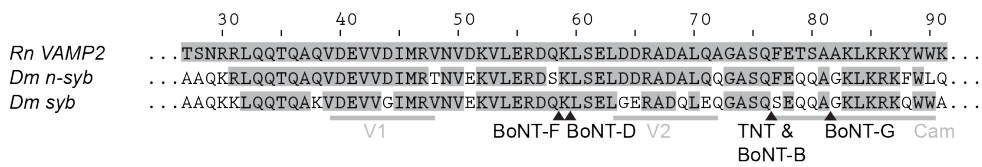


**Figure 3.1 Alignment Synaptobrevin**

Pairwise alignments of *Rattus Norvegicus* VAMP2 (NP\_036795.1) with *Drosophila melanogaster* neuronal Synaptobrevin (NP\_477058.1, isoform a) and Synaptobrevin (gb|AAA28924.1). Gray bars indicate SNARE motifs V1 and V2 and “Cam” indicates a putative Calmodulin binding site. Arrow heads indicate CNT cleavage sites.

### TNT

TNT cleaves rat VAMP2 at Q76-F77 (Schiavo et al., 1992). Cleavage depends critically on the conservation of the V1 motif (39-47) (Pellizzari et al., 1996; Sikorra et al., 2008). The V1-motif is 100 % conserved in *Drosophila* as well as the P3, P2, P1, P1', P2', around the cleavage site. TNT was introduced as an effective tool to interfere with synaptic transmission in *Drosophila* by T. Sweeney 1995. Its effectiveness in cleaving neuronal Synaptobrevin in *Drosophila* has been investigated on a behavioral, biochemical and electrophysiological basis (Sweeney et al., 1995). In biochemical assays TNT exclusively cleaves n-Syb, but not (non-neuronal) Syb. This is most likely explained by the mutated P1' site in Syb and by the less conserved V1-motif.

### ***BoNT-B***

BoNT-B cleaves n-Synaptobrevin at the identical peptide bond as TNT (Q76-F77). Different to TNT, the V2-motif (63-71) is critical for BoNT-B function (Pellizzari et al., 1996; Sikorra et al., 2008). The V2-motif is 100 % conserved in *Drosophila* n-Syb. However, an A72Q substitution downstream of the V2-motif in n-Syb could have influence on BoNT-B cleavage (Sikorra et al. 2008). Overall, potent n-Syb cleavage in *Drosophila* by BoNT-B appears likely.

As the cleavage sites of BoNT-B and TNT are identical, the critical amino acid substitution at P1' should prevent cleavage of Syb for BoNT-B as for TNT. The V2-motif in Syb is mutated at four positions D64G, D65E, A69Q and Q71E. These mutations make proper (non-neuronal) Syb-cleavage even more unlikely than for TNT.

### ***BoNT-D***

BoNT-D cleaves VAMP2 at K59-L60 (Schiavo et al., 1993a) and requires structural conservation in the V1 region. In *Dm* n-Syb the region around the cleavage site is well conserved with a mutation only at the P2 site from Q58S. Sikorra et al. 2008 have shown that substitutions at that position mildly effect BoNT-D mediated cleavage. Overall, proper cleavage of n-Syb by BoNT-D in *Drosophila* appears likely. However, while BoNT-B and TNT are supposed not to cleave Syb, BoNT-D might be an effector on Syb, since all relevant amino acids are well conserved.

### ***BoNT-F***

BoNT-F cleaves VAMP2 at Q58-K59 and also requires structural conservation in the V1 region (Schiavo et al., 1993b). Although the *Dm* n-Syb Q58S substitution is closer to the BoNT-F than to the BoNT-D cleavage site, Sikorra et al. 2008 have shown that substitutions at this site effect BoNT-F cleavage less than BoNT-D cleavage.

### ***BoNT-G***

BoNT-G cleaves VAMP2 at A81-A82 (Schiavo et al., 1994). The influence of amino acid conservation in Synaptobrevin on BoNT-G cleavage was not analyzed in

Sikorra et al 2008. However, the present A82G substitution in Syb and n-Syb should have a strong influence on cleavage since mutations at the P1' site generally strongly interfere with BoNT-cleavage. Also the P2 and P3 sites are mutated in both Syb and n-Syb, making it in general unlikely that BoNT-G cleaves any of the two *Drosophila melanogaster* Synaptobrevin isoforms.

### 3.1.1.2 SNAP-25

Vertebrate SNAP-25 is cleaved by BoNT-A, BoNT-C and BoNT-E.

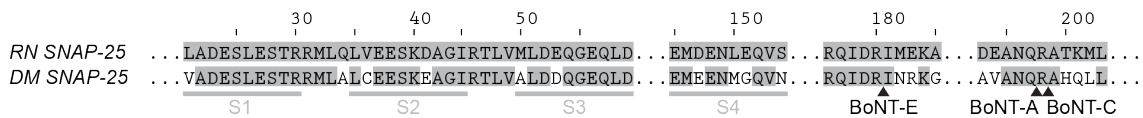


**Figure 3.2 Alignment SNAP-25**

Pairwise alignments between *Rattus norvegicus* SNAP-25 (NP\_001257505.1, isoform a) and *Drosophila melanogaster* SNAP-25 (NP\_001036641.1, isoform a). Gray bars indicate SNARE motifs. Arrow heads indicate CNT cleavage sites.

#### ***BoNT-A and BoNT-E***

BoNT-A cleaves *Rattus norvegicus* SNAP-25 at Q197-R198 and BoNT-E cleaves *Rn* SNAP-25 at R180-I181 (Binz et al., 1994). A biochemical study has shown that *Drosophila melanogaster* SNAP-25 is neither susceptible to BoNT-A nor to BoNT-E (Washbourne et al., 1997).

#### ***BoNT-C***

BoNT-C cleaves *Rn* SNAP-25 at the A198–A199 bond (Vaidyanathan et al., 1999). The influence of single amino acid substitutions and of N- or C-terminal deletions of vertebrate SNAP-25 to BoNT-C cleavage has been analyzed by Jin et al 2007. The respective data do not allow for a definitive prediction on the *Dm* SNAP-25 cleavability to BoNT-C. However substitutions or deletions that greatly affected the susceptibility to BoNT-A and -E often had little effect on BoNT-C cleavage and vice versa, indicating a somewhat different recognition mechanism for BoNT-C than for BoNT-A and -E.

### 3.1.1.3 Syntaxin-1A

*Rn* Syntaxin-1A is cleaved only by BoNT-C.



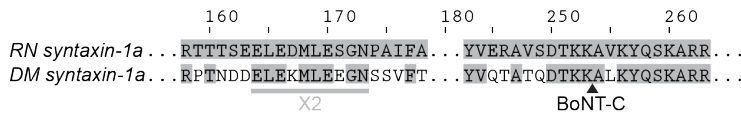


**Figure 3.3 Alignment Syntaxin-1A**

Pairwise alignment of *Rattus norvegicus* Syntaxin-1a (NP\_446240.2) and *Drosophila melanogaster* Syntaxin-1A (NP\_524475.1, isoform a). Gray bars indicate SNARE motifs. Arrow heads indicate CNT cleavage sites.

### **BoNT-C**

BoNT-C cleaves *Rn* Syntaxin-1 at K253-A254 (Schiavo et al., 1995). A study that investigated the cleavability of different vertebrate isoforms of Syntaxin found Syntaxin-1a, 1b, 2 and 3, but not 4 to be cleaved by BoNT-C (Schiavo et al., 1995). In this respect, the X2-motif (164-173) was identified as the putative binding site. The overall grade of primary structure conservation of *Dm* Syntaxin-1A to *Rn* Syntaxin-1A (Percentage ID = 69 %) is higher than between *Rn* Syntaxin-1A and its respective *Rn* isoforms Syntaxin 2 (Percentage ID = 62 %) and 3 (Percentage ID = 63 %). Also the X2-motif as well as the region around the cleavage site are equal or better conserved. These observations associate proper *Dm* Syntaxin-1A cleavage by BoNT-C.

#### **3.1.1.4 Conclusion and selection of BoNTs for generation of transgenic constructs**

6 of the 7 BoNTs were selected for the generation of transgenic flies. The highest probability to effectively cleave its substrates were accounted to BoNT-B, BoNT-C, BoNT-D and BoNT-F. Although probabilities for proper cleavage were predicted low for BoNT-G, it was selected due to the missing detailed data of the importance of primary structure conservation on BoNT-G cleavage. A study could demonstrate that BoNT-A does not cleave *Drosophila* SNAP-25 (Washbourne et al., 1997). It was selected anyways to serve as a negative control.

#### **3.1.2 Synthesis of botulinum toxin light chains**

The genetic code is composed of four different nucleotides. Three subsequent nucleotides encode either for a stop codon or one of the 20 different genetically encoded amino acids. However, 64 different triplet combinations exist (61 without stop-codons) leading to a redundancy in the genetic code. The preference of

different organisms to different codons is commonly referred to as “codon usage bias”. The codon usage in clostridial neurotoxins differs a lot when compared to the general codon usage in vertebrates or invertebrates. We ordered synthetic cDNA of the different botulinum toxins that were adapted to the *Drosophila melanogaster* codon usage and therefore showed elevated GC-content to ensure proper expression in *Drosophila* (GeneOptimizer® by Thermo Fisher Scientific; Table 3.1).

<b>CNT</b>	<b>GC-Content</b>	<b>Codon Adaption Index to <i>Dm</i></b>
TNT wild type (Eisel et al. 1986) (X04436)	29.88	0.54
TNT synthetic (Eisel et al. 1993) (L19522)	48.38	0.78
BoNT-A wild type	29.36	0.52
BoNT-A synthetic	56.27	0.97
BoNT-B wild type (GQ244313)	28.04	0.53
BoNT-B synthetic	55.65	0.98
BoNT-C wild type	27.44	0.5
BoNT-C synthetic	56.74	0.97
BoNT-D wild type (X54254)	27.25	0.48
BoNT-D synthetic	57.4	0.97
BoNT-F wild type	29.19	0.52
BoNT-F synthetic	56.03	0.94
BoNT-G wild type	30.05	0.54
BoNT-G synthetic	56.66	0.98

**Table 3.1 GC-content and codon adaption of different CNT cDNA variants**

GC-Content and Codon Adaption Index was calculated with the GenScript Rare Codon Analysis Tool ([http://www.genscript.com/cgi-bin/tools/rare\\_codon\\_analysis](http://www.genscript.com/cgi-bin/tools/rare_codon_analysis)). A Codon Adaption Index of 1 indicates optimal codon adaption.

### 3.1.3 Transgenic plasmids for embryonic injections

The plasmids that were used for embryonic injections were generated using standard cloning methods. To allow for convenient histochemical detection of the toxins, we fused a 3 x *Flag*-tag to the C-Term of the protein linked with a peptide

spanning 17 amino acids. The *Flag*-tag and linker sequence was identical for all different botulinum toxins and different expression vectors (Figure 3.4).



**Figure 3.4 Scheme of the BoNT gene locus and the expressed protein**

Colored arrows show genes as arranged on the plasmid (and in transgenic flies). Gray arrow indicates expression of the respective fusion protein.

### 3.1.3.1 *Cre*-dependent BoNT-F expression restriction

Embryonic injection of transgenic plasmids yielded no transformants for BoNT-D and -F (see section 3.3), presumably due to leaky expression of the toxic BoNT subspecies. To enhance expression restriction for BoNT-F, we generated an *UAS*-plasmid containing the reporter gene *venus* with a subsequent stop-codon after the transcription initiation site which is flanked by two *LoxP*-sites (Sternberg and Hamilton, 1981) and followed by the BoNT-F cDNA. The *LoxP* sites are derived from coliphage *P1* and constitute recombination sites (Sternberg and Hamilton, 1981). Upon binding of the product of the *cre*-gene, the gene-site flanked by the *loxP* sites is excluded of the main plasmid while it is rejoined at the location of the *loxP* sites. This recombination system is extensively and very successfully used for various transgenic approaches in mainly vertebrate model organisms (Turan et al., 2011). In our construct, before *Cre*-mediated recombination, a RNA-polymerase initiated at the *UAS*-promoter would transcribe the *loxP*-flanked *venus* and discontinue at the following stop codon (*pPB52*). This way, expression restriction is enhanced compared to the sole absence of *GAL4*. After *Cre*-recombination the *venus* and stop-codon are deleted, enabling transcription of the *BoNT-F*-gene (*pPB56*) (Figure 3.5).

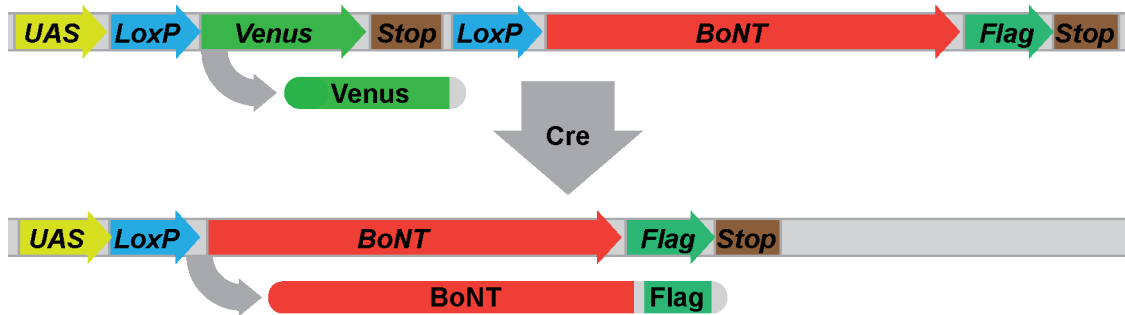


**Figure 3.5 Scheme of the modified BoNT-F construct**

Scheme of *UAS-LoxP-Venus-Stop-LoxP-BoNT-F::Flag* and respective expressed protein before (*pPB52, upper*) and after (*pPB56, lower*) Cre-mediated recombination. Colored arrows show genes as arranged on the plasmid. Gray arrows indicates protein expression / Cre recombination.

### 3.1.4 Transgenic plasmids for cleavage assays

To allow proper immunohistochemical detection of individual cleavage fragments in western blots, we fused a V5-tag to the N-terminus and a HA-tag to the C-terminus of each SNARE protein (*V5::SNARE::HA, pPB22, pPB29* and *pPB30*). Since transgenes are usually expressed only in a fraction of S2 cells after transfection, simple co-transfection with 3 different plasmids containing the *UAS-BoNT*, the *UAS-V5::SNARE::HA* protein and a *GAL4* expressing plasmid would lead to a heterogenic population of S2 cells expressing either only botulinum toxin, SNARE protein, both proteins or none. In this situation, irrespective of the cleavage efficiency of our BoNTs, intact SNARE protein would persist in a fraction of cells and thus lead to false negative results in our cleavage assay. To circumvent this problem, we generated plasmids that contained both, the *BoNTs* and a reverse complementary *Actin-GAL4* (*pPB24-28* and *pPB52*) construct (Figure 3.6). We then co-transfected these plasmids together with a plasmid containing the *UAS-V5::SNARE::HA* construct. Thus every cell that expresses the substrate SNARE protein also expresses botulinum toxin. Cells that have only been transfected with the *UAS-V5::SNARE::HA* plasmid do not express the fusion protein because of the absence of *GAL4*.

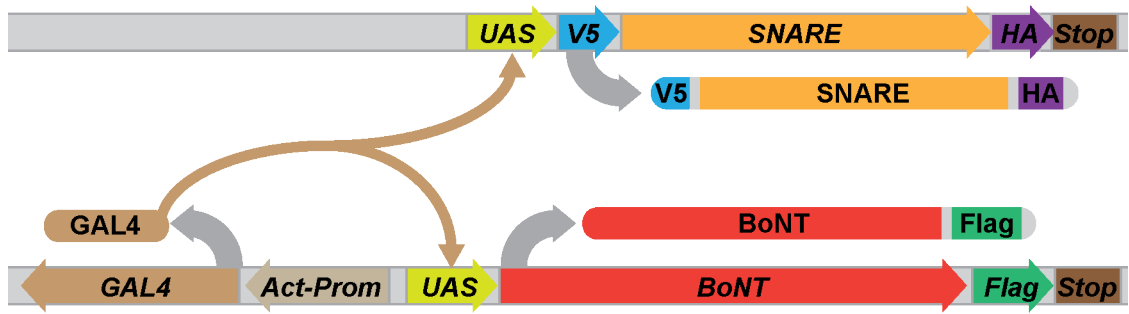


**Figure 3.6 Scheme of expression plasmids for western blots**

Scheme of *pPB22*, *pPB29* and *pPB30* (upper) and *pPB24-28* and *pPB52* (lower). Colored arrows show genes as arranged on the plasmid. Gray arrows indicate expression of the respective fusion protein. Beige curved arrows indicate GAL4 binding to UAS.

### 3.1.5 Immunohistochemical confirmation of the BoNT fusion constructs in *Drosophila* cells

To confirm expression in *Drosophila* cells and immunogenicity of the *Flag*-tag, we stained *Drosophila* S2 cells with a monoclonal anti-*Flag* antibody after expression of the botulinum toxin constructs. For BoNT-A, -B, -C, -F and -G, we co-transfected the plasmids prepared for Phi-C31 mediated transformations (*pPB13-17*) with the *Actin*-promoter driven *GAL4* carrying plasmid *Actin-5C-GAL4* to drive expression. For BoNT-D and the modified BoNT-F construct, we transfected S2 cells with plasmids carrying both the UAS-*BoNT* and *Actin-5c-GAL4* (*pPB55*, *pPB52*, *pPB56*) as described in 3.1.4 on p. 43. The stainings revealed reliable immunogenicity of the fusion constructs (Figure 3.7 A-F), although the BoNT-G signal was slightly lower than for the other tested BoNTs.

To verify the specific expression pattern before and after Cre mediated recombination of the modified UAS-*BoNT-F* construct (section 3.1.3.1), UAS-*LoxP-Venus-Stop-LoxP-BoNT-F::Flag* was treated with Cre-recombinase *in vitro* and successfully recombined clones were separated. We then transfected *Drosophila* S2 cells with the respective un-recombined (*pPB52*) and recombined plasmids (*pPB56*) and double-stained with antibodies directed to the Venus and *Flag*-tag. Dual-channel recordings revealed exclusive Venus staining for the un-recombined plasmids and an exclusive *Flag*-tag signal for the recombined plasmids (Figure 3.7,

G, H and I). Conclusively, *in vitro* recombination and expression restriction in *Drosophila* S2 cells were successful.

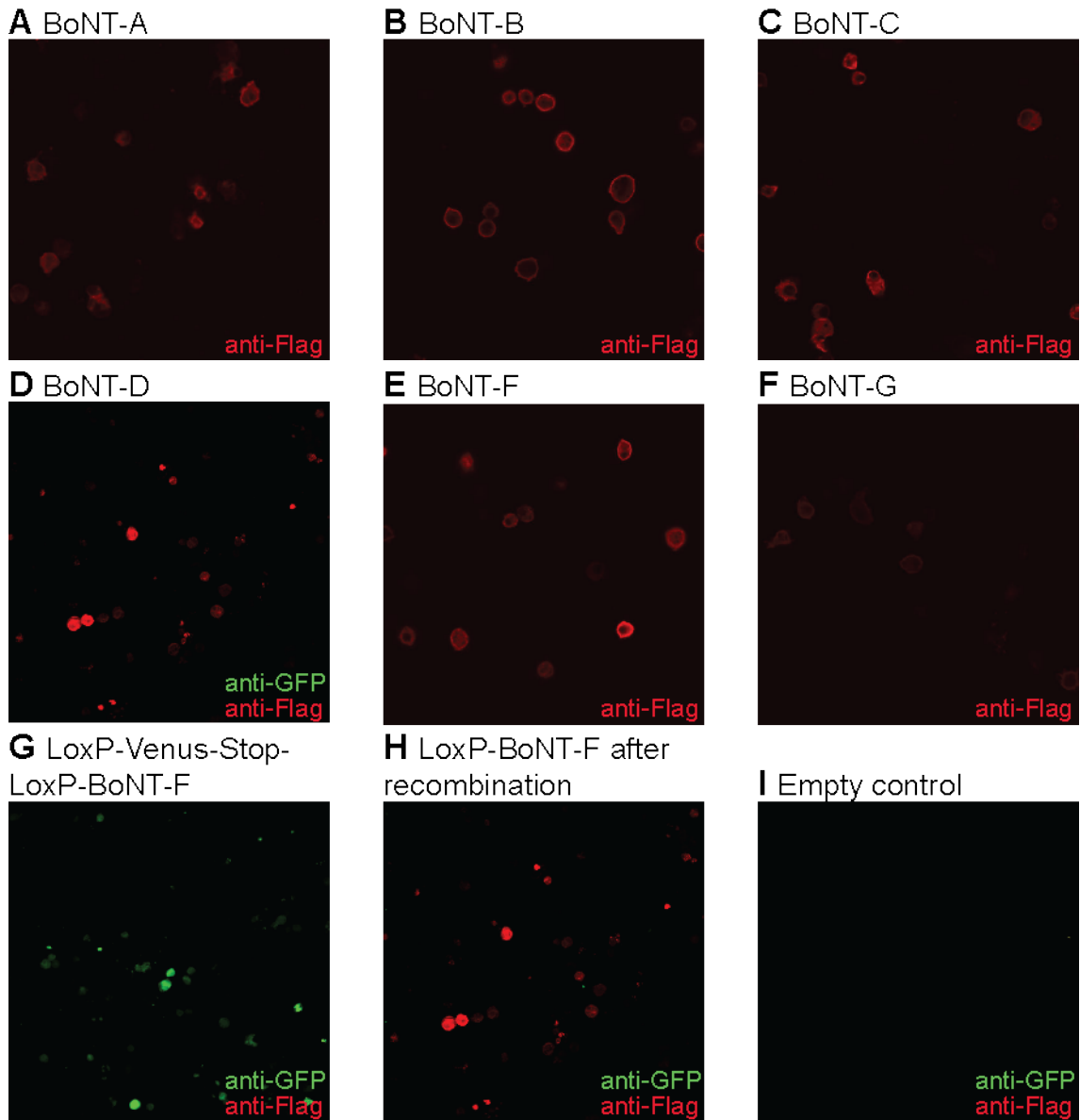


**Figure 3.7 Stainings of BoNTs in S2 cells**

S2 cells were transfected with the following plasmids: **(A)** *UAS-BoNT-A::Flag* (pPB13) + *Actin-5C-GAL4*, **(B)** *UAS-BoNT-B::Flag* (pPB14) + *Actin-5C-GAL4*, **(C)** *UAS-BoNT-C::Flag* (pPB15) + *Actin-5C-GAL4*, **(D)** *UAS-BoNT-D::Flag* (pPB55), **(E)** *UAS-BoNT-F::FLAG* (pPB16) + *Actin-5C-GAL4*, **(F)** *UAS-BoNT-G::FLAG* (pPB17) + *Actin-5C-GAL4*, **(G)** *UAS-LoxP-Venus-Stop-LoxP-BoNT-F::FLAG* (No Cre recombination) (pPB52), **(H)** *UAS-LoxP-BoNT-F::Flag* (pPB52 after Cre recombination: pPB56), **(I)** no plasmid. S2 cells in **A, B, C, E, F** and **I** were co-transfected with *Actin-5C-GAL4* to induce expression of the plasmid. Antibodies for **A, B, C, E and F** were mouse anti-Flag as primary and Cy3 anti-mouse as secondary antibody (dilution 1:1000 in each case). Images were recorded with a confocal microscope at 63 x magnification. Recording settings as well as staining protocol was simultaneously performed and equal for A, B, C, E and F. In addition to mouse anti-Flag as 1<sup>st</sup> and Cy3 anti-mouse as 2<sup>nd</sup>, for D, G, H and I, a primary rabbit anti-GFP antibody and a secondary

Alexa488 anti-rabbit antibody was added. Cy3 and Alexa488 channels were merged for D, G, H and I. Staining protocol and recordings were simultaneously performed and equal for D, G, H and I.

## **3.2 Verification of BoNT mediated proteolysis *in vitro* using western blots**

### **3.2.1 Localization of transgenic Syntaxin-1A in S2 cells**

Syntaxin 1-A is an integral plasma membrane protein. A previous study performed a biochemical analysis of BoNT mediated SNARE protein cleavage and found that BoNT-C mediated Syntaxin-1A cleavage critically depends on membrane integration (Schiavo et al., 1995). We therefore tested whether Syntaxin-1A is expressed in a membrane bound or in an intracellular solved form in *Drosophila* S2 cells. For that, S2 cells were transfected with a Venus::Syntaxin-1A fusion construct (*pTL148*) and the Venus signal was imaged using a confocal microscope (Figure 3.8). To distinguish between a possible membrane-bound and soluble Syntaxin-1A form, we imaged the signal of an mCD8::eGFP construct (*pNH42*), that is localized in the cell membrane and a solvable Venus construct (*pTVW*). The observed signal of the Venus::Syntaxin-1a fusion construct neither matched the intracellular dilution of Venus nor the membrane-bound localization of mCD8::eGFP. Instead, the transgenic Venus::Syntaxin-1a formed doughnut-like shapes of subcellular size that occurred multiple in single cells. Thus Syntaxin seems to localize in the plasma-membrane of S2 cell organelles, but not in the nucleus, which is clearly not stained. This should provide proper cleavage conditions as long as the N-terminal site of the protein is exposed into the cytosol.

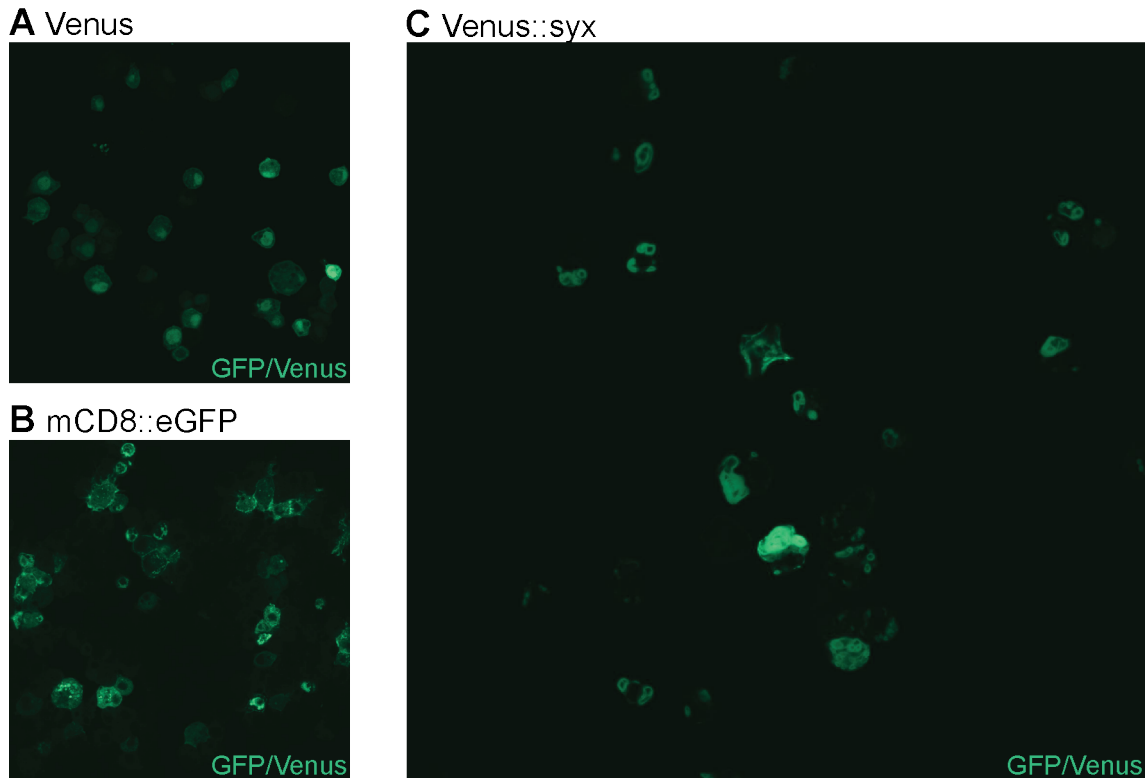


**Figure 3.8 Localization of Syx-1A in S2 cells**

S2 cells were transfected with the following plasmids: **(A)** Solvable Venus (*pTVW*), **(B)** membrane bound mCD8::eGFP (*pNH42*) and **(C)** Venus::Syntaxin-1A fusion protein (*pTL148*). Cells were fixed and natively (without staining) recorded (63x).

### 3.2.2 Western blots

To biochemically test the susceptibility of *Drosophila* SNARE to the different BoNTs, we co-expressed them in different combination in *Drosophila* S2 cells. The expected protein weights without cleavage and respective fragment weights after cleavage are shown in Table 3.2.



Toxin	SNARE protein	Whole protein [kDA]	N-terminal Fragment [kDA]	C-terminal Fragment [kDA]
BoNT-A	HA::SNAP-25::V5 ( <i>Drosophila</i> )	34.27	25.97	8.32
BoNT-A	HA::SNAP-25::V5 ( <i>Rat</i> )	33.92	25.56	8.37
BoNT-B	HA::n-syb::V5 ( <i>Drosophila</i> )	30.05	12.61	17.44
BoNT-C	HA::SNAP-25::V5 ( <i>Drosophila</i> )	34.27	26.12	8.16
BoNT-C	HA::SNAP-25::V5 ( <i>Rat</i> )	33.92	25.72	8.22
BoNT-C	HA::syx1a::V5 ( <i>Drosophila</i> )	46.54	33.39	13.17
BoNT-C	HA::syx1a::V5 ( <i>Rat</i> )	43.64	32.42	11.23
BoNT-D	HA::n-syb::V5 ( <i>Drosophila</i> )	30.05	10.82	19.24
BoNT-F	HA::n-syb::V5 ( <i>Drosophila</i> )	30.05	10.69	19.37
BoNT-G	HA::n-syb::V5 ( <i>Drosophila</i> )	30.05	13.22	16.84

**Table 3.2 SNARE protein and fragment molecular weight**

Molecular weights were calculated by Scripps' ProteinCalculator v3.3 <http://www.scripps.edu/~cdputnam/protcalc.html> by primary structure information.

Lyses was performed 48 hours after incubation at 31 °C. As negative controls, we loaded blots with protein from S2 cells that were only transfected with *Act-5C-GAL4* or with plasmids containing the different BoNTs and *Act-5C-GAL4 (pPB24-28)* and stained with V5- and HA-antibodies. The negative controls did not reveal detectable bands in any case, whereas the positive  $\alpha$ - or  $\beta$ -tubulin loading-controls always revealed detectable bands. This shows that bands corresponding to SNARE fusion proteins or its fragments did result from specific antibody binding.

The resulting western blots of co-expressed BoNT- and SNARE- proteins revealed a clear effect of BoNT expression on SNARE integrity (Figure 3.9 for overview, see Figure 3.10 on p. 51 - Figure 3.12 on p. 52 for original blots with additional controls). Appearance of a band corresponding to the cleavage fragments was observed in every tested combination and only in the presence of the respective botulinum toxin. This was also the case for BoNT-A (Figure 3.9, lower left panel), although previous publications reported *Dm* SNAP-25 to be resistant for BoNT-A (Washbourne et al., 1997). The nevertheless presence of a fragment band indicates a high sensibility for proteolysis in our assays.

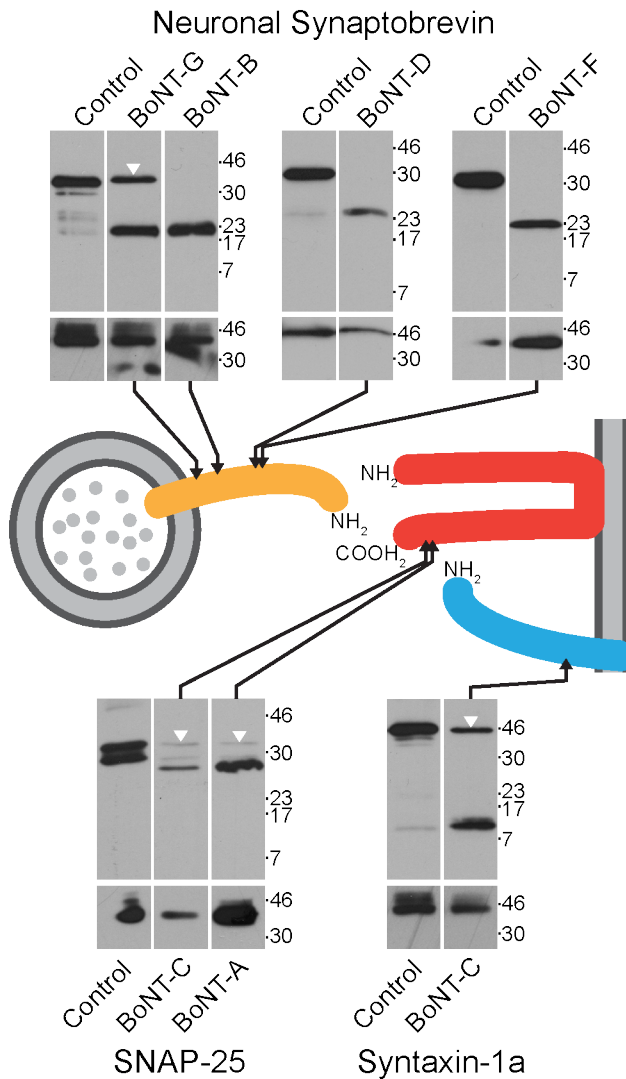


**Figure 3.9 Overview on western blots of BoNT mediated proteolysis of SNARE proteins**

Neuronal Synaptobrevin (orange), SNAP-25 (red) and Syntaxin-1a (blue) and respective BoNT cleavage sites (black arrows) are schematically outlined. SNARE protein cDNAs were tagged at both ends (V5::SNARE::HA) and co-transfected in *Drosophila* S2 cells together with the respective BoNTs. Cells were cultured, lysed and blotted. Control lanes represent SNARE proteins without BoNTs. Staining of the blot was performed with anti-HA for n-Syb and Syx and with anti-V5 for SNAP-25. Lower blots display loading controls with anti-beta-tubulin for BoNT-D and anti-alpha-tubulin for the other blots. White arrows represent remaining intact SNARE protein bands that indicate incomplete SNARE protein cleavage. Lanes in one panel derive from one gel and film. Lane order was changed in respect to the original film.

Disappearance of the intact protein band after BoNT-expression was only observed for BoNT-B, BoNT-F and BoNT-D. In other cases the intact protein only

decreased in the presence of the respective BoNTs indicating incomplete cleavage (BoNT-A, BoNT-C and BoNT-G).

Co-expression of SNAP-25 with BoNT-C or BoNT-A yielded no C-terminal fragment band using HA-antibody stainings, whereas N-Terminal stainings using the V5-antibody revealed intact cleavage fragments. This suggests either rapid degradation of the particular small (< 10 kDa) C-terminal fragment or loss of its immunogenicity.

As described in section 3.2.1 on p. 46, improper localization or expression of the respective SNARE-protein in S2 cells might lead to wrong negative cleavage results in our assays. As a positive cleavage control, we thus tested whether the vertebrate isoforms of SNAP-25 and Syntaxin-1A were cleaved by the respective BoNTs. Both, BoNT-C and BoNT-A successfully cleaved *Rattus norvegicus* SNAP-25 without remaining intact SNARE bands (Figure 3.11, **B**, lane 6 & 9 respectively). Similarly BoNT-C co-expression led to complete *Rn* Syntaxin-1a cleavage (Figure 3.12, **A**, lane 3). Thus, the observed incomplete degradation of *Drosophila* isoforms of these BoNTs reflects biochemical incompatibility of these proteins and not limitations of our cleavage assays. Regarding n-Syb cleavage, no such positive controls were performed, as multiple BoNTs already led to complete cleavage of the *Drosophila* isoform.

In order to test whether the modifications for Cre-dependent recombination in the *UAS-BoNT-F* construct (3.1.3.1 on p. 42) allow the intended expression restriction, cleavage in western blots was examined. Successful expression restriction is indicated by appearance of the intact n-Syb band, although the appearance of also the cleavage fragment band indicates persisting (minor) BoNT-F expression (Figure 3.12, **B**, lane 7). After Cre-recombination of the modified BoNT-F construct no intact n-Syb band was recognizable, showing unimpaired expression and cleavage (Figure 3.12, **B**, lane 5) as intended.

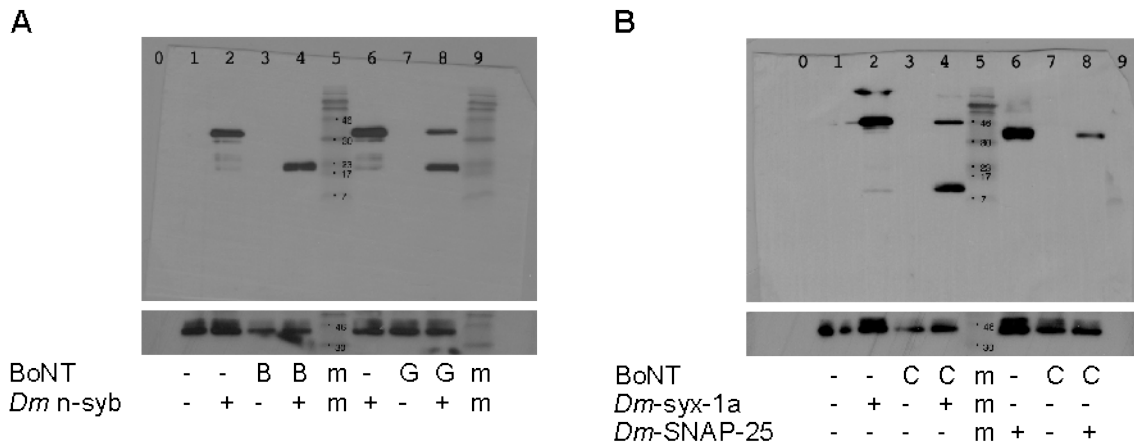


**Figure 3.10 Original western blot**

Overlay of blot and film. Blot stained with anti-HA. Asterisks indicate lanes in Figure 3.9 (film only). Marker unit is kDA. Lower blot represents loading controls with anti-alpha-tubulin. **A: 1:** Control, **2:** *Dm* n-Syb (*pPB22*)\*, **3:** BoNT-B (*pPB25*), **4:** *Dm* n-Syb (*pPB22*) + BoNT-B (*pPB25*)\*, **5:** Marker Color Plus 7709s, **6:** *Dm* n-Syb (*pPB22*), **7:** BoNT-G (*pPB28*), **8:** *Dm* n-Syb (*pPB22*) + BoNT-G (*pPB28*)\*, **9:** Marker Color Plus 7709s. **B: 1:** Control, **2:** *Dm* Syx (*pPB29*)\*, **3:** BoNT-C (*pPB26*), **4:** *Dm* Syx (*pPB29*) + BoNT-C (*pPB26*)\*, **5:** Marker Color Plus 7709s, **6:** *Dm* SNAP-25 (*pPB30*), **7:** BoNT-C (*pPB26*), **8:** *Dm* SNAP-25 (*pPB30*) + BoNT-C (*pPB26*).

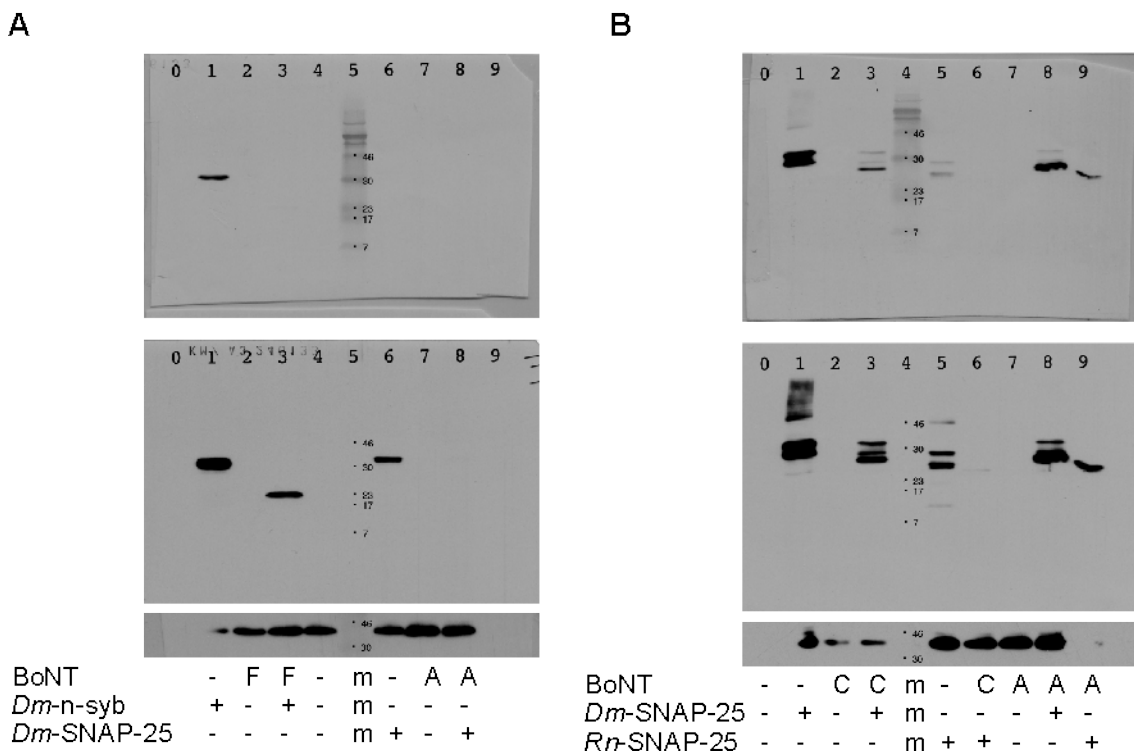


**Figure 3.11 Original western blot**

Overlay of blot and film after short exposure (upper blot) and long exposure (middle blot). Lower blot represents loading controls with anti-alpha-tubulin. Asterisks indicate lanes in Figure 3.9. Marker unit is kDA. **A:** stained with anti-HA. **1:** *Dm* n-Syb (*pPB22*)\*, **2:** BoNT-F (*pPB27*), **3:** *Dm* n-Syb (*pPB22*) + BoNT-F (*pPB27*)\*, **4:** Control, **5:** Marker Color Plus 7709s,

6: *Dm* SNAP-25 (*pPB30*), 7: BoNT-A (*pPB24*), 8: *Dm* SNAP-25 (*pPB30*) + BoNT-A (*pPB24*).  
**B:** stained with anti-V5. 0: Control, 1: *Dm* SNAP-25 (*pPB30*)\*, 2: BoNT-C (*pPB26*), 3: *Dm* SNAP-25 (*pPB30*) + BoNT-C (*pPB26*)\*, 4: Marker Color Plus 7709s, 5: *Rn* SNAP-25 (*pPB39*), 6: *Rn* SNAP-25 (*pPB39*) + BoNT-C (*pPB26*), 7: BoNT-A (*pPB24*), 8: *Dm* SNAP-25 (*pPB30*) + BoNT-A (*pPB24*)\*, 9: *Rn* SNAP-25 (*pPB39*) + BoNT-A (*pPB24*).

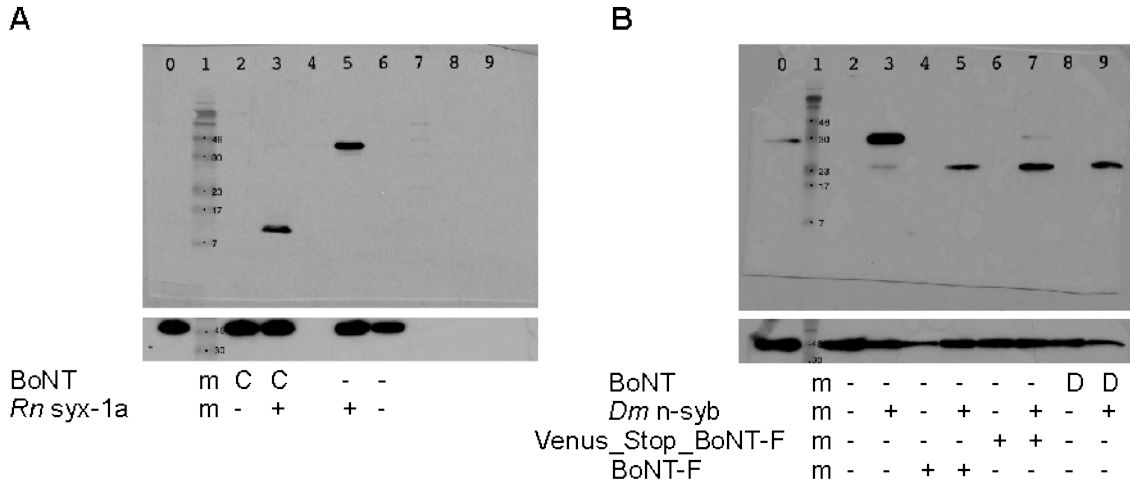


**Figure 3.12 Original western blot**

Overlay of blot and film. Blot stained with anti-HA. Marker unit is kDa. Asterisks indicate lanes in Figure 3.9. Lower blot represents loading controls with anti-beta-tubulin. **A:** 1: Marker Color Plus 7709s, 2: BoNT-C (*pPB26*), 3: *Rn* Syx (*pPB38*) + BoNT-C (*pPB26*), 5: *Rn*-Syx1a (*pPB38*), 6: Control. **B:** 1: Marker Color Plus 7709s, 2: Control, 3: *Dm* n-Syb (*pPB22*)\* 4: LoxP\_BoNT-F (*pPB56*), 5: LoxP\_BoNT-F (*pPB56*) + *Dm*-n-Syb (*pPB22*), 6: LoxP\_Venus\_Stop\_LoxP\_BoNT-F (*pPB52*), 7: LoxP\_Venus\_Stop\_LoxP\_BoNT-F (*pPB52*) + *Dm*-n-Syb (*pPB22*), 8: BoNT-D (*pPB55*), 9: *Dm* n-Syb (*pPB22*) + BoNT-D (*pPB55*)\*.

### 3.3 Generation of transgenic flies

Embryonic injections were carried out by BestGene Inc. (California). At first, *BoNT-A*, *BoNT-B*, *BoNT-C*, *BoNT-F* and *BoNT-G* were selected for Phi-C31 mediated injections (Bischof et al., 2007). This injection protocol allows selection of different fly strains that feature a defined target site for insertion of the transgene. An advantage of this method is that all *BoNTs* are inserted into the same locus on the same chromosome allowing for better comparison of the effectiveness of the different botulinum toxins. Furthermore, induced as well as presumed leaky expression can be tuned by selection of different target sites located in more or less active gene sites.

Using the Phi-C31 method no transgenic flies could be generated for BoNT-B and -F constructs. Remarkably, as assumed by primary structure conservation analysis (section 3.1.1 on p. 36) and biochemical assays (section 3.2 on p. 46), those were

the most effective BoNTs. We thus suggested that, due to leaky expression in the absence of *GAL4*, toxicity caused the failure in generating transgenic BoNT-B and -F flies. After consultation with BestGene Inc., we selected 4 additional target sites for BoNT-B and -F constructs including those associated with lowest leaky expression levels. Using this approach no additional transgenic flies could be generated. We then developed different expression vectors allowing for P-Element mediated insertions. Using this protocol, the transgene is inserted randomly into different gene loci of *w<sup>1118</sup>* flies. With this approach generation of 4 different transgenic BoNT-B fly strains on the X and 2nd chromosome was successful. BoNT-F and BoNT-D also yielded transgenic flies, however those flies were barely vital or fertile and failed to generate sufficient progeny to establish a stock. A subsequent injection trial with 200 embryos of the modified *UAS-LoxP-Venus-Stop-LoxP-BoNT-F::FLAG* construct (described in 3.1.3.1 on p. 42) inserted into a plasmid for P-element mediated transformation (*pPB51*), yielded 8 viable and fertile transgenic fly lines, whereas P-element mediated injections into 600 embryos of the unmodified BoNT-F (*pPB41*) construct yielded no transformants (Table 3.3).

	Calos strain 8622	Basler strain 24485 Bellen strain 9743	Bellen strain 9725, 9738 and strain 34763	P-Element
<i>UAS-BoNT-A (pPB13)</i>	3 / 200	-	-	-
<i>UAS-BoNT-B (pPB14, pPB40)</i>	0 / 400	0 / 200	0 / 400	5 / 400
<i>UAS-BoNT-C (pPB15)</i>	3 / 200	-	-	-
<i>UAS-BoNT-D (pPB54)</i>	-	-	-	0 / 600
<i>UAS-BoNT-F (pPB16, pPB41)</i>	0 / 400	0 / 200	0 / 400	0 / 600
<i>UAS-BoNT-G (pPB17)</i>	5 / 200	-	0 / 400	-
<i>UAS-LoxP-Venus-Stop-LoxP-BoNT-F::FLAG (pPB51)</i>	-	-	-	8/200

**Table 3.3 Success of Injection**

Overview on the number of transgenic animals after embryonic injections carried out by BestGene Inc. Numbers before slash display yield of viable transgenic flies and numbers after the slash the count of injected embryos. The respective plasmids for injection trials were *pPB13-17* for Phi-C31 mediated transformations and *pPB40, pPB41, pPB51* and *pPB54* for P-element mediated transformations.

## 3.4 CNT effect on survival and development

### 3.4.1 Assessment of lethality after expression in neurons

Previous investigations have shown that pan-neuronal and motoneuronal TNT expression lead to death at early developmental stages (Sweeney et al., 1995). Following this observation, we tested the potency of BoNT expression *in vivo*. We assessed the ability of BoNTs to induce lethality by driving expression with the pan-neuronal *elav-GAL4* and the glutamatergic motoneuron-specific *OK6-GAL4* enhancers (Figure 3.13). The respective *GAL4*-line was crossed to an *UAS-BoNT* line, whereas either the *GAL4*-line or the *UAS-BoNT* line were heterozygous to a balancer chromosome with a dominant marker. Effective toxins thus led to a fraction (*f*) of marker positive progeny of 1, whereas ineffective toxins led to an even proportion of marker positive and marker negative progeny. In accordance with the results from previous studies (Sweeney et al., 1995), pan-neuronal and motoneuronal *UAS-TNT-E* expression effectively interfered with fly development (Figure 3.13). Amongst the botulinum toxins *UAS-BoNT-B* and *-C* were equally effective and led to complete lethality after expression with both driver lines (all  $f = 1$ ,  $p < 0.0001$ ; binominal test). *UAS-BoNT-A* led to (incomplete) lethality only after pan-neuronal ( $f = 0.97$ ,  $p < 0.0001$ ), but not motoneuronal expression ( $f = 0.48$ ,  $p = 0.65$ ), whereas *UAS-BoNT-G* expression did not show any effect with both *GAL4*-lines (*elav*:  $f = 0.47$ ,  $p = 0.86$ ; *OK6*:  $f = 0.49$ ,  $p = 1$ ).

To sum up, only *UAS-BoNT-B* and *-C* led to induced lethality after expression in neuronal populations that are essential for life. We thus focused on these effective toxins in the next set of experiments.

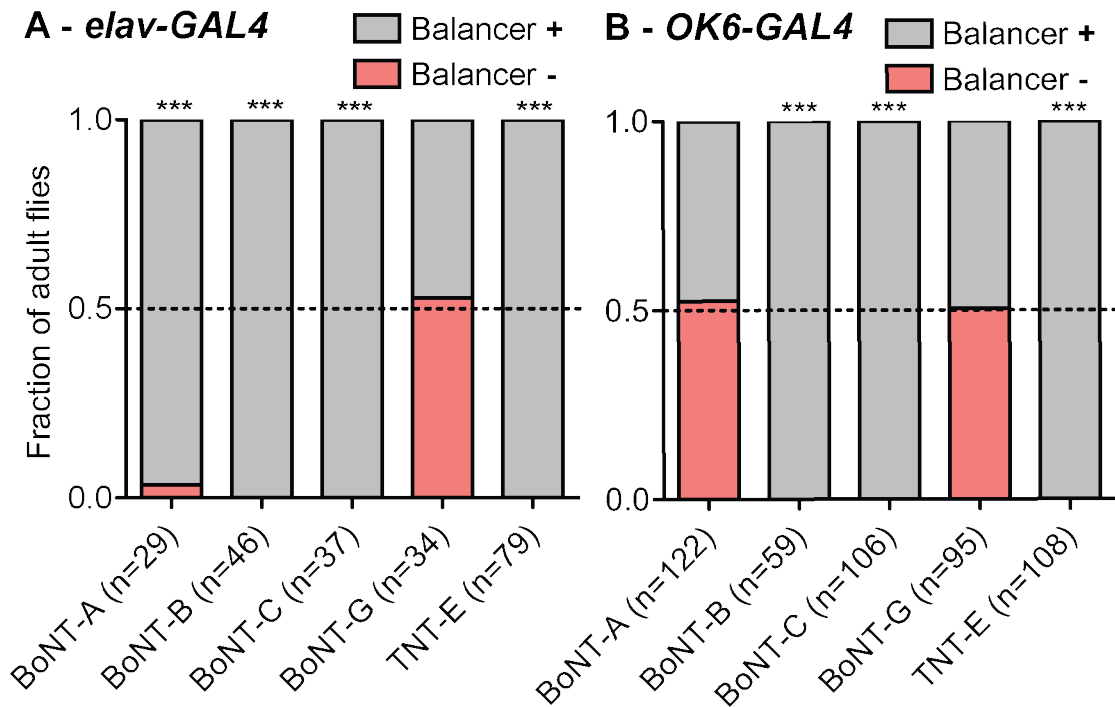


**Figure 3.13 Assessment of lethality after expression in neurons**

The different CNTs were balanced with balancer chromosomes with a morphological phenotype (*Cyo* or *TM3-Sb*) and crossed to either **(A)** *elav-GAL4* or **(B)** *OK6-GAL4*. Progeny was counted at 4-8 consecutive days. Balancer-positive and Balancer-negative flies are represented in gray and red respectively. The dashed line indicates a balanced ratio.

### 3.4.2 Assessment of lethality after expression in muscles

To assess the neuron-specificity of the toxins' actions, we expressed them using the muscle-specific driver line *G7-GAL4*.



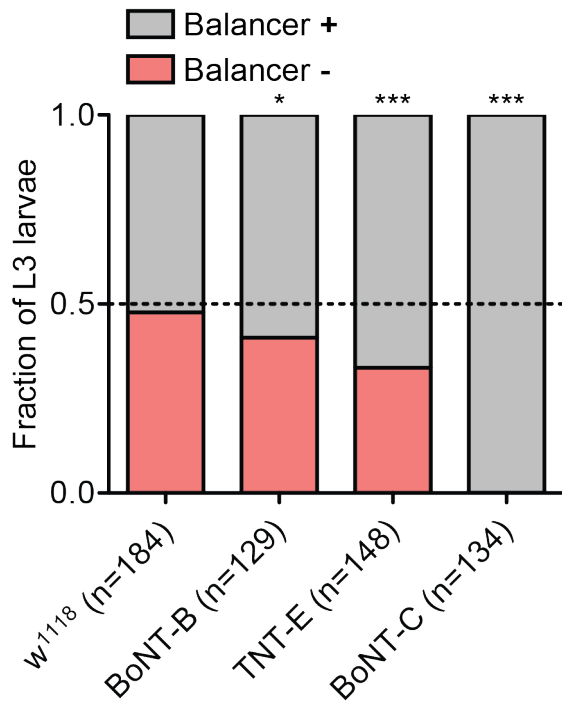


**Figure 3.14 Assessment of lethality after expression in muscles**

*G7-GAL4* (on 2<sup>nd</sup> chromosome) was balanced with *Cyo Act-GFP* and crossed to the respective *UAS-CNT* lines or *w<sup>1118</sup>* and L3 progeny was collected, sorted by the presence of a GFP signal and separately counted. GFP-positive and GFP-negative larvae are represented in grey and red respectively. The dashed line indicates a balanced ratio.

Flies of the *w<sup>1118</sup>* control group appeared to have a well-balanced proportion of progeny indicating that neither *G7-GAL4* nor the used balancer chromosome solely influence the proportion of larval progeny (binominal test;  $f = 0.52$ ,  $p = 0.61$ ). Both, *UAS-BoNT-B* ( $f = 0.59$ ,  $p = 0.05$ ) and *UAS-TNT* ( $f = 0.67$ ,  $p < 0.0001$ ) expression with *G7-GAL4* seemed to exhibit a slight but significant disadvantage on larval development as indicated by the moderate shift from a 50:50 ratio. However, *UAS-BoNT-C* expression led to lethality after muscle-specific expression ( $f = 1$ ,  $p < 0.0001$ ). Its effect is thus clearly not neuron-specific but appears in muscles and presumably also in other non-neuronal cell types as indicated by the lethal phenotype after expression with *GMR-GAL4* (section 3.6.1 on page 61).

### 3.4.3 Assessment of lethality after *UAS-Cre* dependent *UAS-BoNT-F* expression

To drive expression of the generated BoNT-F construct, we combined an insertion of an *UAS*-dependent Cre-recombinase on the 2<sup>nd</sup> chromosome (Heidmann and Lehner, 2001) with an insertion of the *UAS-LoxP-Venus-Stop-LoxP-BoNT-F::FLAG* construct on the 3<sup>rd</sup> chromosome. We balanced both chromosomes with morphological detectable balancer chromosomes and crossed these to *elav-GAL4* and *OK6-GAL4*. As effective Cre-expression, subsequent *LoxP*-recombination and resulting BoNT-F expression should lead to lethality when driven with these *GAL4*-lines, no balancer-negative progeny was expected for an effective protein expression. Viable, balancer-negative flies hatched for both *GAL4*-lines, indicating ineffectiveness of the construct (Table 3.4). We thus discontinued the experiments with the *UAS-LoxP-Venus-Stop-LoxP-BoNT-F::FLAG* construct.

	Cyo- Sb-	Cyo+ Sb-	Cyo- Sb+	Cyo+ Sb+
<i>Elav-GAL4</i> ; + ; + x <i>w*</i> / <i>y</i> ; <i>UAS-Cre</i> / <i>Cyo</i> ; <i>UAS-LoxP-Venus-Stop-LoxP-BoNT-F::FLAG</i> / <i>TM3,Sb</i>	4	2	7	1
<i>OK6-GAL4</i> ; + ; + x <i>w*</i> / <i>y</i> ; <i>UAS-Cre/Cyo</i> ; <i>UAS-LoxP-Venus-Stop-LoxP-BoNT-F::FLAG</i> / <i>TM3,Sb</i>	22	16	18	11

**Table 3.4 Lethal effect of *UAS-Cre* dependent *UAS-BoNT-F* expression**

Numbers indicate the total amount of the first generation progeny that carry a specific combination of the morphological markers *Cyo* and *Sb*.

### 3.4.4 Overview on BoNT *in vitro* cleavage, transgenesis and induced lethality

Toxin	Cleavage efficiency	Transformants	Lethality with <i>elav-GAL4</i>	Lethality with <i>OK6-GAL4</i>	Lethality with <i>G7-GAL4</i>
TeNT			+ (f=1, p<0.0001, n=79)	+ (f=1, p<0.0001, n=108)	(-) (f=0.67, p<0.0001, n=148)
BoNT-A	+	phi-C31: BDSC #8622, 3 <sup>rd</sup> chromosome	(+) (f=0.97, p<0.0001, n=29)	- (f=0.48, p=0.65, n=122)	
BoNT-B	++	P-element: X and 2 <sup>nd</sup> chromosome	+ (f=1, p<0.0001, n=46)	+ (f=1, p<0.0001, n=59)	(-) (f=0.59, p=0.05, n=129)
BoNT-C	+	phi-C31: BDSC #8622, 3 <sup>rd</sup> chromosome	+ (f=1, p<0.0001, n=37)	+ (f = 1, p<0.0001, n=106)	+ (f=1, p<0.0001, n=134)
BoNT-D	++	-			
BoNT-F	++	-			
BoNT-G	+	phi-C31: BDSC #8622, 3 <sup>rd</sup> chromosome	- (f=0.47, p=0.86, n=34)	- (f=0.49, p=1, n=95)	

**Table 3.5 Overview on BoNT *in vitro* cleavage, transgenesis and induced lethality**

Cleavage efficiency was estimated by western blots (Figure 3.9 on p. 49). Complete cleavage is indicated by ++ and incomplete cleavage by +. Primarily, *BoNT-A*, *-B*, *-C*, *-F* and *-G* were Phi-C31 dependent injected into targeted gene loci. After 5 unsuccessful attempts to integrate into different loci, P-element mediated injections were performed. For lethality assays balanced *UAS-CNT* flies were cell-specifically over-expressed in either motoneurons (*OK6-GAL4*), in all neurons (*elav-GAL4*) or larval muscles (*G7-GAL4*). Effective toxins led to a fraction (f) of marker positive progeny of 1, whereas ineffective toxins led to an even proportion of marker positive and marker negative progeny. - indicates unaltered survival, (-) slightly reduced survival, (+) incomplete lethality with few survivors and + complete lethality. *G7-GAL4* controls did not show an effect on larval survival (f=0.52, p=0.61, n=184).

### 3.5 Effects of CNT expression on larval behavior

The previous experiments demonstrated that *UAS-BoNT-B* and *-C* crucially affected neuronal function in developing animals. To measure the acute effect of *BoNT-B* and *-C* expression in developed neurons, we combined the *UAS*-constructs with the temperature-sensitive *tub-GAL80<sup>ts</sup>* construct (TARGET system (McGuire et al.,

2003)) using multiple steps of balancing and backcrossing of the respective transgenes. The TARGET system allows for temporal control gene expression, as GAL4 and thereby *UAS*-activation is inhibited at low temperatures (18 °C) and activated at high temperatures (31°C), mediated by the activity of the GAL4 suppressor *GAL80<sup>ts</sup>* at low temperatures only. We then measured the course of the spontaneous larval peristaltic movement frequency (Suster and Bate, 2002) as a function of time after a temperature shift to 31 °C that leads to expression induction (Figure 3.15). Again *UAS-TNT-E* served as a measure to classify the efficiency of *UAS-BoNTs*. To quantify the decay of larval activity, the length of incubation necessary for a 50 % suppression of movement frequency on the basis of fitted curves (mf50-values) was calculated. Further, pairwise statistical comparisons of the experimental groups with the respective controls were made at each time point. In addition to the genetic controls, flies of the same genotype that were held at 31 °C for 1 h served as un-induced controls.

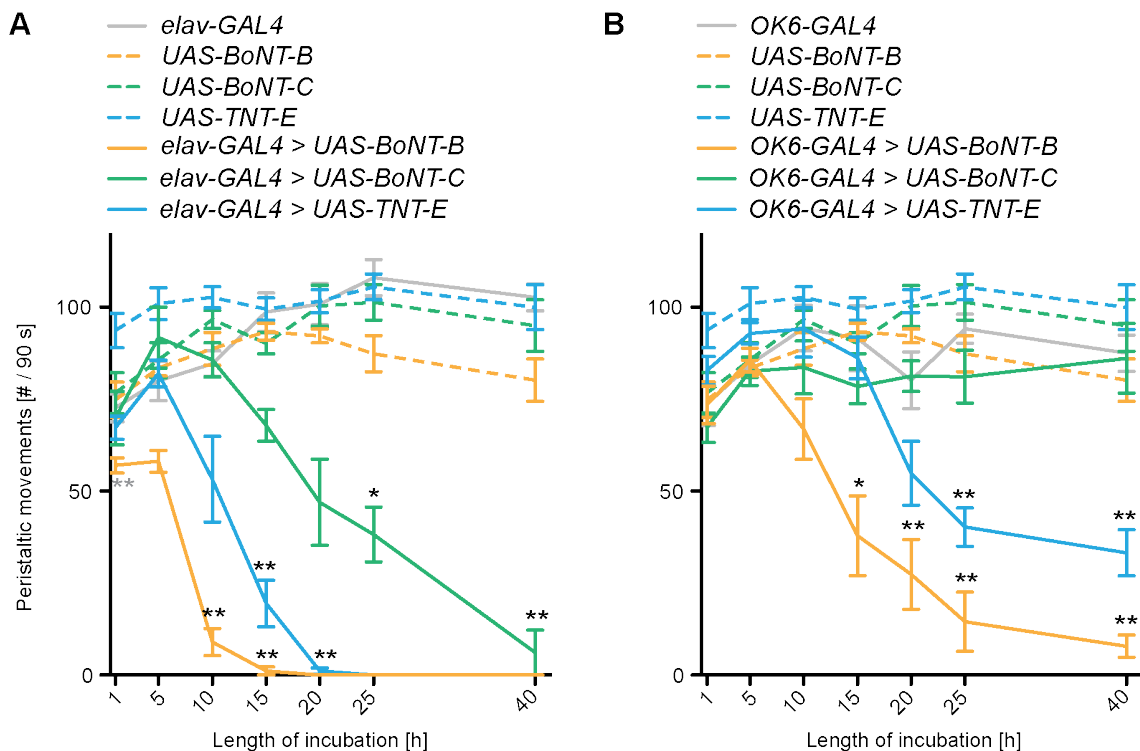


**Figure 3.15 Decrease of larval activity after induction of CNT expression in neurons**

As lines were combined with the *tub-GAL80<sup>ts</sup>* construct for conditional expression, graphs display the frequency of peristaltic movements at different time points after expression induction (temperature shift to 31 °C) of CNTs with either **(A)** *elav-GAL4* or **(B)** *OK6-GAL4*.

Black stars indicate the lowest level of significance from an experimental group at a certain length of incubation to differ from its genetic *GAL4*-control, *UAS*-control and to larvae of the same genotype that were incubated for 1 h. Thus, significance was only attributed to experimental groups that significantly differed from all three controls. Gray stars indicate that differently to the other experimental groups, *elav-GAL4 > UAS-BoNT-B* larvae already yielded statistical significance from their genetic controls after 1 h after the onset of incubation. Error bars represent the SEM. 6 (control) to 8 (experimental) larvae were tested for each group.

Pan-neuronal expression (Figure 3.15, A) of *UAS-BoNT-C* after 25 h induction led to significantly reduced locomotion in larvae compared to the uninduced control (*elav > BoNT-C* 1 h vs 25 h after induction:  $p = 0.01$ ,  $U = 7.0$ ; Mann-Whitney U-Test;  $mf50 = 22.78$  h), but paralysis occurred not to be total in the observed time window of 40 h. *Elav-GAL4* driven *BoNT-B* expression already yielded significant reduced locomotion after 1 h incubation (*elav > BoNT-B* vs *elav*:  $p = 0.0097$ ,  $U = 3.5$  and *BoNT-B*:  $p = 0.0027$ ,  $U = 2.0$ ), whereas the peristaltic of larvae transgenic for the *UAS-BoNT-B* construct only was not significantly altered. Nevertheless, compared to the “uninduced” controls pan-neuronal expression of *UAS-TNT-E* and *UAS-BoNT-B* led to significant weaker performance of larvae after 15 h (*elav > TNT* 1 h vs 15 h:  $p = 0.0002$ ,  $U = 0.0$ ;  $mf50 = 12.09$  h) and 10 h (*elav > BoNT-B* 1 h vs 10 h:  $p = 0.0002$ ,  $U = 0.0$ ;  $mf50 = 8.75$  h) incubation and complete paralysis after 25 h and 20 h, respectively.

Using the motoneuron specific driver line *OK6-GAL4* to drive expression (Figure 3.15, B), even after 40 h induction at high temperature (31 °C) no significant alteration of the behavior of *UAS-BoNT-C*-expressing larvae was detected (all  $p > 0.05$ ). In contrast, *UAS-TNT-E* and *UAS-BoNT-B* motoneuronal expression led to a robust suppression with significantly weaker performance after 25 h (*OK6 > TNT-E* 1 h vs 25 h:  $p = 0.0013$ ,  $U = 1.0$ ;  $mf50 = 22.08$  h) and 15 h (*OK6 > BoNT-B* 1 h vs 15 h:  $p = 0.0207$ ,  $U = 10.0$ ;  $mf50 = 15.24$  h) incubation, respectively, without inducing complete paralysis in the observed time window.

In conclusion, *UAS-BoNT-C* takes longer than *UAS-TNT-E* to impair larval activity after pan-neuronal expression and is ineffective after induced motoneuronal expression. *UAS-BoNT-B* on the other side decreases larval peristaltic activity even

faster than *UAS-TNT-E*, independent from the used *GAL4*-line. This indicates an overall higher potency of the newly generated botulinum toxin type B.

### 3.6 CNT effect in the visual system

A study has shown that *UAS-TNT* failed to significantly interfere with the adult flies' ability to detect movement after expression in photoreceptor cells (Rister and Heisenberg, 2006). In order to test whether expression of the botulinum toxins sufficiently blocks photoreceptor function, the different CNTs as well as the heat sensitive *shibire<sup>ts</sup>* construct were expressed via two different *GAL4*-lines: *GMR-GAL4* and *RH1-GAL4*. These two *GAL4*-lines differ in some ways: *GMR-GAL4* drives expression in all photoreceptor subtypes (R1-R8) (Freeman, 1996), while expression is restricted to R1-R6 for *RH1-GAL4* (Mollereau et al., 2000). Another difference is the onset of expression during fly development: *GMR-GAL4* drives expression under the control of glass multiple reporter (GMR) promoter elements and starts in the the developing eye (Freeman, 1996). Some effectors driven by *GMR-GAL4*, like i.e. *UAS-TNT* lead to severe morphological defects in the developing eye, when expression is unrestricted (Rister and Heisenberg, 2006). *RH1-GAL4* induced expression starts in the late pupa (Kumar and Ready, 1995) and unrestricted expression of *UAS-TNT* does not lead to a morphological phenotype (Rister and Heisenberg, 2006).

#### 3.6.1 Developmental effects of CNT expression

To assess developmental effects, we expressed the different CNTs in the eye using *Rh1-GAL4* and *GMR-GAL4*. As mentioned above, *RH1-GAL4* expression starts in late pupa and effectors as *UAS-TNT* do not effect the morphological phenotype of the *Drosophila* eye (Rister and Heisenberg, 2006). Consistently, all *Rh1-GAL4* positive flies used for behavioral measurements that expressed effectors as *UAS-shibire<sup>ts</sup>*, *UAS-BoNT-B*, *UAS-BoNT-C* and *UAS-TNT* did not show a macroscopically detectable morphological eye phenotype (data not shown). Contrary to that, *GMR-GAL4*-driven CNT expression led to morphological eye phenotypes of varying degrees depending on the used neurotoxin (Figure 3.16).

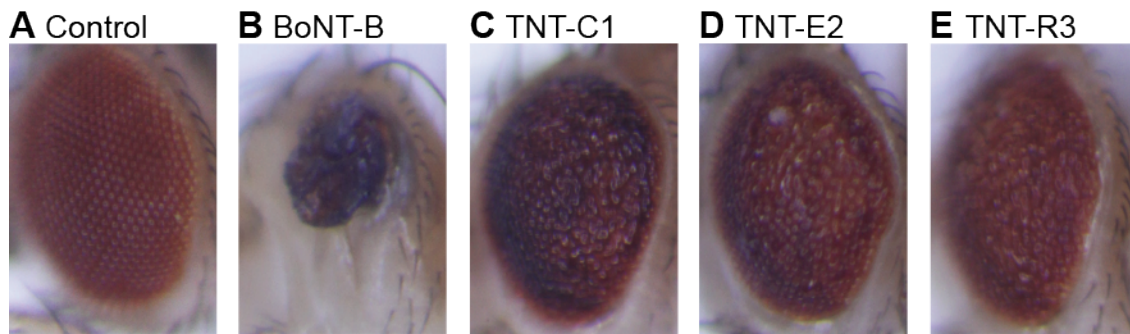


**Figure 3.16 Eye morphology after CNT expression**

*GMR-GAL4* was crossed to (A) *w<sup>1118</sup>*, (B) *UAS-BoNT-B*, (C) *UAS-TNT-C1*, (D) *UAS-TNT-E2* and (E) *UAS-TNT-R3*. All flies were raised at 25°C.

*UAS-BoNT-C* led to lethality after expression with *GMR-GAL4*. Interestingly, this was also the case, when it was combined with *tub-GAL80<sup>ts</sup>* and expression was restricted at 18 °C. In this case flies develop into mature pupae while the mature flies seem to fail to escape the pupa. The three different *UAS-TNT* (TNT-C1, TNT-E2 (used in experiments) and TNT-R3) insertions all produce a similar “rough-eye phenotype”, whereas *UAS-BoNT-B* produces a stronger morphological phenotype with heavy dysplastic eyes. For *UAS-BoNT-B* and *UAS-TNT*, combination with *tub-GAL80<sup>ts</sup>* prohibited the macroscopically determinable morphological phenotype when raised at 18 °C. These results indicate a high potency of *UAS-BoNT-B* to interfere with function of developing cells. However, *tub-GAL80<sup>ts</sup>*-mediated expression restriction can successfully circumvent these developmental defects.

**3.6.2 CNT effect on optomotor response behavior**

**3.6.2.1 Evaluation of the “Buchner-ball” setup**

For composition of the setup see 2.7.3 on p. 25.

To measure motion vision dependent behavior (optomotor response, OMR) in flies, we build a setup adapted from Buchner 1976 - the so called “Buchner-Ball-apparatus”. The next measurements serve to show that our setup reliably measures flies OMR as a function of various stimulus variables.

## Evaluation of *Shibire<sup>ts</sup>* induction

During first measurements with our setup we discovered a strong dependence of the flies' activity and performance on air temperature and humidity. Since the fly is positioned directly inside the (in comparison to the fly's body volume) strong air stream of >1 l/min, that is carrying the Styrofoam ball, it was assumed to be a major determining factor for the fly activity. We thus amplified the setup to control for both: humidity and temperature of the air stream. By that, we were able (1) to influence the fly's activity and endurance, (2) to create constant measurement conditions, regardless of measurement history (heating up of the setup), weather and air source (humidity) and ambient temperature and (3) to enable activation of heat sensitive constructs as the *shibire<sup>ts</sup>* mutant. Orienting measurements suggested a temperature of 31 °C and moderate augmentation of humidity to provide good conditions for long lasting and reliable measurements. To test whether this temperature was sufficient to induce *Shibire<sup>ts</sup>* effectively, we tested flies expressing the mutant allele pan-neuronally (*elav-GAL4*) and measured their overall activity in turning the Styrofoam ball after a temperature shift from the permissive temperature (25 °C) to the restrictive temperature (31 °C) (Figure 3.17, A). To check whether the chosen temperatures were sufficient, we also tested a temperature shift from 24 °C to 33 °C (Figure 3.17, B).

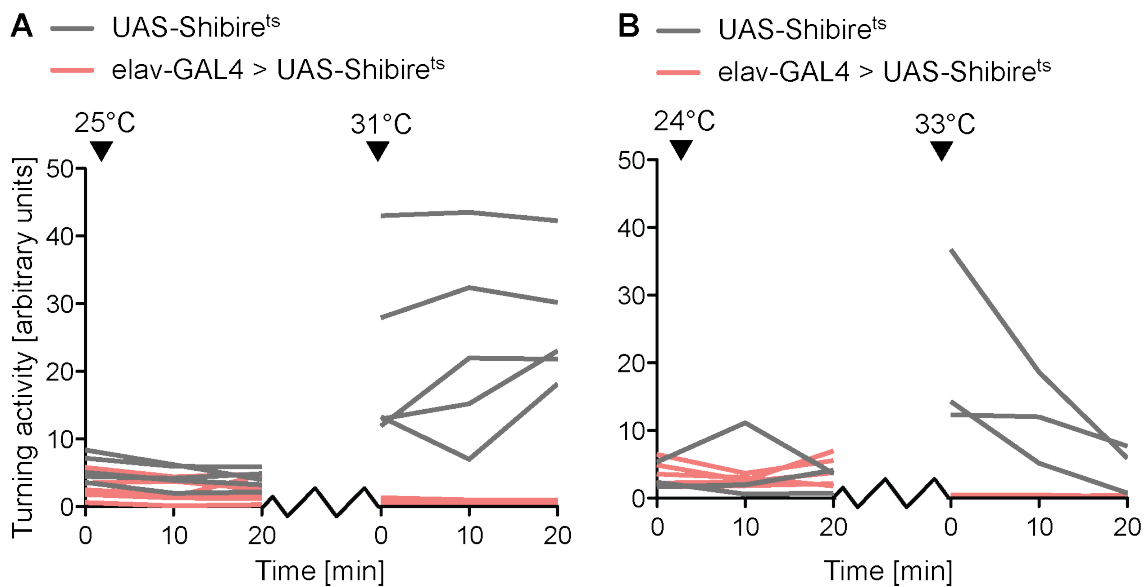


**Figure 3.17 Effect of pan-neuronal *Shibire<sup>ts</sup>* expression**



Lines display movement activity of individual flies. X axis show the duration of measurement. Triangles mark the temperature shift from **(A)** 25 °C to 31 °C and **(B)** 24 °C to 33 °C. The temperature shift takes 5-15 minutes (span between 20 and 0 minutes on x-axis) and differs for **(A)** and **(B)** and individual flies. A full contrast zebra striped pattern was presented to the flies that rotated with 3.3 Hz and changed direction every 6 minutes. Flies were raised at 21 °C.

The measurements (Figure 3.17) show reliable paralysis of *Shi<sup>ts</sup>* expressing flies after the temperature shift to either 31 °C or 33 °C, that appears slightly stronger at 33 °C. The activity of all control flies strongly increases after the temperature shift, but also limits the endurance of the flies which can be observed by the activity-decay after the temperature shift to 33 °C. At 25 °C and 24 °C, activity levels appear similar between the experimental and control groups. In conclusion, the effect of *UAS-Shibire<sup>ts</sup>* can be well triggered at 31 °C with restriction at 25 °C in our setup.

### ***Influence of contrast and pattern frequency on OMR***

We wanted to be able to detect even subtle influence of different effectors at the photoreceptor synapse on the flies' optomotor response. We thus included the limits of spatial and temporal visual resolution into the spectra of tested variables (Figure 3.18). To determine these limits, different contrasts of the presented pattern (no pattern, 2 %, 5 %, 20 % and 100 %) and pattern frequencies (0.1 Hz, 1 Hz, 10 Hz, 30 Hz and 45 Hz) were used to test the OMR of wild type *WTB* flies. The pattern with 100 % contrast was presented with and without ambient light.

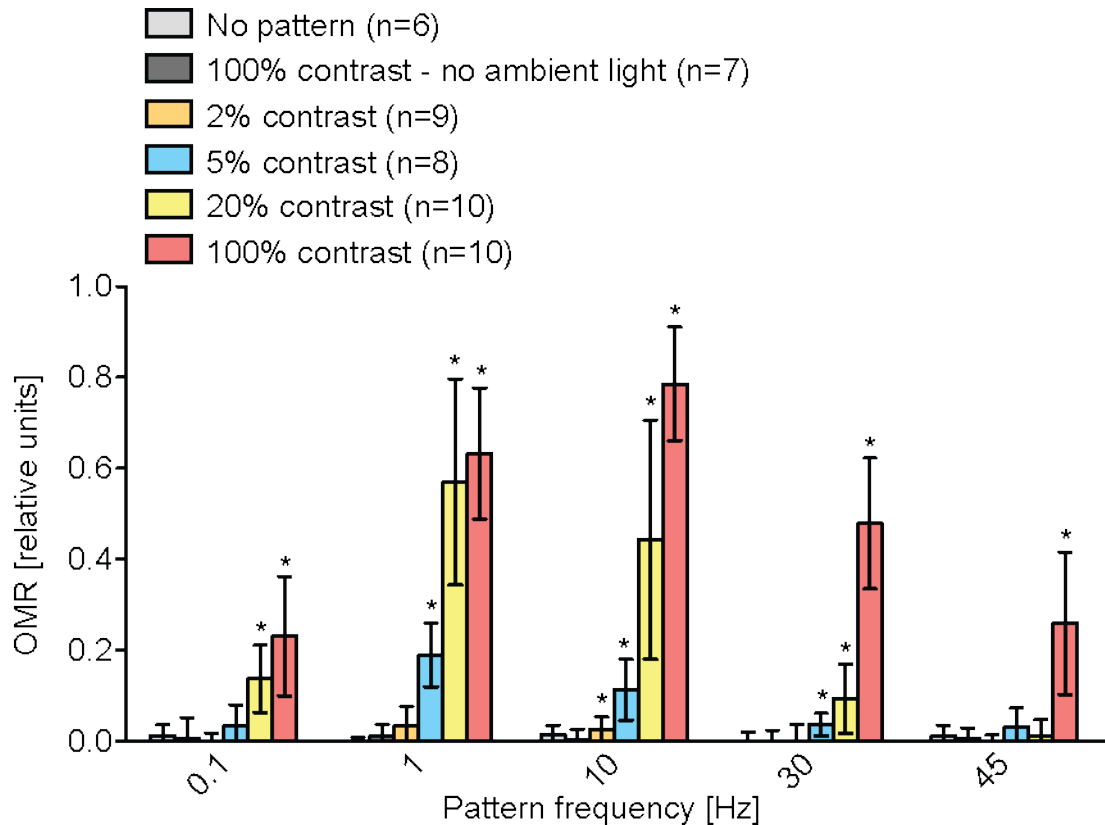


**Figure 3.18 Influence of different stimulus variables on OMR**

WTB flies were divided into different groups with differently contrasted stimulus patterns and each fly was tested multiple times under 5 different pattern frequencies. Stars represent significance to differ from zero (Wilcoxon Signed Rank Test;  $p < 0.05$ ). For “No pattern”, flies were presented a blank transparent paper, whereas for 2 %, 5 % and 20 % contrast different strengths of black bars were printed on transparent paper. The values do not represent actual Michelson contrast values, but different gray scale values as adjusted in Adobe Illustrator©. For 100 % contrast, a beamless black rubber plot was glued to the transparent paper, at least reaching a Michelson contrast of  $> 95$  %. For the group “100% contrast – no ambient light” the same pattern was used, but the surrounding LEDs were turned off. Experiments were performed at 31 °C fly temperature. Error bars represent SD.

Independent of the used pattern frequency, WTB-flies did not show any OMR when no pattern or the 100 % contrast pattern without ambient light was presented (Wilcoxon Signed Rank Test comparison with zero; *No pattern*: 0.1 Hz:  $p = 0.2785$ ; 1 Hz:  $p = 0.4076$ ; 10 Hz:  $p = 0.2031$ ; 20 Hz:  $p = 1.0$ ; 40 Hz:  $p = 0.5887$ . *100 % contrast - no ambient light*: 0.1 Hz:  $p = 1.0$ ; 1 Hz:  $p = 0.5862$ ; 10 Hz:  $p = 0.8643$ ; 20 Hz:  $p = 0.5827$ ; 40 Hz:  $p = 0.7835$ ). This shows that the flies’ behavior indeed depends on the detection of the presented illuminated pattern and not on other cues, such as sound, air movement, vibration or unintended visual marks as glue

stains. Furthermore a strong influence of the variables pattern frequency and contrast strength on OMR behavior could be detected. Low pattern contrast of 2 % yielded significant OMR in WTB flies only at pattern frequencies of 10Hz (0.1 Hz:  $p = 0.9512$ ; 1 Hz:  $p = 0.0567$ ; 10 Hz:  $p = 0.0352$ ; 20 Hz:  $p = 0.7647$ ; 40 Hz:  $p = 0.9425$ ), whereas 5 % contrast led to significant OMR at 1 Hz, 10 Hz and 30 Hz pattern frequency (0.1 Hz:  $p = 0.1071$ ; 1 Hz:  $p = 0.0137$ ; 10 Hz:  $p = 0.0142$ ; 20 Hz:  $p = 0.035$ ; 40 Hz:  $p = 0.076$ ). High pattern contrast of 20% (0.1 Hz:  $p = 0.008$ ; 1 Hz:  $p = 0.002$ ; 10 Hz:  $p = 0.008$ ; 20 Hz:  $p = 0.0142$ ; 40 Hz:  $p = 0.3829$ ) and 100% (0.1 Hz:  $p = 0.0059$ ; 1 Hz:  $p = 0.0058$ ; 10 Hz:  $p = 0.0059$ ; 20 Hz:  $p = 0.0059$ ; 40 Hz:  $p = 0.0020$ ) were sufficient to elicit significant OMR at all pattern frequencies except 45 Hz for 20 % contrast. Overall 1 Hz - 30 Hz pattern frequency elicited the strongest OMR values, while at the extreme ends only high contrast patterns were sufficient. Low contrast anticipate the flies' ability to detect fast moving patterns and vice versa. Also the peak optomotor response activity in regard to the contrast frequency is modulated by the contrast strength and shifted from 1 Hz for contrasts  $\leq 20\%$  to 10 Hz for 100 % contrast.

### ***Comparison of wild type OMR with an established OMR-defective genotype***

To test whether measurements with our custom build optomotor response setup were sufficient to detect motion vision phenotypes, we compared the optomotor response of *wild type Berlin (WTB)* and *optomotorblind<sup>H31</sup> (omb<sup>H31</sup>)* flies. The latter strain is characterized by the absence of the Lobula plate giant neurons HS and VS and resulting absence of optomotor behavior (Heisenberg et al., 1978; Schwarz et al., 1990) (Figure 3.19). The observed results show significant differences of the two genotypes for every tested pattern frequency (Mann-Whitney U-Test; 0.1 Hz:  $p = 0.0235$ ,  $U = 3.5$ ; 1 Hz:  $p = 0.002$ ,  $U = 0.0$ ; 10 Hz:  $p = 0.0058$ ,  $U = 0.0$ ; 20 Hz:  $p = 0.002$ ,  $U = 0.0$ ; 40 Hz:  $p = 0.002$ ,  $U = 0.0$ ). Conclusively, our setup can be used to detect differences in optomotor behavior of flies of different genotypes.

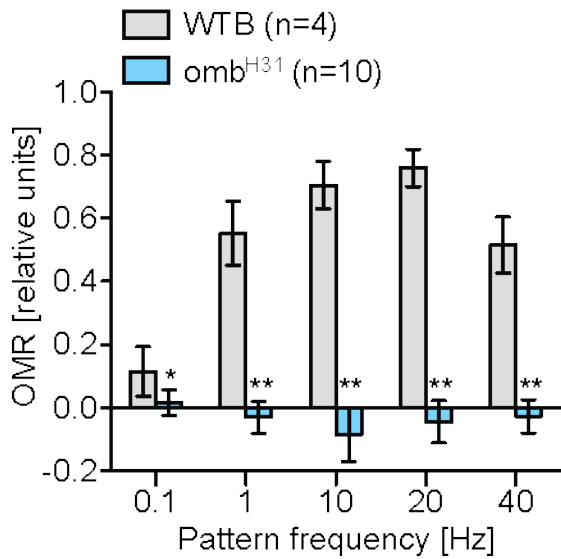


**Figure 3.19 OMR of *omb<sup>H31</sup>* vs *WTB***

Stars represent significance of *omb<sup>H31</sup>* to differ from *WTB*. The Mann-Whitney U-Test was used for pairwise comparisons. Measurements were performed at 31 °C fly temperature. Error bars represent SD.

The above measurements led us to select a certain measurement regime that was used for all following OMR experiments if not stated otherwise (see 2.7.3.4 on page 33 for details). It allows for induction of both used temperature sensitive constructs *shibire<sup>ts</sup>* and the temperature sensitive *tub-GAL80<sup>ts</sup>* that blocks *GAL4* binding: 24 h before measurements, flies were separated into vials that were incubated at 31 °C, only the “not incubated” controls were held at 18 °C. Measurements were carried out at 31 °C. After positioning the fly into the setup, it was heated until the target temperature of 31 °C was reached in a stable manner (usually 5-10 minutes). During heating, the drum did not move and illumination was turned on. Only 100 % contrast pattern was used. Directly after reaching the target temperature, the drum started rotating. 10 different measurement units of 90 seconds were applied (-0.1 Hz, 0.1 Hz, -1 Hz, 1 Hz, -10 Hz, 10 Hz, -30 Hz, 30 Hz, -45 Hz, 45 Hz pattern frequency). All 10 units were executed 9 times, while the order of the units was randomized. A whole measurement usually took 2 hours and 20 - 35 minutes (90 seconds x 10 x 9 + time for initial heating + time for drum rotation changes).

### 3.6.2.2 OMR after CNT expression with *GMR-GAL4*

#### ***UAS-TNT expression with GMR-GAL4 leaves OMR unaltered.***

*UAS-TNT-E* was shown not to be effective in suppressing OMR behavior after restricted expression to adult photoreceptors using *GMR-GAL4* (Rister and Heisenberg, 2006). We wanted to test whether we could reproduce these findings with our setup and measurement regime and could indeed not find any significant differences (Mann-Whitney U-Test; *GMR* > *TNT* (not incubated) vs *GMR* > *TNT* (incubated): all  $p > 0.05$ ) in the OMR after expression of *UAS-TNT-E* in the adult photoreceptor.

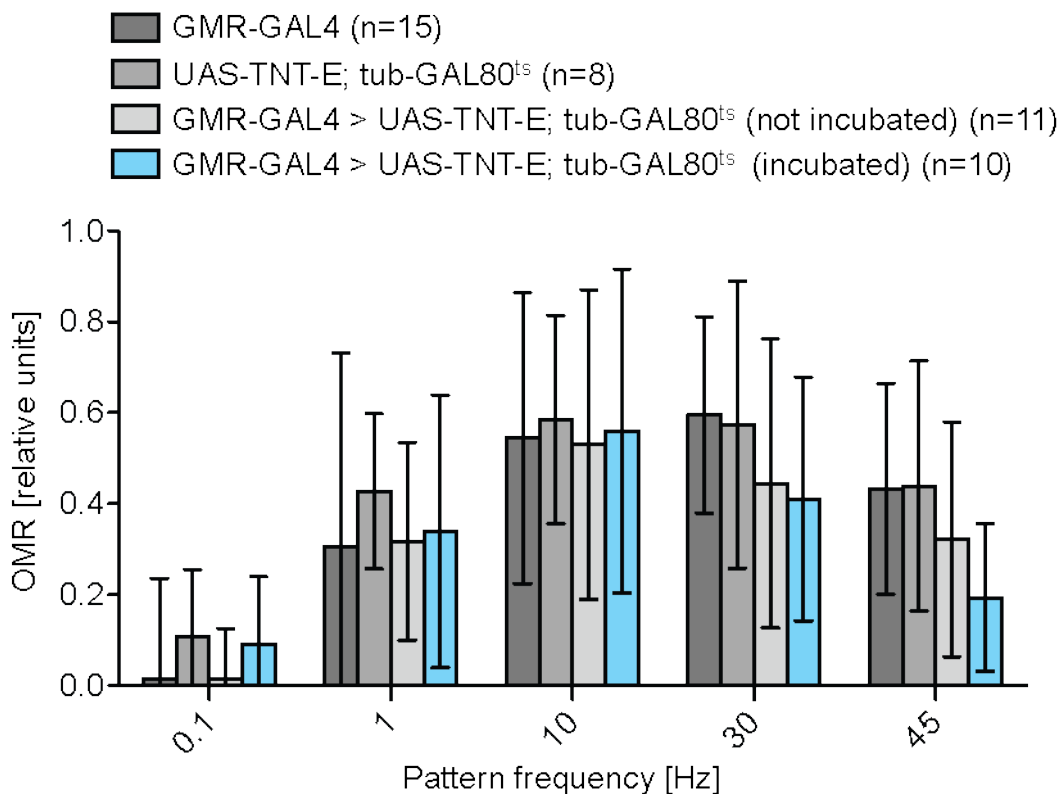


**Figure 3.20 *GMR-GAL4* > *UAS-TNT* effect on OMR in the adult fly**

All flies were raised at 18 °C. *GAL4*- and *UAS*-control, as well as the experimental group were incubated at 31 °C 24 h before the experiment. Only the non incubated group was left at 18 °C until the experiment, but also measured at 31 °C. Error bars represent SD.

#### ***UAS-Shibire<sup>ts</sup> suppresses OMR after expression with GMR-GAL4***

In a next step, it was tested whether effectors that interfere with presynaptic vesicle release other than CNTs could influence the flies' OMR. Therefore, we

expressed *Shibire<sup>ts</sup>* in the adult photoreceptor cells after a temperature shift to 31 °C using *GMR-GAL4* (Figure 3.21)

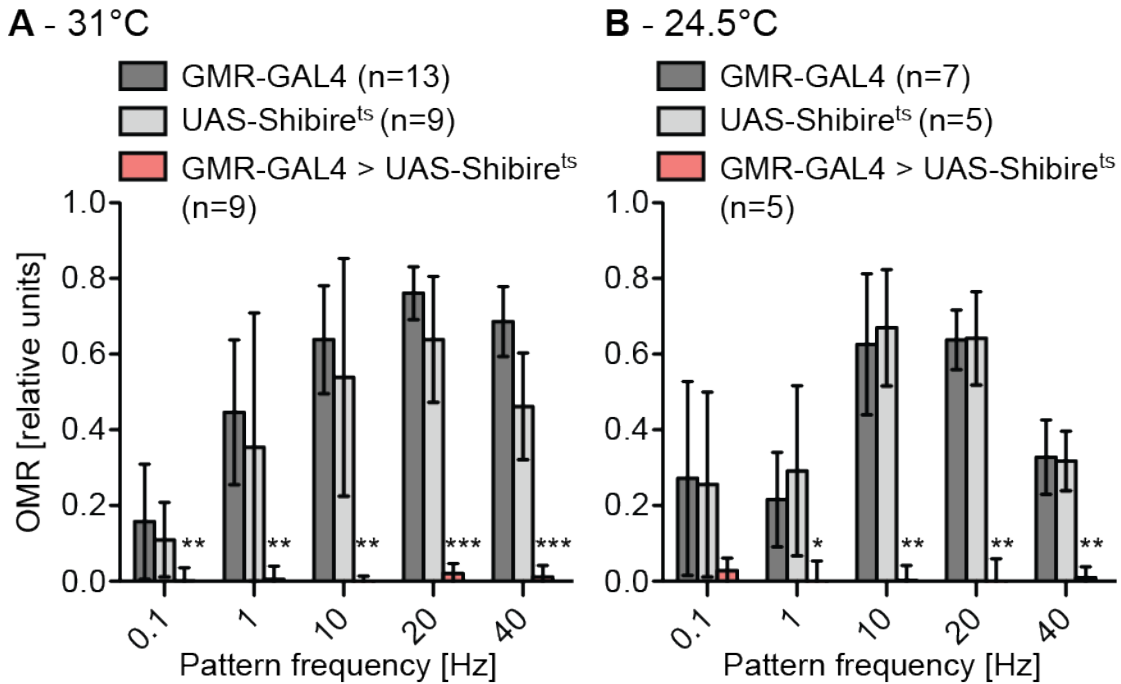


**Figure 3.21 *GMR-GAL4 > UAS-Shibire<sup>ts</sup>* effect on OMR**

Flies were crossed and raised at 21°C. Stars represent lowest significance levels of *GMR-GAL4 > UAS-Shibire<sup>ts</sup>* to differ from both controls. Flies were incubated **(A)** at 25 °C 24 h before the experiment and measured at 31 °C, **(B)** at 21 °C 24 h before the experiment and measured at 24.5 °C. Please note that for **(B)** the actual measurement temperature sometimes could exceed the target temperature up to 25.7 °C. Error bars represent SD.

Expression of the *Shibire<sup>ts</sup>* allele leads to complete diminishment of OMR in the experimental group at 31 °C at all tested pattern frequencies (Mann-Whitney U-Test; 0.1 Hz: *GMR- > Shibire<sup>ts</sup>* vs *GMR*:  $p = 0.001$ ,  $U = 9.0$  and *GMR > Shibire<sup>ts</sup>* vs *Shibire<sup>ts</sup>*:  $p = 0.0096$ ,  $U = 11.0$ ; 1 Hz:  $p = 0.0001$ ,  $U = 0.0$  and  $p = 0.0061$ ,  $U = 9.0$ ; 10 Hz:  $p = 0.0001$ ,  $U = 0.0$  and  $p = 0.0061$ ,  $U = 9.0$ ; 20 Hz:  $p = 0.0001$ ,  $U = 0.0$  and  $p = 0.0004$ ,  $U = 0.0$ ; 40 Hz:  $p = 0.0001$ ,  $U = 0.0$  and  $p = 0.0004$ ,  $U = 0.0$ ). To control for unspecific effects of the effector gene, we also measured the flies' OMR at 24.5 °C. Surprisingly, these flies also did not show any OMR except for a pattern frequency of 0.1 Hz (comparison of groups as above; 0.1 Hz:  $p = 0.1432$ ,  $U = 8.0$  and  $p = 0.1196$ ,  $U = 7.5$ ; 1 Hz:  $p = 0.0101$ ,  $U = 2.0$  and  $p = 0.048$ ,  $U = 5.0$ ; 10 Hz:  $p = 0.0057$ ,  $U = 0.0$  and  $p = 0.0057$ ,  $U = 0.0$ ; 20 Hz:  $p = 0.0025$ ,  $U = 0.0$  and  $p = 0.0025$ ,  $U = 0.0$ ; 40 Hz:  $p = 0.0025$ ,  $U = 0.0$  and  $p = 0.0054$ ,  $U = 0.0$ ). In

conclusion, OMR can be sufficiently suppressed using *GMR-GAL4* driven *UAS-Shibire<sup>ts</sup>*, however the effect is not temperature-dependent in the range of tested temperatures.

### ***Expression of UAS-BoNT-B with GMR leads to defects of OMR at high pattern frequencies***

We tested whether the newly generated *UAS-BoNT-B* construct would effect OMR after expression in adult photoreceptors. No significant differences between controls and experimental flies were discovered at the pattern frequency range of 0.1 - 10 Hz (Mann-Whitney U-Test; 0.1 Hz: *GMR* > *BoNT-B* (incubated) vs *GMR* > *BoNT-B* (not incubated):  $p = 0.3685$ ,  $U = 61.0$ ; 1 Hz: *GMR* > *BoNT-B* (incubated) vs *GMR* > *BoNT-B* (not incubated):  $p = 0.0123$ ,  $U = 31.5$  and *GMR* > *BoNT-B* (incubated) vs *BoNT-B*:  $p = 0.3558$ ,  $U = 45.5$ ; 10 Hz: *GMR* > *BoNT-B* (incubated) vs *GMR* > *BoNT-B* (not incubated):  $p = 0.7647$ ,  $U = 72.0$ ). At 45 Hz, expression using *GMR-GAL4* yielded a slight leaky effect at low temperature (*GMR* > *BoNT-B* (not incubated) vs *GMR*:  $p = 0.0483$ ,  $U = 37.0$  and vs *BoNT-B*:  $p = 0.0023$ ,  $U = 15.5$ ). However, in contrast to TNT (Figure 3.20), expression of *UAS-BoNT-B* led to a significant decrease in vision dependent motion behavior at the fastest frequencies of 30-45 Hz (30 Hz: *GMR* > *BoNT-B* (incubated) vs *GMR* > *BoNT-B* (not incubated):  $p = 0.0012$ ,  $U = 18.0$  and vs *BoNT-B*,  $p = 0.0003$ ,  $U = 7.0$  and vs *GMR*:  $p < 0.0001$ ,  $U = 0.0$ ; 45 Hz:  $p = 0.0001$ ,  $U = 7.0$  and  $p < 0.0001$ ,  $U = 0.0$  and  $p < 0.0001$ ,  $U = 0$ ) (Figure 3.22). Therefore, using *BoNT-B* as effector alters photoreceptor function at the limits of temporal motion vision resolution.

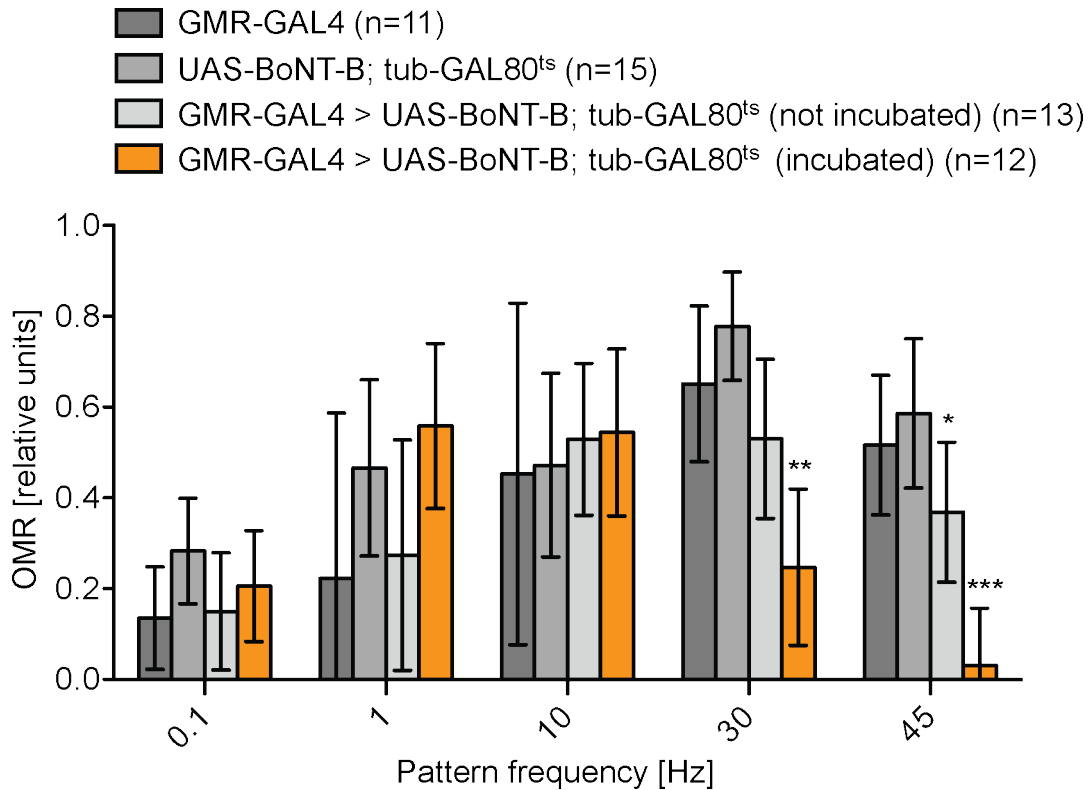


**Figure 3.22 *GMR-GAL4 > UAS-BoNT-B* effect on OMR in the adult fly**

All flies were raised at 18 °C. *GAL4*- and *UAS*-control, as well as the experimental group were incubated at 31 °C 24 h before the experiment. Only the not incubated group was left at 18 °C until the experiment, but also measured at 31 °C. Stars represent the lowest level of significance of the experimental group to differ from the other 3 control groups. Also significance levels of the not incubated group to differ from the *GAL4*- and *UAS*-control group was tested. Error bars represent SD.

### 3.6.2.3 Expression of effectors using *Rh1-GAL4*

*Rh1-GAL4* driven expression starts in late pupal development when eye and lamina development are largely finished (Kumar and Ready, 1995; Mollereau et al., 2000). Thus, expression of effectors as *UAS-TNT* do not influence the morphology of the eye. We tested whether the newly generated effectors influence the flies' ability to detect motion after expression with *Rh1-GAL4* and compared their effect to *UAS-TNT-E* and *Shibire<sup>ts</sup>* (Figure 3.23).



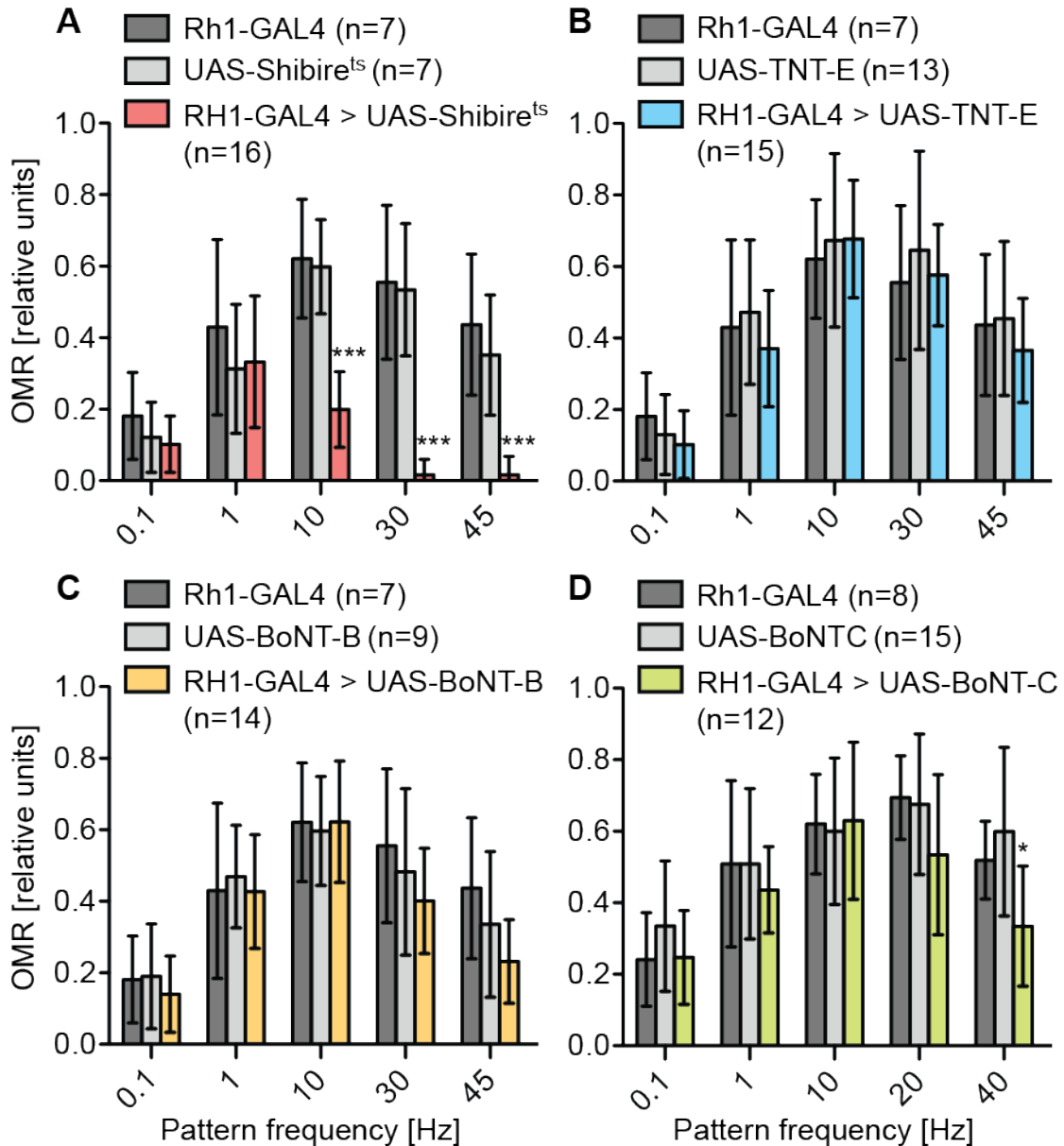


**Figure 3.23 OMR after expression of different effectors with *Rh1-GAL4***

All flies were raised at 25 °C and incubated at 31 °C 24 h before measurement. Note that all groups for A-C were part of the same measurement cycle and were measured in an alternating manner. The group *Rh1-GAL4* was identical for A-C. Stars represent the minimal level of significance for the experimental group to differ from both controls. The control lines *UAS-BoNT-B* and *UAS-TNT-E* showed a very bright orange eye colour when combined with *w<sup>1118</sup>*. To increase eye colour depth we combined them with *UAS-Tag64*, an arbitrary *UAS*-construct with *w<sup>1118</sup>* background that was previously tested with our setup and kindly provided by Nicole Hartmann.

Neither *UAS-BoNT-B* nor *UAS-TNT-E* did significantly change OMR behavior after expression with *Rh1-GAL4* (Mann-Whitney U-Test; all  $p > 0.05$ ). On the other hand, *UAS-BoNT-C* slightly reduces OMR performance at 40 Hz (40 Hz: *Rh1* > *BoNT-C* vs

*Rh1*:  $p = 0.0185$ ,  $U = 17.0$  and vs *BoNT-C*:  $p = 0.0021$ ,  $U = 26.5$ , all other frequencies  $p > 0.05$ ). A previous paper reports that flies with *Rh1-GAL4*-driven *UAS-Shibire<sup>ts</sup>*-expression were “motion blind” (Rister et al., 2007). Although OMR performance was strongly decreased in our experiment, flies still could detect motion at low stimulation frequencies (0.1 Hz: *Rh1* > *UAS-Shibire<sup>ts</sup>* vs *Rh1*:  $p = 0.0414$ ,  $U = 25$  and vs *UAS-Shibire<sup>ts</sup>*:  $p = 0.5028$ ,  $U = 45.5$ ; 1 Hz:  $p = 0.3326$ ,  $U = 41.0$  and  $p = 0.6639$ ,  $U = 49$ ; 10 Hz:  $p = 0.0002$ ,  $U = 0.0$  and  $p = 0.0002$ ,  $U = 0.0$ ; 30 Hz,  $p = 0.0002$ ,  $U = 0.0$  and  $p = 0.0002$ ,  $U = 0.0$ ; 45 Hz,  $p = 0.0003$ ,  $U = 1.0$  and  $p = 0.0002$ ,  $U = 0.0$ ). To test whether this discrepant findings reflected the different used *RH1-GAL4* insertion (3<sup>rd</sup> chromosome vs 2<sup>nd</sup> chromosome, the utilized *UAS-Shibire<sup>ts</sup>* insertion was identical) in our experiment, we tested the *UAS-Shibire<sup>ts</sup>* effect with another *Rh1-GAL4* insertion on the 2<sup>nd</sup> chromosome (Figure 3.24 A).

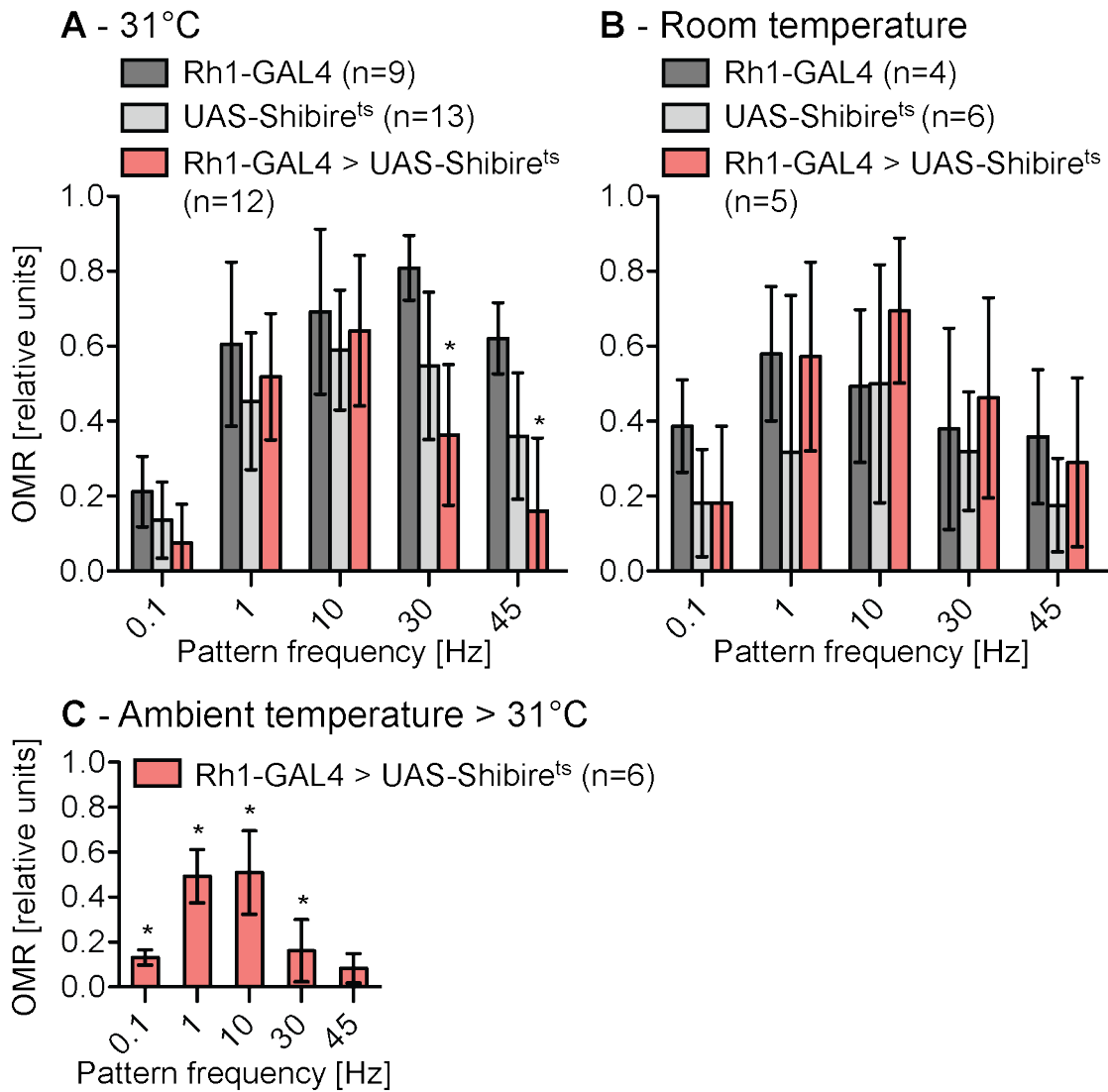


**Figure 3.24** *Rh1-GAL4 (on 2<sup>nd</sup>) > UAS-Shibire<sup>ts</sup>*

Flies were crossed and raised at 21 °C. Flies in **A** and **C** were incubated at 31 °C for 24 h before the experiment, **B** were incubated at 21 °C. No target temperature was assigned for **B** and the setup chamber was opened to allow air circulation to keep setup temperature < 25 °C. For **C**, the target temperature was 31 °C and additionally the temperature in the whole recording chamber was elevated to temperatures above 31 °C. Stars represent the minimal level of significance for the experimental group to differ from both controls for **A** and **B** whereas stars represent level of significance to differ from 0 for **C**.

Also for this *GAL4*-line we could not reproduce a complete loss of OMR performance after *Shibire<sup>ts</sup>* expression and induction (31 °C, 0.1 Hz: *Rh1* > *Shibire<sup>ts</sup>* vs *Rh1*:  $p = 0.0128$ ,  $U = 18.5$  and vs *Shibire<sup>ts</sup>*:  $p = 0.1018$ ,  $U = 47.5$ ; 1 Hz: *Rh1* > *Shibire<sup>ts</sup>* vs *Rh1*:  $p = 0.2546$ ,  $U = 37.5$ ; 10 Hz: vs *Rh1*:  $p = 0.1882$ ,  $U = 35.0$ ; 30 Hz: vs *Rh1*:  $p = 0.0003$ ,  $U = 2.0$  and vs *Shibire<sup>ts</sup>*:  $p = 0.0296$ ,  $U = 37.5$ ; 45 Hz:  $p = 0.0004$ ,  $U = 4.0$  and  $p = 0.0105$ ,  $U = 30.5$ ). The even less pronounced deficit after

expression with *Rh1-GAL4* on 2<sup>nd</sup> chromosome (Figure 3.24 A) in comparison to expression with *Rh1-GAL4* on the 3<sup>rd</sup> chromosome (Figure 3.23 A) might be linked to the different raising temperatures used in these experiments (21 °C vs 25 °C).

Although tested and evaluated in various approaches (see Figure 3.17), we could yet not fully exclude our air stream temperature to be the cause of the incomplete reduction of OMR performance by *Shibire<sup>ts</sup>*. To test this, we manually elevated the temperature of the complete recording chamber to temperatures > 31 °C (Figure 3.24, C). Still no complete reduction of the OMR could be observed, showing that our obtained results do not reflect insufficient temperature elevation of the flies' body by the air stream (Wilcoxon Signed Rank Test, significance to differ from zero; 0.1 Hz: p = 0.0355, 1 Hz: p = 0.0313; 10 Hz: p = 0.0313; 30 Hz: 0.0313; 45 Hz: 0.0625).

Expression of *UAS-Shibire<sup>ts</sup>* with *GMR-GAL4* leads to complete suppression of OMR also at a non-restrictive temperature of 24.5 °C (Figure 3.21 on page 69), questioning the specificity of the observed *Shibire<sup>ts</sup>* effect. To determine if *Shibire<sup>ts</sup>* alters the OMR of flies even at low temperatures when driven by *Rh1-GAL4*, we measured OMR at room temperature (Figure 3.24, B) and could not detect statistic significant defects (all p > 0.5). This indicates that the observed *Shibire<sup>ts</sup>* effect for *RH1-GAL4* is indeed caused by the temperature specific conformational change of the mutated *dynamain* allele.

## 4 Discussion

### 4.1 Generation of transgenic *UAS-BoNT*-flies

In our study we selected 6 different BoNT-subtypes for expression in *Drosophila*: BoNT-A, -B, -C, -D, -F and -G. Whereas insertions of *UAS-BoNT-A*, -C and -G directly led to transgenic progeny after phiC31 injection, *UAS-BoNT-B* insertion yielded transgenic flies only after a shift to P-Element insertion and no transgenic flies could be generated for *UAS-BoNT-D* and -F using these insertion methods. Notably, we chose transfection conditions which should reduce toxic effects of the inserted constructs, like 18 °C injection temperature and low copy numbers. The difficulties to integrate *UAS-BoNT-B*, -D and -F correlates with a high cleavage efficiency of these toxins as estimated by our biochemical data (Figure 3.9 on p. 49). Therefore toxic effects on SNARE targets already in the absence of the GAL4 transcription factor due to leaky expression are suggested. A possible higher affinity of BoNT-F and -D to either n-Syb or its ubiquitously expressed homologue Syb (Chin et al., 1993; DiAntonio et al., 1993; Hua et al., 1998) could provide a possible explanation for the fact that insertions of *UAS-BoNT-B* yielded transgenic flies, while those of *UAS-BoNT-D* and -F did not. Amino acid conservation at the p1'-position (the first C-terminal amino acid in respect to the cleavage site ) of the respective target SNAREs is considered to be most critical for proper CNT-cleavage as experimentally proven for BoNT-A and -E (Vaidyanathan et al., 1999), for BoNT-B (Schmidt and Bostian, 1997), BoNT-D, BoNT-F and TNT (Sikorra et al., 2008). The cleavage site of *Drosophila* Syb for BoNT-B and TNT features an amino acid substitution at the critical p1' position (Figure 3.1 on p. 37) making sufficient Syb-cleavage unlikely. This is reflected by our experiments showing equally low influence of non-neuronal expression of BoNT-B and TNT (section 3.4.2 on p. 55). The putative cleavage site on Syb for BoNT-D and -F however appears to be even better conserved than the cleavage site on n-Syb. On one hand this provides a likely explanation for a higher toxicity of these constructs upon leaky expression

and resulting failure to generate transgenic flies. On the other hand it challenges the role of BoNT-D and -F as neurospecific toxins in *Drosophila* in general.

We still aimed to test whether in principal a more powerful expression restriction could circumvent the toxic leak expression of BoNT-D and -F by utilizing an alternative genetic approach using a *loxP* flanked marker protein and additional stop codons preceding the BoNT-F cDNA (section 3.1.3.1 on p. 42). Indeed, this dual expression restriction of the *UAS-LoxP-Venus-Stop-LoxP-BoNT-F::Flag* construct seemed to effectively reduce leaky expression after embryonic injections resulting in 8 viable and fertile individual transformants after the first set of injections for P-element mediated integration (Table 3.3 on p. 53). We verified expression restriction before recombination and proper expression after recombination *in vitro* (Figure 3.7 G-H on p. 45). We also demonstrated proper cleavage restriction of n-Syb before recombination and after recombination unaltered cleavage potency in respect to the original *UAS-BoNT-F* construct in western blot experiments (Figure 3.12, B, lane 5 & 7 on p. 52). We thus generated transgenic flies combining our transgenic *UAS-LoxP-Venus-Stop-LoxP-BoNT-F::Flag* flies with an *UAS-Cre* construct (Heidmann and Lehner, 2001). However, co-expression of these constructs using *OK6-GAL4* did not result in lethality, as would be expected for a proper working construct. We thus discontinued our efforts in generating transgenic *UAS-BoNT-F* flies.

## **4.2 Varying effectivity of *UAS-BoNT* constructs in larval survival and behavior**

*UAS-BoNT-G* expression only led to weak cleavage of n-Syb in western blots and consequently did not affect fly survival (Figure 3.9 on p. 49, Figure 3.13 on p. 55). A likely explanation for this missing cleavage potency is an amino acid substitution in *Drosophila* n-Syb at the at the critical p1' position of the BoNT-G cleavage site.

A previous study using *in vitro* assays for proteolytic activity suggested that *Drosophila* SNAP-25 was not susceptible to BoNT-A (Washbourne et al., 1997). In our experiments *UAS-BoNT-A* led to incomplete cleavage of its *Drosophila* substrate In *Drosophila* S2 cell cultures and to partial lethality after neuronal

expression (Figure 3.9 on p. 49 and Figure 3.13 on p. 55). Whether this discrepancy derives from different experimental settings (in vitro vs in vivo) or from a putatively higher BoNT concentration after overexpression in S2 cells and neurons compared to the in vitro concentrations used by Washbourne et al., remains speculative. Taken into account the weak impact of *UAS-BoNT-A* and *-G* in our biochemical and lethality experiments, they appeared to be overall insufficient effectors in *Drosophila*.

*UAS-BoNT-C* partially cleaves its substrates SNAP-25 and Syntaxin-1A in our biochemical assays (Figure 3.9 on p. 49). It efficiently interferes with fly survival after expression in neurons and also in muscles and is thus not a neuron-specific effector (Figure 3.13 on p. 55. and Figure 3.14 on p. 56). Since BoNT-A seems to cleave SNAP-25 equally effective as BoNT-C, but does not sufficiently interfere with fly survival, the observed *UAS-BoNT-C* effect is more likely to be mediated by cleavage of Syntaxin-1A than of SNAP-25. Despite its role in neuroexocytosis, Syntaxin-1A plays a key role in non-neuronal secretion in *Drosophila* (Schulze et al., 1995). Another potential target for *UAS-BoNT-C* mediated cleavage is SNAP-24, a SNAP-25 homologue which is also involved in neurotransmission and non-neuronal cell function (Niemeyer and Schwarz, 2000; Vilinsky et al., 2002). Together potential *UAS-BoNT-C* mediated cleavage of Syntaxin-1A or SNAP-24 provide a sufficient explanation for the observed non-neuronal toxicity of expressed BoNT-C. Compared to *UAS-BoNT-B* and *UAS-TNT-E*, pan-neuronal *UAS-BoNT-C* expression requires longer incubation time to interfere with larval motor behavior (88 % longer than *UAS-TNT-E*, 160 % longer than *UAS-BoNT-B*, based on mf50-values) and is ineffective after induced expression in motoneurons (Figure 3.15 on p. 59). Although these characteristics limit the potential usage of *UAS-BoNT-C*, it could prove a useful tool where general, non-neuronal cell toxicity is desired. Thus it represents an alternative for established tools such as transgenes carrying the apoptosis activating gene *reaper* (White et al., 1996) or the mutated Diphtheria toxin A-chain DTI (Han et al., 2000).

In contrast to *UAS-BoNT-A*, *C* and *-G*, *UAS-BoNT-B* led to complete cleavage of its substrate neuronal Synaptobrevin in western blots (Figure 3.9 on p. 49). Similar as

for *UAS-TNT-E*, pan-neuronal and motoneuronal expression of *UAS-BoNT-B* is lethal while expression in muscle cells only exerts a minor influence on survival (Figure 3.13 on p. 55. and Figure 3.14 on p. 56). Both toxins thus seem to act equally neuron-specifically. *UAS-BoNT-B* however appeared to be more potent than *UAS-TNT-E* as it affected larval behavior faster, irrespective of the GAL4-line used (28 % for *elav-GAL4*, 33 % faster for *OK6-GAL4*, based on fm50-values; Figure 3.15 on p. 59). This should prove useful for neuroscientific analysis especially with *GAL4*-lines exhibiting low transgene expression levels.

Although BoNT-B and TNT cleave their substrate at the identical peptide bond, distinct binding and recognition sites on n-Syb that cause differences in the properties of these two toxins have been described (Hua and Charlton, 1999). Whereas TNT requires ongoing exocytosis events to cleave n-Syb, BoNT-B is also effective at inactive synapses. The different requirements on synaptic activity of the two toxins may constitute an advantage of *UAS-BoNT-B*: Before experiments, flies are raised under stable environmental stimulus conditions. In this period, TNT would be unable to cleave n-Syb in resting neuron populations, whereas BoNT-B could effectively interfere with synaptically silent nerve cells. Distinct zippering states of neuronal SNARE in different stages of presynaptic cycling are supposed to account for the varying exposure of the binding and recognition sites for BoNT-B and TNT (Hua and Charlton, 1999). Additionally, these different features could provide a new approach for the analysis of active zone processes in *Drosophila*: A recent study made use of these toxins by injections into *Crayfish* motoneurons. The authors tested whether the vesicle release probabilities at tonic and phasic synapses are determined by different SNARE zippering states (Prashad and Charlton, 2014). The concept of employing these toxins as reporters for zippering states of SNARE proteins could potentially be translated into research in *Drosophila*. Also a combination of these reporters with genetic alterations of other molecular players that are known to interact with SNARE proteins could help to identify the mechanisms and molecular interactions that underlie SNARE zippering.



### 4.3 Effect of BoNT-expression in the visual system of *Drosophila*

We used two different *GAL4*-lines to drive transgene expression in the visual system, *RH1-GAL4* and *GMR-GAL4* (see section 3.6 on p. 61). Unrestricted *GMR-GAL4* driven *UAS-BoNT-B* expression led to a strong morphological phenotype with heavily dysplastic eyes, whereas *UAS-TNT* expression led to a milder “rough-eye” phenotype (section 3.6.1 on p. 61). This difference might reflect the observed overall more potency of *UAS-BoNT-B* in comparison to *UAS-TNT* in disrupting neuronal function by n-Syb cleavage. A study that made use of eye specific gene deletions found that deletion of n-Syb resulted in a rough eye phenotype whereas deletion of Syb resulted in a dysplastic phenotype similar as observed for *UAS-BoNT-B* expression (Bhattacharya et al., 2002). These results raise the question whether *UAS-BoNT-B* relevantly interferes with other proteins than n-Syb, especially with (non-neuronal) Syb. The missing higher potency of *UAS-BoNT-B* to interfere with non-neuronal viability, as demonstrated by our experiments using toxin expression in developing muscle cells (see 3.4.2 on p. 55), however strongly argues against this scenario. Similarly our considerations on BoNT substrate specificity based on *Drosophila* n-Syb/Syb primary structure conservation do not support Syb cleavage by BoNT-B (see 3.1.1.1 on p. 37). Conditional expression using *tub-GAL80<sup>ts</sup>* successfully prevented the development of a morphological phenotype for *UAS-TNT* and *UAS-BoNT-B*.

Expression of *UAS-BoNT-C* with *GMR-GAL4* did not yield viable progeny. A recent research paper provides a possible explanation for these findings: *GMR-GAL4* is shown to not only promote expression in photoreceptors, but also in non-neuronal tissues as tracheae, leg and wing discs (Li et al., 2012). The different effect in inducing lethality with *GMR-GAL4* between *UAS-BoNT-B* and *UAS-BoNT-C* is likely to be explained by the observed toxic effect of *UAS-BoNT-C* not only on neuronal, but also non-neuronal cells (section 3.4.2 on page 55). Surprisingly the combination of *GMR-GAL4* with *UAS-BoNT-C* and *tub-GAL80<sup>ts</sup>* still did not yield viable flies when raised at 18 °C, indicating escape of the induced expression restriction. Notably, *tub-GAL80<sup>ts</sup>* mediated conditional expression of *UAS-BoNT-C* works with other (unrestricted lethal) *GAL4*-lines as *elav-GAL4* or *OK6-GAL4* where

viable flies hatch at 18 °C. In accordance with the fact that *RH1-GAL4* promotes expression after eye maturation, no morphological phenotypes were observed for unrestricted expression with any CNT (Rister and Heisenberg, 2006).

We aimed to test whether our newly generated BoNT constructs were effective in disrupting signal transmission in *Drosophila* photoreceptor cells. For this purpose we created a “Buchner-ball”-setup allowing to test the OMR-response on a wide scale of stimulus variables including luminance, contrast, pattern frequency, pattern type and the fly’s temperature. We generated a software to control the setup and to allow to create and modify complex measurement protocols to dynamically change these stimulus variables. One special feature of our setup was the possibility to constantly measure and regulate the air stream and the fly’s temperature dynamically by a feedback loop circuitry. This in principal provides the possibility to switch on and off temperature sensitive constructs as *Shibire<sup>ts</sup>*. Also high temperature induces stress and thus provides a method to ensure high fly activity during measurements (Figure 3.17 on p. 63, A, wild type controls). In various experiments we demonstrated that we could (1) measure flies optomotor response as a function of multiple stimulus variables (Figure 3.18 on p. 65), (2) reproduce behavioral phenotypes of defect mutants (Figure 3.19 on p. 67) and (3) induce temperature sensitive phenotypes by controlling the flies temperature during measurements (Figure 3.17 on p. 63).

We observed a complete loss of OMR after *UAS-Shibire<sup>ts</sup>* expression with *GMR-GAL4* not only at the restrictive (31 °C) but also at the permissive temperature (25 °C) (Figure 3.21 on p. 69). These results are in contrast with findings from Kitamoto 2001 where *UAS-Shibire<sup>ts</sup>* expression with *GMR-GAL4* resulted in a complete loss of behavioral response to light at the restrictive temperature (30 °C) and wild type-like behavior at the permissive temperature (19 °C) (Kitamoto, 2001). A plausible explanation for these discrepant findings is of course the much higher used permissive temperature in our experiments compared to Kitamoto (25 °C vs 19 °C), although in our experiments flies expressing *UAS-Shibire<sup>ts</sup>* pan-neuronally using *elav-GAL4* did not show majorly reduced locomotion activity at 25 °C compared to wild type controls (Figure 3.17, A on p. 63). The recording

temperature could not be practicably reduced below 25 °C, because the temperature inside the recording chamber usually spanned around 25 °C due to heat emission of the technical components. The Peltier elements principally allowed active cooling of the air stream, but this was accompanied by water condensation inside the air channel leading to obstruction of the latter. In accordance with our results, another study finds *GMR-GAL4 > UAS-Shibire<sup>ts</sup>* flies not to show any phototactic behavior also at a permissive temperature of 18 °C (Keller, 2002). Correspondingly, Gonzalez-Bellido et al. 2009 described “decelerated phototransduction and reduced neurotransmitter release” for *UAS-Shibire<sup>ts</sup>* expression with *RH1-GAL4* at the permissive temperature of 19 °C (Gonzalez-Bellido et al., 2009). These findings go along with unnaturally bundled microtubules and other ultrastructural changes in photoreceptors, that are not confined to the active zone of the synapse. As *GMR-GAL4* starts expression earlier during development and is believed to be an overall stronger driver line compared to *Rh1-GAL4* such effects are imaginable to also appear with *GMR-GAL4*. This provides a possible explanation for the effect at permissive temperatures observed by Keller and us. These results also underlie, that without showing a temperature dependent effect restriction, we can not surely account the observed effects of *UAS-Shibire<sup>ts</sup>* expression with *GMR-GAL4* to result from specific interference at the level of the presynapse.

Previous papers report flies that drive *UAS-Shibire<sup>ts</sup>* expression with *RH1-GAL4* to be “motion blind” (Rister et al., 2007). Although OMR performance was decreased in our experiment especially at high pattern turning frequencies, flies still could detect motion at low stimulation frequencies (Figure 3.23, A on p. 72 and Figure 3.24 on p. 74). Different *RH1-GAL4* insertions as well as different temperature induction protocols including heating up of the whole recording chamber to > 31 °C could also not completely deplete OMR. The most likely reason for the observed discrepancy of our experimental results to those of Rister et al. is a putative high sensitivity of our setup to motion responses because of the very optimal stimulus conditions, as the very bright presentation of high contrast patterns and the (intended) huge stress for the flies during recordings. Under less favourable

stimulus conditions, OMR might indeed be absent as it is the case in our experiments at very fast contrast frequencies (Figure 3.23 on p. 72, A, 30 and 45 Hz). Our intention of testing *UAS-Shibire<sup>ts</sup>* in these *GAL4*-lines was to show that disruption of neuroexocytosis using these *GAL4*-lines is sufficient to generate a “motion-blind” phenotype, in the sense of a “positive control”. As mentioned above, this goal could neither be completely achieved for *GMR-GAL4*, nor for *RH1-GAL4*.

*UAS-BoNT-C* could not be expressed in adult flies using *GMR-GAL4* due to lethality. Expression with *RH1-GAL4* however led to a slight significant reduction of OMR at highest pattern frequencies. As described above *UAS-BoNT-C* can not be seen as a neuron-specific tool, but is highly effective in promoting lethality in developing animals. The definite target of *UAS-BoNT-C* action could not be determined with certainty. It thus remains speculative what molecular target or targets mediate the observed phenotype after expression with *RH1-GAL4*. A cleavage of neuronal SNARE proteins and subsequent diminution of neuroexocytosis appears equally likely as effects on SNARE proteins mediating more general cell function. Thus, no certain conclusion of the involvement of SNAP-25 and Syntaxin-1A in neuroexocytosis in photoreceptor cells in *Drosophila* can be drawn from these experimental results.

*UAS-BoNT-B* significantly influences vision dependent motion behavior after expression in the “TNT-insensitive” photoreceptor cells using *GMR-GAL4*, but no complete blockade of photoreceptor function and only at high frequencies could be observed. These results reflect a common obstacle of *UAS-TNT-E* and *UAS-BoNT-B* to abolish photoreceptor function in *Drosophila*. Rister and Heisenberg 2006 discussed that n-Syb might be protected from TNT cleavage because of the calcium binding messenger protein Calmodulin, that appears to be involved in synaptic transmission in *Drosophila* photoreceptor cells (Xu et al., 1998). N-Syb features a binding site for Calmodulin overlapping with the cleavage site for TNT and BoNT-B (De Haro et al., 2003). Following this hypothesis, *UAS-BoNT-B* seems to somehow better overcome the assumed competitive Calmodulin “shielding” of the cleavage site. This could be simply due to a higher synaptic concentration or more favorable binding kinetics as reflected by the observed higher potency of *UAS-BoNT-B*

compared to *UAS-TNT-E*. Another explanation is provided by the putative different dependence on the active state of the synapse for substrate cleavage of BoNT-B and TNT. As a result of the differentially located binding sites on n-Syb of these two neurotoxins, TNT requires ongoing exocytosis events to cleave its SNARE substrate whereas BoNT-B is also effective at inactive synapses (Hua et al., 1998). Since Calmodulin binding critically depends on a high  $Ca^{2+}$  concentration, the blockade of the n-Syb cleavage site should break down at inactive synapses enabling cleavage for BoNT-B, but not for TNT (Di Giovanni et al., 2010).

The higher potency of *UAS-BoNT-B* compared to *UAS-TNT-E* led to a coherent more pronounced effect of leaky toxin expression in optomotor response experiments. This was observed for larval motor behavior where un-induced *UAS-BoNT-B* led to slight but significant decrease in larval peristaltic with *elav-GAL4*. In optomotor response experiments, *UAS-BoNT-B* led to a minor phenotype at the fastest pattern frequency in the un-induced control group despite expression restriction using *tub-GAL80<sup>ts</sup>* (Figure 3.20 on p. 68 and Figure 3.22 on p. 71).

No significant OMR-deficits could be detected after expression of *UAS-BoNT-B* using *RH1-GAL4*. This discrepancy does assumably not reflect actual differences of the expression patterns of these *GAL4*-lines but rather the common impression of *RH1-GAL4* being a weaker driver line compared to *GMR-GAL4*.

In conclusion, none of our tested BoNTs led to complete motion blindness as would be expected after complete block of neuroexocytosis after expression in photoreceptors regardless of the *GAL4*-line tested. However expression of *UAS-BoNT-B* with *GMR-GAL4* led to a significant OMR-response suppression restricted to higher frequencies. *UAS-BoNT-B* can thus only partially supersede *UAS-TNT* as an effective tool for the blockade of neurotransmitter release in the “TNT-insensitive” photoreceptor cells. Testing this toxin in other “TNT-insensitive” cells as mushroom body neurons (Thum et al., 2006) or Lamina monopolar neurons (Zhu et al., 2009) would be highly desirable.

## 5 Conclusion

Of the originally 6 different botulinum toxins that were selected for transgenic insertion, we can introduce two toxins as effective new transgenes in *Drosophila*: *UAS-BoNT-C* and *UAS-BoNT-B*. As our experiments in the visual system imply, *UAS-BoNT-B* can only partially advantageously supersede *UAS-TNT* as an effective tool for the blockade of neurotransmitter release in the “TNT-insensitive” photoreceptors. We however are confident that these toxins represent a useful addition to the *Drosophila* toolkit for various other applications. *UAS-BoNT-C* effectively exerts toxicity in neurons and muscles, and alters behavior after induced pan-neuronal but not motoneuronal expression. In contrast *UAS-BoNT-B* is a specific suppressor of neuronal function and interferes with behavior most effectively compared to the other tested CNTs. Although cleaving neuronal Synaptobrevin at the identical peptide bond, BoNT-B and TNT are supposed to harbor distinct features cleaving its substrate differently dependent on the state of SNARE zippering. This may provide the possibility to utilize these toxins for analysis of the molecular interactions that govern SNARE function during transmitter release. Correspondingly, BoNT-B should be useful in interfering with the SNARE machinery in resting neurons. It thus represents a means - complementary to TNT - to specifically suppress neuronal activity in *Drosophila*.

## 6 References

- Adams ME, Olivera BM (1994) Neurotoxins: overview of an emerging research technology. *Trends Neurosci* 17:151–155.
- Ashburner M (1989) *Drosophila*. A laboratory handbook. Cold Spring Harbor Laboratory Press.
- Bhattacharya S, Stewart BA, Niemeyer BA, Burgess RW, McCabe BD, Lin P, Boulianne G, O’Kane CJ, Schwarz TL (2002) Members of the synaptobrevin/vesicle-associated membrane protein (VAMP) family in *Drosophila* are functionally interchangeable in vivo for neurotransmitter release and cell viability. *Proceedings of the National Academy of Sciences* 99:13867–13872.
- Binz T, Blasi J, Yamasaki S, Baumeister A, Link E, Südhof TC, Jahn R, Niemann H (1994) Proteolysis of SNAP-25 by types E and A botulinum neurotoxins. *J Biol Chem* 269:1617–1620.
- Bischof J, Maeda RK, Hediger M, Karch F, Basler K (2007) An optimized transgenesis system for *Drosophila* using germ-line-specific phiC31 integrases. *Proc Natl Acad Sci USA* 104:3312–3317.
- Borst A (2009) *Drosophila's View on Insect Vision: Current Biology*. Current biology.
- Brand AH, Perrimon N (1993) Targeted gene expression as a means of altering cell fates and generating dominant phenotypes. *Development* 118:401–415.
- Breidenbach MA, Brunger AT (2005) New insights into clostridial neurotoxin-SNARE interactions. *Trends Mol Med* 11:377–381.
- Bruns D, Jahn R (2002) Molecular determinants of exocytosis. *Pflugers Arch* 443:333–338.
- Buchner E (1976) *Elementary movement detectors in an insect visual system* - Springer. Biological Cybernetics.
- Chen YA, Scheller RH (2001) SNARE-mediated membrane fusion. *Nat Rev Mol Cell Biol* 2:98–106.
- Chin AC, Burgess RW, Wong BR, Schwarz TL, Scheller RH (1993) Differential expression of transcripts from *syb*, a *Drosophila melanogaster* gene encoding VAMP (synaptobrevin) that is abundant in non-neuronal cells. *Gene* 131:175–181.
- De Haro L, Quetglas S, Iborra C, Lévêque C, Seagar M (2003) Calmodulin-dependent regulation of a lipid binding domain in the v-SNARE synaptobrevin and its role in vesicular fusion. *Biol Cell* 95:459–464.
- Di Giovanni J, Iborra C, Maulet Y, Lévêque C, Far El O, Seagar M (2010) Calcium-dependent regulation of SNARE-mediated membrane fusion by calmodulin. *J Biol Chem* 285:23665–23675.
- DiAntonio A, Burgess RW, Chin AC, Deitcher DL, Scheller RH, Schwarz TL (1993) Identification and characterization of *Drosophila* genes for synaptic vesicle proteins. *J Neurosci* 13:4924–4935.
- Dietzl G, Chen D, Schnorrer F, Su K-C, Barinova Y, Fellner M, Gasser B, Kinsey K, Oettel S, Scheiblaue S, Couto A, Marra V, Keleman K, Dickson BJ (2007) A genome-wide transgenic RNAi library for conditional gene inactivation in *Drosophila*. *Nature* 448:151–156.
- Freeman M (1996) Reiterative Use of the EGF Receptor Triggers Differentiation of All Cell Types in the *Drosophila* Eye. *Cell*.

- Schwarz H, Roth H, Poeck B, Sigl A, Kerscher S, Jonschker B, Pak WL, Heisenberg M, Pflugfelder GO (1990) Genetic and Molecular Characterization of the Optomotor-Blind Gene Locus in *Drosophila Melanogaster*. *Genetics* 126:91.
- Gonzalez-Bellido PT, Wardill TJ, Kostyleva R, Meinertzhagen IA, Juusola M (2009) Overexpressing Temperature-Sensitive Dynamin Decelerates Phototransduction and Bundles Microtubules in *Drosophila* Photoreceptors. ... of Neuroscience.
- Han DD, Stein D, Stevens LM (2000) Investigating the function of follicular subpopulations during *Drosophila* oogenesis through hormone-dependent enhancer-targeted cell ablation. *Development* 127:573–583.
- Heidmann D, Lehner CF (2001) Reduction of Cre recombinase toxicity in proliferating *Drosophila* cells by estrogen-dependent activity regulation. *Dev Genes Evol* 211:458–465.
- Heisenberg M, Wonneberger R, Wolf R (1978) Optomotor-blind<sup>H31</sup>?a*Drosophila* mutant of the lobula plate giant neurons. *J Comp Physiol* 124:287–296.
- Hua S-Y, Raciborska DA, Trimble WS, Charlton MP (1998) Different VAMP/Synaptobrevin Complexes for Spontaneous and Evoked Transmitter Release at the Crayfish Neuromuscular Junction. *Journal of Neurophysiology* 80:3233–3246.
- Hua SY, Charlton MP (1999) Activity-dependent changes in partial VAMP complexes during neurotransmitter release. *Nat Neurosci* 2:1078–1083.
- Jenett A et al. (2012) A GAL4-driver line resource for *Drosophila* neurobiology. *Cell Rep* 2:991–1001.
- Jin R, Sikorra S, Stegmann CM, Pich A, Binz T, and Brunger AT (2007) Structural and biochemical studies of botulinum neurotoxin serotype C1 light chain protease: implications for dual substrate specificity. *Biochemistry*, 46:10685–10693
- Keller A (2002) Genetic intervention in sensory systems of a fly. *Dissertation*:1–111.
- Kitamoto T (2001) Conditional modification of behavior in *Drosophila* by targeted expression of a temperature-sensitive shibire allele in defined neurons. *J Neurobiol* 47:81–92.
- Kumar JP, Ready DF (1995) Rhodopsin plays an essential structural role in *Drosophila* photoreceptor development. *Development* 121:4359–4370.
- Li W-Z, Li S-L, Zheng HY, Zhang S-P, Xue L (2012) A broad expression profile of the GMR-GAL4 driver in *Drosophila melanogaster*. *Genet Mol Res* 11:1997–2002.
- McGuire SE, Le PT, Osborn AJ, Matsumoto K, Davis RL (2003) Spatiotemporal rescue of memory dysfunction in *Drosophila*. *Science* 302:1765–1768.
- McMahon HT, Ushkaryov YA, Edelman L, Link E, Binz T, Niemann H, Jahn R, Südhof TC (1993) Cellubrevin is a ubiquitous tetanus-toxin substrate homologous to a putative synaptic vesicle fusion protein. *Nature* 364:346–349.
- Mollereau B, Wernet MF, Beaufile P, Killian D, Pichaud F, Kühnlein R, Desplan C (2000) A green fluorescent protein enhancer trap screen in *Drosophila* photoreceptor cells. *Mech Dev* 93:151–160.
- Neuser K, Triphan T, Mronz M, Poeck B, Strauss R (2008) Analysis of a spatial orientation memory in *Drosophila*. *Nature* 453:1244–1247.



- Niemeyer BA, Schwarz TL (2000) SNAP-24, a *Drosophila* SNAP-25 homologue on granule membranes, is a putative mediator of secretion and granule-granule fusion in salivary glands. *J Cell Sci* 113 ( Pt 22):4055–4064.
- Nouvian R, Neef J, Bulankina AV, Reisinger E, Pangršič T, Frank T, Sikorra S, Brose N, Binz T, Moser T (2011) Nouvian\_ExocytosisSnare2011. *Nature Publishing Group* 14:411–413.
- Pellizzari R, Rossetto O, Lozzi L, Giovedi S, Johnson E, Shone CC, Montecucco C (1996) Structural determinants of the specificity for synaptic vesicle-associated membrane protein/synaptobrevin of tetanus and botulinum type B and G neurotoxins. *J Biol Chem* 271:20353–20358.
- Pfeiffer BD, Ngo T-TB, Hibbard KL, Murphy C, Jenett A, Truman JW, Rubin GM (2010) Refinement of tools for targeted gene expression in *Drosophila*. *Genetics* 186:735–755.
- Prashad RC, Charlton MP (2014) SNARE zippering and synaptic strength. *PLoS ONE* 9:e95130.
- Rister J, Heisenberg M (2006) Distinct functions of neuronal synaptobrevin in developing and mature fly photoreceptors. *J Neurobiol* 66:1271–1284.
- Rister J, Pauls D, Schnell B, Ting C-Y, Lee C-H, Sinakevitch I, Morante J, Strausfeld NJ, Ito K, Heisenberg M (2007) Dissection of the peripheral motion channel in the visual system of *Drosophila melanogaster*. *Neuron* 56:155–170.
- Sakaba T, Stein A, Jahn R, Neher E (2005) Distinct kinetic changes in neurotransmitter release after SNARE protein cleavage. *Science* 309:491–494.
- Schiavo G, Benfenati F, Poulain B, Rossetto O, de Laureto PP, DasGupta BR, Montecucco C (1992) Tetanus and botulinum-B neurotoxins block neurotransmitter release by proteolytic cleavage of synaptobrevin. *Nature* 359:832–835.
- Schiavo G, Malizio C, Trimble WS, Polverino de Laureto P, Milan G, Sugiyama H, Johnson EA, Montecucco C (1994) Botulinum G neurotoxin cleaves VAMP/synaptobrevin at a single Ala-Ala peptide bond. *J Biol Chem* 269:20213–20216.
- Schiavo G, Matteoli M, Montecucco C (2000) Neurotoxins Affecting Neuroexocytosis. *Physiol Rev* 80:717–766.
- Schiavo G, Rossetto O, Catsicas S, Polverino de Laureto P, DasGupta BR, Benfenati F, Montecucco C (1993a) Identification of the nerve terminal targets of botulinum neurotoxin serotypes A, D, and E. *J Biol Chem* 268:23784–23787.
- Schiavo G, Shone CC, Bennett MK, Scheller RH, Montecucco C (1995) Botulinum neurotoxin type C cleaves a single Lys-Ala bond within the carboxyl-terminal region of syntaxins. *J Biol Chem* 270:10566–10570.
- Schiavo G, Shone CC, Rossetto O, Alexander FC, Montecucco C (1993b) Botulinum neurotoxin serotype F is a zinc endopeptidase specific for VAMP/synaptobrevin. *J Biol Chem* 268:11516–11519.
- Schmidt JJ, Bostian KA (1997) Endoproteinase activity of type A botulinum neurotoxin: substrate requirements and activation by serum albumin. *J Protein Chem* 16:19–26.
- Schulze KL, Broadie K, Perin MS, Bellen HJ (1995) Genetic and electrophysiological studies of *Drosophila* syntaxin-1A demonstrate its role in nonneuronal secretion and neurotransmission. *Cell* 80:311–320.

- Sikorra S, Henke T, Galli T, Binz T (2008) Substrate recognition mechanism of VAMP/synaptobrevin-cleaving clostridial neurotoxins. *J Biol Chem* 283:21145–21152.
- Sternberg N, Hamilton D (1981) Bacteriophage P1 site-specific recombination. I. Recombination between loxP sites. *J Mol Biol* 150:467–486.
- Suster ML, Bate M (2002) Embryonic assembly of a central pattern generator without sensory input. *Nature* 416:174–178.
- Südhof TC (2012) The Presynaptic Active Zone. *Neuron* 75:11–25.
- Sweeney ST, Broadie K, Keane J, Niemann H, O’Kane CJ (1995) Targeted expression of tetanus toxin light chain in *Drosophila* specifically eliminates synaptic transmission and causes behavioral defects. *Neuron* 14:341–351.
- Thum AS, Knapek S, Rister J, Dierichs-Schmitt E, Heisenberg M, Tanimoto H (2006) Differential potencies of effector genes in adult *Drosophila*. *J Comp Neurol* 498:194–203.
- Turan S, Galla M, Ernst E, Qiao J, Voelkel C, Schiedlmeier B, Zehe C, Bode J (2011) Recombinase-mediated cassette exchange (RMCE): traditional concepts and current challenges. *J Mol Biol* 407:193–221.
- Umezaki Y, Yasuyama K, Nakagoshi H, Tomioka K (2011) Blocking synaptic transmission with tetanus toxin light chain reveals modes of neurotransmission in the PDF-positive circadian clock neurons of *Drosophila melanogaster*. *J Insect Physiol* 57:1290–1299.
- Vaidyanathan VV, Yoshino K, Jahnz M, Dörries C, Bade S, Nauenburg S, Niemann H, Binz T (1999) Proteolysis of SNAP-25 isoforms by botulinum neurotoxin types A, C, and E: domains and amino acid residues controlling the formation of enzyme-substrate complexes and cleavage. *J Neurochem* 72:327–337.
- Vilinsky I, Stewart BA, Drummond J, Robinson I, Deitcher DL (2002) A *Drosophila* SNAP-25 null mutant reveals context-dependent redundancy with SNAP-24 in neurotransmission. *Genetics* 162:259–271.
- Washbourne P, Pellizzari R, Baldini G, Wilson MC, Montecucco C (1997) Botulinum neurotoxin types A and E require the SNARE motif in SNAP-25 for proteolysis. *FEBS Lett* 418:1–5.
- Waterhouse AM, Procter JB, Martin DMA, Clamp M, Barton GJ (2009) Jalview Version 2--a multiple sequence alignment editor and analysis workbench. *Bioinformatics* 25:1189–1191.
- White K, Tahaoglu E, Steller H (1996) Cell Killing by the *Drosophila* Gene reaper. *Science* 271:805–807.
- Xu XZ, Wes PD, Chen H, Li HS, Yu M, Morgan S, Liu Y, Montell C (1998) Retinal targets for calmodulin include proteins implicated in synaptic transmission. *J Biol Chem* 273:31297–31307.
- Zhu Y, Nern A, Zipursky SL, Frye MA (2009) Peripheral visual circuits functionally segregate motion and phototaxis behaviors in the fly. *Curr Biol* 19:613–619.

# **Danksagung**

Vielen Dank Kirsa und Tobi, dass ihr mich bei diesem Projekt betreut habt.

Vielen Dank Manfred und Robert für die intensive Begleitung.

Vielen Dank auch an Nicole, Jennifer, Dmitrij, Nadine, Mila und Martin.

# Philipp Backhaus

philipp.backhaus@ukmuenster.de

---

PERSÖNLICHE INFORMATIONEN	Geburtsdatum: 30.09.1987 Geburtsort: Paderborn, Deutschland	
AUSBILDUNG	<b>Medizinstudium Universität Würzburg</b> <b>Ludwig-Erhard Berufskolleg, Paderborn</b> Allgemeine Hochschulreife	04/2008-05/2015 2007
KLINISCHE TÄTIGKEIT	<b>Uniklinik Münster</b> Assistenzarzt Nuklearmedizin / Radiologie	07/2015-
FORSCHUNG	<b>Promotion Physiologisches Institut Würzburg</b> <i>„Effects of Transgenic Expression of Botulinum Toxins in Drosophila“</i>	2010 –
PUBLIKATIONEN	<i>„Effects of Transgenic Expression of Botulinum Toxins in Drosophila“</i> Backhaus P, Langenhan T, Kirscha N (2016) Journal of Neurogenetics (DOI: 10.3109/01677063.2016.1166223) -Posterpräsentation bei der 92. Jahrestagung der <i>Deutschen Physiologischen Gesellschaft</i> , Heidelberg -Posterpräsentation bei dem internationalen Symposium <i>„Molecular models for diseases of the nervous system“</i> des Sonderforschungsbereich 581 -Posterpräsentation bei dem internationalen Kongress <i>„Biochemical Chemistry, Molecular Biology and Cybernetics of Cell Functions“</i> in Klosters, Schweiz	06/2016   03/2013 04/2012 01/2012